DEPARTMENT OF TRANSPORTATION

Performance Monitoring of Olmsted CR 117 and 104 and Aggregate Base Material Update

Kyle Hoegh, Principal Investigator
Minnesota Department of Transportation

December 2023

Research Project
Final Report 2024-01

LRRB
LOCAL ROAD RESEARCH BOARD

To request this document in an alternative format, such as braille or large print, call 651-366-4718 or 1-800-657-3774 (Greater Minnesota) or email your request to ADArequest.dot@state.mn.us. Please request at least one week in advance.

Technical Report Documentation Page

1. Report No.	2.	3. Recipients Accession No.	
MN 2024-01			
4. Title and Subtitle Performance Monitoring of Olmsted CR 117 and 104 and Aggregate Base Material Update		5. Report Date December 2023 6.	
7. Author(s) Kyle Hoegh, P.E., Ph.D.		8. Performing Organization Report No.	
9. Performing Organization Name and Address Minnesota Department of Transportation Office of Materials and Road Research 1400 Gervais Avenue Maplewood, Minnesota 55109-2044		10. Project/Task/Work Unit No. 11. Contract (C) or Grant (G) No. (c) LAB986	
12. Sponsoring Organization Name and Address Minnesota Department of Transportation Office of Research & Innovation 395 John Ireland Boulevard, MS 330 St. Paul, Minnesota 55155-1899		13. Type of Report and Period Covered Final Report 14. Sponsoring Agency Code	
15. Supplementary Notes http://mdl.mndot.gov/			

16. Abstract (Limit: 250 words)

A performance monitoring and forensic study was conducted on several test sections with varying base and pavement characteristics. This report includes the performance data from the current phase, which was extended until pavement reconstruction, with the previously reported data, collected since original construction of the test sections. Each of the three original test sections were prepared with a different combination of base type and asphalt binder type. Three different crushed limestone base types were used in the construction: (Section 1) standard Class 5, (Section 2) permeable aggregate base (PAB), and (Section 3) Class 5 modified. Two different types of asphalt binders, PG 58-28 and PG 58-34, were incorporated to evaluate the effects of cold temperature cracking. All asphalt mixtures were designed according to MnDOT Specification 2350. In addition to the comparisons among sections, each road section was constructed, both with and without transverse sawn-and-sealed regularly spaced joints, to evaluate the relative performance for ride and cracking (both spacing and crack severity) of sawing and sealing (S&S) versus allowing thermal cracking to relieve tensile stress without sawing and sealing (non-S&S). Prior to reconstruction, the severity of cracking in Section 1 was significantly higher than in Sections 2 and 3, with no severe cracking observed in Section 3. This study confirmed previous research efforts on this project, indicating that the combination of PG58-34 binder with Class 5 modified base material (Section 3) and PAB base (Section 2) performed well as compared to the control section. Seasonal trends of reduced stiffness during spring thaw followed by rapid recovery were also observed in the FWD analysis.

17. Document Analysis/Descriptors	18. Availability Statement		
PG grade, base type, stiffness, freeze thaw, saw and seal, performance monitoring	No restrictions. Document available from: National Technical Information Services, Alexandria, Virginia 22312		
19. Security Class (this report) Unclassified	20. Security Class (this page) Unclassified	21. No. of Pages 79	22. Price

Performance Monitoring of Olmsted CR 117 and 104 and Aggregate Base Material Update

Final Report

Prepared by:

Kyle Hoegh, P.E., Ph.D.
Minnesota Department of Transportation
Office of Materials and Road Research
1400 Gervais Avenue
Maplewood, Minnesota 55109-2044

December 2023

Published by:

Minnesota Department of Transportation
Office of Research & Innovation
395 John Ireland Boulevard, MS 330
St. Paul, Minnesota 55155-1899

Acknowledgements

The author would like to express appreciation to the Local Road Research Board for providing financial support for this project and to the Minnesota Department of Transportation for its support of this research. Thanks to Dr. Shongtao Dai for supervising and guiding this research and the previous principal investigators (most recently Matthew Lebens) for reporting previous findings that this final phase of the research is based on. The authors would like to thank those serving on the TAP throughout the previous projects, as well as Technical Liaison for the current phase of the project, Kaye Bieniek, for insights that contributed to the success of the study.

Table of Contents

Chapter 1: Introduction 1

1.1 Background 1

1.2 Objective 1

1.3 Scope 1

Chapter 2: Project Analysis 3

2.1 Site and Research Platform Description 3

Chapter 3: Performance Monitoring and Traffic Analysis 10

3.1 Traffic 10

3.2 Automated Distress Surveys 12

3.3 Visual Distress Surveys 14

Chapter 4: Project Data Analysis and Forensics 29

4.1 Falling Weight Deflectometer (FWD) Data Analysis 29

4.1.1 FWD Major Trends 29

4.1.2 2010 Spring Thaw Period Intensive FWD Testing 39

4.1.3 2012 Fall Freezing Period Intensive FWD Testing 42

4.2 Ground Penetrating Radar Forensic Analysis 46

4.3 Cone Penetrometer (CPT) Methodology and Results 58

4.4 Base Layer Forensic Analysis 63

Chapter 5: Crushed Limestone Base Materials Survey 65

5.1 Agency Survey Description 65

5.2 Agency Survey Results 66

Chapter 6 Conclusions and Recommendations 67

Table of Tables

Table 2.1 Test sections for Olmsted County Research Project 5

Table 2.2 Aggregate Base Gradations 8

Table 3.1 2015 Visual distress survey data summary for Test Sections 15

Table 4.1 2008 Average Back-Calculated Resilient Moduli 29

Table 4.2 2009 Average Back-Calculated Resilient Moduli 30

Table 4.3 2010 Average Back-Calculated Resilient Moduli 30

Table 4.4 2011 Average Back-Calculated Resilient Moduli 31

Table 4.5 2012 Average Back-Calculated Resilient Moduli 31

Table 4.6 2014 Average Back-Calculated Resilient Moduli 32

Table 4.7 CPT Measured Tip Stress (PSI) for Each Sounding 62

Table 4.8 Gradation Pre-Compaction, Post-Compaction, and Post-Failure of All 3 Sections 63

Table of Figures

Figure 2.1 Olmsted County, MN Research Site Location 3

Figure 2.2 Olmsted County Roads 104 & 117 – Research Site Location 4

Figure 2.3 Test Section Map for Olmsted County Research Project 6

Figure 2.4 Olmsted County Road 117 (Station 105+00) 03/27/2002 8

Figure 2.5 Olmsted County Road 117 (Station 105+00) 11/25/2014 9

Figure 2.6 Typical Sections on Olmsted County Research Project 9

Figure 3.1 Traffic Count History on Olmsted County Research Project by Section Updated with Most Recent Measurements 10

Figure 3.2 Traffic Counts Including HCADT on Olmsted County Research Project 11

Figure 3.3 IRI Results for Each Section through Reconstruction 13

Figure 3.4 2007-2016 Pavement Roughness Index – Test Sections Only 14

Figure 3.5 2008-2015 Approximate Cracking Length Observed by Visual Surveys 16

Figure 3.6 Photo-Based Versus Traditional Cracking Measurements for the Multiple Sections 17

Figure 3.7 Example Photo-Based Distress Mapping Result from Section 1A 105+00 to 105+50 18

Figure 3.8 Example 10 Ft. by 12 Ft. Photo-Based Distress Mapping Result from Section 1A 105+00 to 105+30, Where the Transparent Green Box Shows the Mapped Area and Corresponding Photo 19

Figure 3.9 Comparison of Visual Crack Length in Each Section Showing Minimal Distress Increases in Sections 1A, and 1B, and Relatively Substantial Increases in Sections 2A, 2B, 3A, and 3B 20

Figure 3.10 Breakdown of Section 1A by 50 Ft.-Sections Comparison of Visual Crack Length in Each Section. 21

Figure 3.11 Wheel path Cracking Observed in Section 1A 23

Figure 3.12 Centerline Construction Joint Deterioration and Cracking, Section 1B 24

Figure 3.13 Fatigue Cracking in Section 1A 25

Figure 3.14 Transverse Crack in Section 1B 26

Figure 3.15 Secondary Cracking, Section 1B 27

Figure 3.16 Minor Surface Cracking Beginning Section 3 28

Figure 4.1 2008-2014 Average Back-Calculated Asphalt Pavement Resilient Moduli for Section 1 33

Figure 4.2 2008-2014 Average Back-Calculated Asphalt Pavement Resilient Moduli for Section 2 33

Figure 4.3 2008-2014 Average Back-Calculated Asphalt Pavement Resilient Moduli for Section 3 34

Figure 4.4 2008-2014 Average Back-Calculated Aggregate Base Resilient Moduli for Section 1 35

Figure 4.5 2008-2014 Average Back-Calculated Aggregate Base Resilient Moduli for Section 2 35

Figure 4.6 2008-2014 Average Back-Calculated Aggregate Base Resilient Moduli for Section 3 36

Figure 4.7 2008-2014 Average Back-Calculated Subgrade Resilient Moduli for Section 1 37

Figure 4.8 2008-2014 Average Back-Calculated Subgrade Resilient Moduli for Section 2 38

Figure 4.9 2008-2014 Average Back-Calculated Subgrade Resilient Moduli for Section 3 38

Figure 4.10 Average Daily Temperature (^{o}F) During 2010 Thaw Period 39

Figure 4.11 Asphalt Resilient Modulus, Spring 2010 40

Figure 4.12 Aggregate Base Resilient Modulus, Spring 2010 41

Figure 4.13 Subgrade Resilient Modulus, Spring 2010 42

Figure 4.14 Average Daily Temperature (°F) During 2012 Freeze Period 43

Figure 4.15 Asphalt resilient Modulus, Fall 2012 44

Figure 4.16 Aggregate Base Resilient Modulus, Fall 2012 45

Figure 4.17 Subgrade Resilient Modulus, Fall 2012 46

Figure 4.18 GPR Antenna (Yellow Object Mounted to the Front of the Van) During Data Collection on Asphalt Pavement Construction 47

Figure 4.19 3D Reconstruction at Showing the AC Thickness in the Center 5 Ft. of Eastbound Section 1A Starting at Stationing 105 to Station 115 48

Figure 4.20 3D Reconstruction at 4 Different Angles Throughout the Title Specified Section 49

Figure 4.21 3D Reconstruction at 4 Different Angles Throughout the Title Specified Section 50

Figure 4.22 3D Reconstruction at 4 Different Angles Throughout the Title Specified Section 51

Figure 4.23 3D Reconstruction at 4 Different Angles Throughout the Title Specified Section 52

Figure 4.24 3D Reconstruction at 4 Different Angles Throughout the Title Specified Section 53

Figure 4.25 3D Reconstruction at 4 Different Angles Throughout the Title Specified Section 54

Figure 4.26 3D Reconstruction at 4 Different Angles Throughout the Title Specified Section 54

Figure 4.27 3D Reconstruction at 4 Different Angles Throughout the Title Specified Section 55

Figure 4.28 3D Reconstruction at 4 Different Angles Throughout the Title Specified Section 56

Figure 4.29 3D Reconstruction at 4 Different Angles Throughout the Title Specified Section 57

Figure 4.30 3D Reconstruction at 4 Different Angles Throughout the Title Specified Section 58

Figure 4.31 Cone Penetrometer (CPT) Testing Locations 59

Figure 4.32 Cone Penetrometer (CPT) Probe and Vehicle 60

Figure 4.33 CPT Soil Type Classification Chart [5] 61

Figure 4.34 Percent Passing at Sieve Size #4 or Smaller for Class 5 (Shown in Gray), Class 5 Modified (Shown in Blue), and PAB (Shown in Orange), for Post Compaction (Indicated by Squares) and Post Failure (Indicated by Xs) 64

Executive Summary

The objective of this project was to evaluate the effect of performance graded (PG) binder type, base type, and sawed and sealed (S&S) vs non-S&S pavement sections, including an evaluation of seasonal effects on pavement and base-layer stiffness. This was accomplished through the continuation of a performance monitoring study, over a five-year period or until pavement reconstruction, of several test sections on two low-volume roads, Olmsted County Road (CR) 104 and CR 117, southwest of Rochester, Minnesota. The analyses described in this report represents findings from previous phases of the project as well as 2015 to 2019 and forensics conducted prior to reconstruction of the pavement in 2022.

The objectives were accomplished through the testing and monitoring of the original test sections. Each of the three original test sections were prepared with a different combination of base type and asphalt binder type. Three different crushed limestone base types were used in the construction: (Section 1) standard Class 5, (Section 2) permeable aggregate base (PAB), and (Section 3) Class 5 modified. Two different types of asphalt binders, PG 58-28 and PG 58-34, were incorporated to evaluate the effects of cold temperature cracking. All asphalt mixtures were designed according to MnDOT Specification 2350. In addition to the comparison among sections, each road section was constructed, both with and without transverse sawn-and-sealed regularly spaced joints, to evaluate the relative performance for ride and cracking (both spacing and crack severity) of sawing and sealing (S&S) versus allowing thermal cracking to relieve tensile stress without sawing and sealing (non-S&S).

The performance monitoring study includes the following monitoring activities: traffic counts, falling weight deflectometer (FWD), automated pavement distress surveys (Pathways), visual pavement distress surveys, and cone penetrometer (CPT) testing. In addition to some of the tests listed previously, ground penetrating radar (GPR) testing was also conducted in the final phase to learn more about the as-built asphalt layer thickness variation. Traffic count surveys were conducted to estimate the traffic volume and types of vehicles present on the test sections to determine load-related performance characteristics. The FWD testing data was used to back-calculate layer moduli and to determine seasonal, moisture, and temperature dependent in-situ stiffness. Additional detailed analysis of the FWD monitoring activities began this phase to provide further insights to the effects of time and varying temperature on the measured results. CPT testing was employed previously to acquire information about the strength of the subsurface materials. The automated and visual pavement distress surveys were used to quantify and categorize localized pavement distresses to differentiate section performance. A more controlled photo-based distress survey was introduced in this final phase to allow for a more systematic approach, which validated the findings of the more variable visual distress surveys previously conducted.

This study confirmed previous research efforts on this project, indicating that the Class 5 modified base material (Section 3) in combination with PG 58-34 binder is the best performing of the three base types and may be considered an effective substitution for conventional Class 5 crushed limestone base materials of the type commonly available in Olmsted County, Minnesota. Test Section 2, constructed with PAB base in combination with PG 58-28 binder (with similar traffic as test Section 1 consisting of

conventional Class 5) also performed well. The data from the previous study led to an addition to the MnDOT standard Specification 3138 of a new gradation category named CLASS 5Q. This study (phase 4) has clarified the results, showing a continuation of the trends observed previously. Prior to reconstruction, the severity of cracking in Section 1 was significantly higher than in Sections 2 and 3 with no severe cracking observed in Section 3. While minor cracking started to increase in Section 3 at a higher level than Section 2 prior to pavement reconstruction, it was still significantly lower than Section 1. Additionally, Section 3 showed significantly lower international roughness index (IRI) than Sections 1 and 2 through the end of measurements prior to reconstruction.

Chapter 1: Introduction

1.1 Background

Three previous 5-year research projects were completed at this site prior to this final phase: (LRRB #767); *Investigation of Flexible Pavement Performance in Relation to Aggregate Base and Asphalt Mixture Low-temp Characteristics* (LRRB #825); and *Performance Monitoring of Olmsted CR 117 and 104 and Aggregate Base Material* (LRRB #899), funded jointly by the Minnesota Local Road Research Board (LRRB) and the Minnesota Department of Transportation's (MnDOT's) Office of Materials and Road Research (OMRR). The original objectives were to evaluate the constructability and performance of three aggregate base types and two asphalt mixtures, specifically to:

- Examine the performance of larger top-size gradations of crushed limestone aggregate base types versus the control Class 5 aggregate base.
- Evaluate the properties (permeability, strength, and resilient modulus) of these material types in relation to freeze-thaw cycles.
- Evaluate the low-temperature cracking resistance of the different asphalt binders to saw-and-seal construction.

At the completion of the third study period, the test sections still had not failed. Therefore, it was determined that an additional phase would be beneficial to continue data collection for a period of time in which the deterioration process leading up to pavement reconstruction could be observed and forensic activities could be conducted. The final phase of the performance evaluation was then initiated at the original project location and followed the same general testing and monitoring protocols with more detailed distress surveys and additional evaluation of previously collected falling weight deflectometer (FWD) data, more controlled photo-based distress mapping, and ground penetrating radar subsurface evaluation.

1.2 Objective

The overall objective of this project has been to evaluate the effectiveness of PG binder and base types. This was accomplished through a follow-up performance monitoring study, over a 5-year period, then conducting forensic activities prior to reconstruction. The analyses described herein, presents the results of this follow-up study, following similar methodology. More detailed distress tracking methods were also introduced as part of this phase of the project.

1.3 Scope

The performance monitoring study included the following monitoring activities: traffic counts, FWD, automated pavement distress surveys (Pathways), and visual pavement distress surveys. The FWD testing was used to back-calculate layer moduli and to determine seasonal, moisture, and temperature dependent in-situ stiffness at various times of the year to observe the effects of temperature and time on the measured results. Traffic count surveys were conducted to estimate the traffic volume and types

of vehicles present on the test sections to determine the load-related performance of the test sections. The pavement distress surveys were used to quantify and compare localized pavement and other distresses. Previously, cone penetrometer (CPT) testing was also employed to acquire information about the strength of the subsurface materials. Local agencies near this project were previously surveyed to acquire information about current practices for the use of crushed limestone base materials. Relevant activities were continued during the initial 5 years of phase 4 of the project, followed by forensic activities after pavement failure prior to reconstruction. Additional FWD analysis and GPR data collection and analysis were also conducted during this phase.

Chapter 2: Project Analysis

2.1 Site and Research Platform Description

The objectives of this project were accomplished through the testing and monitoring of six test sections on two low-volume roads, Olmsted County Road (CR) 104 and CR 117, located southwest of Rochester, Minnesota (see Figures 2.1 and 2.2).

Figure 2.1 Olmsted County, MN Research Site Location

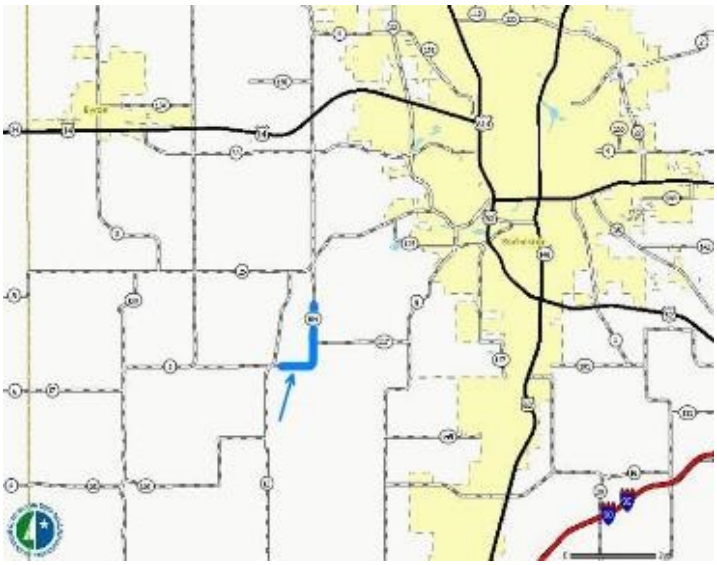

Figure 2.2 Olmsted County Roads 104 & 117 – Research Site Location

Three test sections were developed, each with a different combination of base type and asphalt binder type (see Table 2.1 and Figure 2.3). The sections were constructed as part of the reconstruction effort of two low volume roads. A top layer of different crushed limestone base types was added over an in-place crushed limestone Class 5 road base; Section 1 had Class 5, Section 2 had Permeable Aggregate Base (PAB), and Section 3 had Class 5 modified. The control section (Section 1) had only Class 5 base and consisted of 152 mm (6 in) of conventional Class 5 over 152 mm (6 in) of in-place Class 5. The PAB section (Section 2) consisted of 76 mm (3 in) of Class 5 modified (as a paving platform) over 152 mm (6 in) of PAB over 152 mm (6 in) of conventional Class 5. The Class 5 modified section consisted of 152 mm (6 in) of Class 5 modified over 154 mm (6 in) of conventional Class 5. Each test section was further divided in the S&S and non-S&S.

Table 2.1 Test sections for Olmsted County Research Project

Test section	County Road	Station	Asphalt Binder	Asphalt Thickness, mm (in)	Saw-and-Seal	Base Type	Thickness, mm (in)	Length, m (ft)
1a (S&S)	117	105+00 to 115+00	2350 (58-28)	152 (6)	Yes	CL 5	305 (12)	305 (1000)
1b	117	120+00 to 125+00	2350 (58-28)	152 (6)	No	CL 5	305 (12)	152 (500)
2a	117	153+00 to 158+00	2350 (58-34)	152 (6)	No	PAB	381 (15)	152 (500)
2b (S&S)	117	159+00 to 168+00	2350 (58-34)	152 (6)	Yes	PAB	381 (15)	305 (1000)
3a	104	12+00 to 20+00	2350 (58-34)	152 (6)	No	CL 5 mod.	305 (12)	244 (800)
3b (S&S)	104	30+00 to 40+00	2350 (58-34)	152 (6)	Yes	CL 5 mod.	305 (12)	305 (1000)

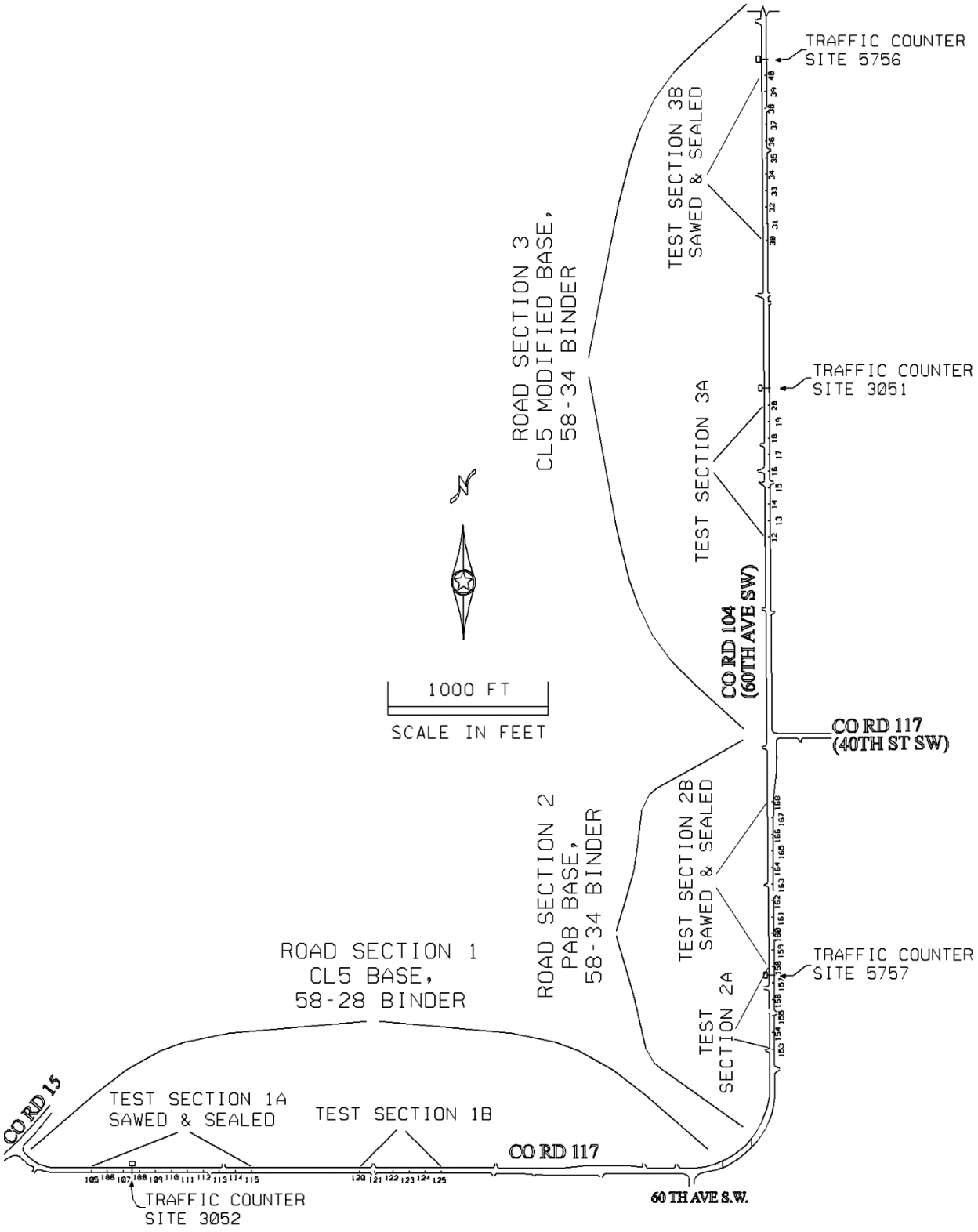

Figure 2.3 Test Section Map for Olmsted County Research Project

Two different types of performance graded asphalt binders, PG 58-28 and PG 58-34, were used to evaluate the effects of cold temperature cracking. At the time of construction, both binders were commonly used in the wearing courses of low-volume roads in Minnesota. The PG 58-34 is a polymer modified binder which is more expensive than the PG 58-28 but offers better cold weather cracking resistance. The three road sections each contained both sawed and sealed and non-sawed and sealed pavement test subsections, where the pavement was allowed to crack. The non-sawed-and-sealed subsections were 1b, 2a, and 3a. This was done to assess the relative performance for ride and cracking (both spacing and crack deterioration) of sawing and sealing versus allowing thermal cracking to relieve tensile stresses.

Another goal of this research was to examine the performance of larger top-size gradations of crushed limestone. The primary grading aggregate available in the studied region of Minnesota is crushed limestone of the type used on this project. Attempting to crush the limestone materials down to a conventional Class 5 often results in excessive fine particles, which are not easy to remedy. The resulting material often fails to meet specifications and suffers from performance loss; particularly in spring (wet) conditions. Handling and compaction of this material is also known to cause additional particle size degradation. Therefore, post-compaction gradation tests were performed to quantify that effect. Reduced performance due to excessive initial fine material and particle degradation, along with the difficulty (expense) of meeting Class 5 specifications with the crushed limestone materials, were reasons for comparing the conventional Class 5 in road Section 1, and larger top-size (less crushed) aggregates installed in road Sections 2 and 3. Additionally, a follow-up gradation after failure was conducted to assess any changes in gradation after service life.

The three different test sections were constructed with three base gradations; a summary of the pre- and post-compaction gradation as well as post-failure results is shown in table 2.2. The conventional Class 5 aggregate base contains a very high percentage of material passing the 0.075 mm (#200) sieve and did not meet MnDOT's specification for Class 5 (10 percent maximum fines) even prior to compaction. The Class 5M (modified) base material used in this project is a custom gradation specification that has a higher nominal top size (2") than a standard Class 5. The reduced crushing necessary for production resulted in a material that would meet the standard MnDOT Class 5 specification limits for material passing the 0.075 mm (#200) sieve; 8.9%. The permeable aggregate base (PAB) is also a custom gradation that has an even higher nominal top size (3"), contains very little material passing the 4.7 mm (#4) sieve, and is very permeable. Additional analysis of the gradation after pavement failure is given in section 4.4, "Base Layer Forensic Analysis" of this report.

Table 2.2 Aggregate Base Gradations

Sieve Size (in) *Cl5 Spec	Class 5		Class 5M		PAB	
	Pre	Post	Pre	Post	Pre	Post
3					100.0	
2 1/2					97.3	
2			100.0	100.0	84.7	100.0
1 1/2				100.0		100.0
1 1/4				99.4		52.0
1 100	100.0		90.4	95.3	37.0	37.5
3/4 90-100	100.0	100.0	77.0	86.9	23.3	23.0
5/8		98.5		77.1		15.0
1/2		90.4		66.7		10.5
3/8 50-90	77.9	79.5	47.9	57.7	8.7	8.0
#4 35-80	51.3	56.2	31.0	41.5	4.8	5.5
#8		38.5		30.8		4.5
#10 20-65	31.8	36.0	21.5	28.8		4.0
#16		28.2		23.7		3.5
#30		22.6		19.4		3.0
#40 10-35	18.0	20.8	12.9	17.7		3.0
#50		19.5		16.6		3.0
#140		17.5		14.6		2.5
#200 3-10	12.0	14.7	8.9	12.3		2.3

Figures 2.4 and 2.5 show the roadway at station 105 in 2002 soon after construction, and again in fall of 2014. Figure 2.6 shows the as-built cross sections of the different test sections on this project.

Figure 2.4 Olmsted County Road 117 (Station 105+00) 03/27/2002

Figure 2.5 Olmsted County Road 117 (Station 105+00) 11/25/2014

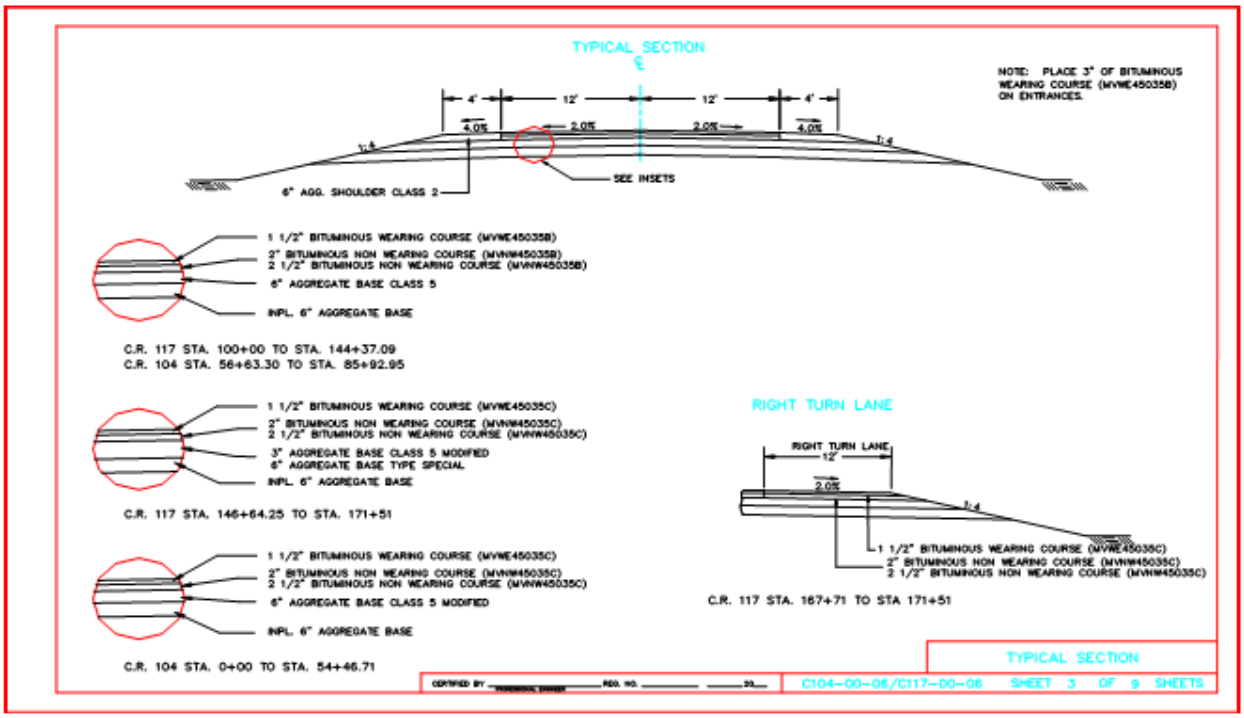

Figure 2.6 Typical Sections on Olmsted County Research Project

Chapter 3: Performance Monitoring and Traffic Analysis

To evaluate the performance of each of the test sections, MnDOT compiled and analyzed Traffic Counts, Automated Pavement Distress, and Visual Pavement Distress. Data from previous years was included when available. In the last phase of the project, updated pavement distress methods were introduced in the analysis of each of these testing parameters when appropriate.

3.1 Traffic

Traffic data was collected since 2002 at Section 1 (counter 3052), Section 2 (counter 5757), and Section 3 (counter 3051 and 5756) with locations indicated on Figure 2.3 in Chapter 2 previously. Figure 3.1 shows the traffic trends for all 3 of the studied sections over the years as characterized by AADT. It can be observed that Sections 1 and 2 experienced similar levels of traffic that remained relatively consistent. It can also be observed that Section 3 experienced an increase in traffic levels before leveling off at 3 to 4 times larger in magnitude than Sections 1 and 2 toward the end of the project.

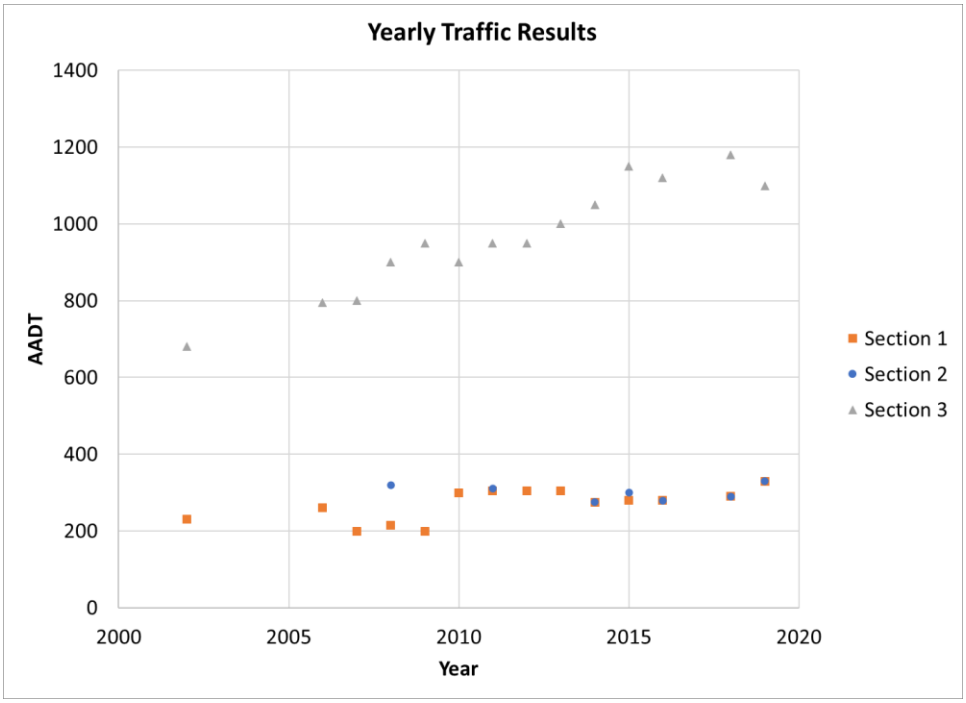

Figure 3.1 Traffic Count History on Olmsted County Research Project by Section Updated with Most Recent Measurements

Figure 3.2 shows results accounting for heavy trucks using an HCADT measure. Initially, there was not a large difference in loading between the two different ends of Section 3; however, there was an uptick in heavy vehicles in Section 3a as compared to 3b (HCADT = 140 vs 58) observed in 2015. Section 2 continued to have a higher level of heavy commercial vehicles than Section 1, with Section 3 showing

the highest levels. The AADT at counter 3052 (CR 117; TS1a) was 280, with 2.5% heavy commercial vehicles, and AADT at counter 5757 (CR 117; TS2a) was 300, with 12.3% heavy commercial vehicles. On CR 104, AADT at counter 3051 (CR 104; TS3a) was 1150, with 12.2% heavy commercial vehicles, and AADT at counter 5756 (CR 104; TS3b) was also 1150, with 5.0% heavy commercial vehicles. (Figure 3.2)

The overall traffic loading was low throughout the project for the robust cross sections in-place and was not sufficient to cause rapid damage to any of the test sections. Section 1 consistently recorded the lowest overall traffic loading along with Section 2. However, Section 1 declined the most in condition and performance. Sections 2 and 3 remained in significantly better condition than Section 1, suggesting better performance despite higher traffic levels (especially Section 3). This suggests the PAB and Class 5 modified outperformed the Class 5 despite higher traffic levels.

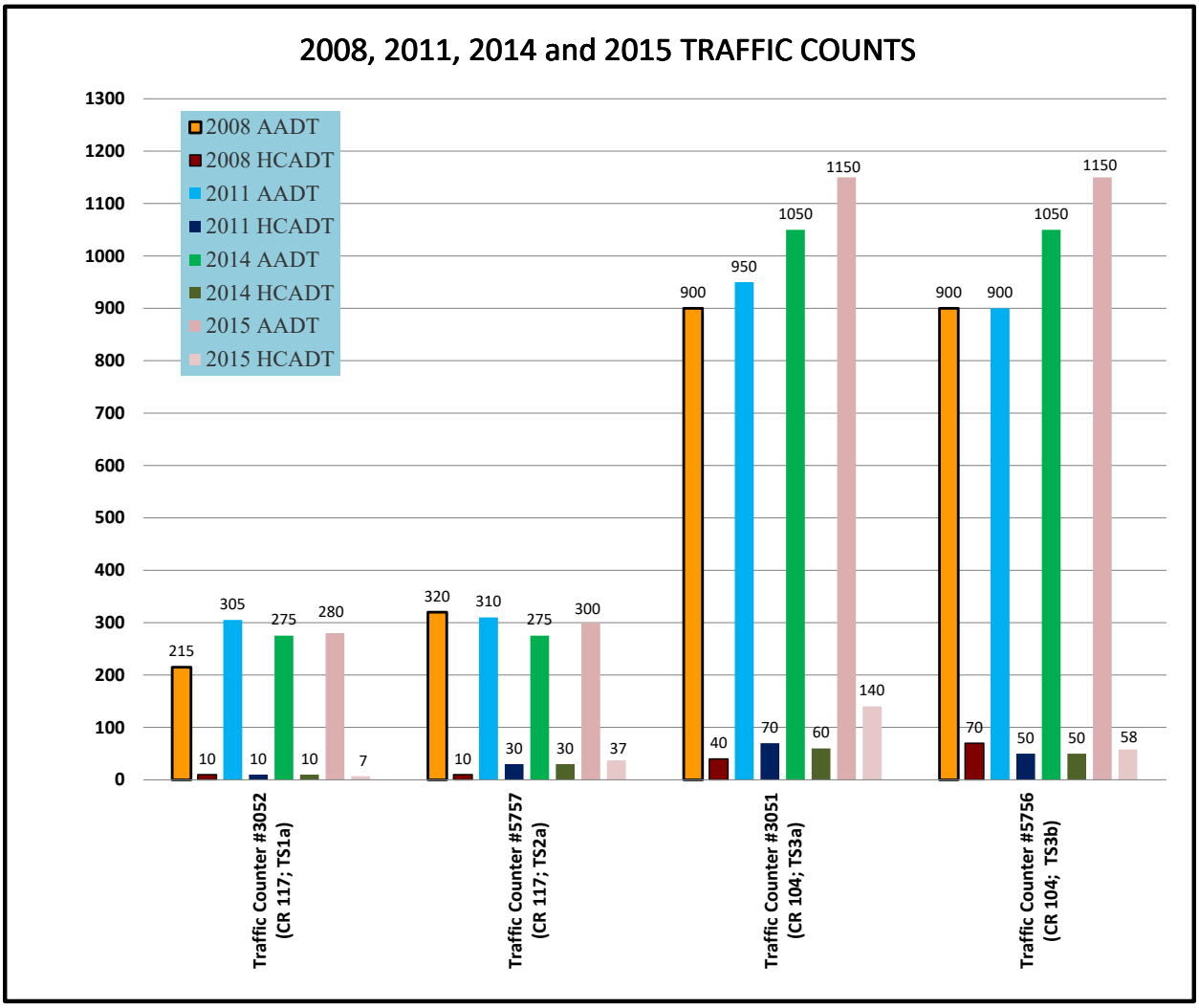

Figure 3.2 Traffic Counts Including HCADT on Olmsted County Research Project

3.2 Automated Distress Surveys

Automated distress and roughness surveys were performed on the test sections of this project using the MnDOT Pathways survey van. While updates to the hardware and software didn't always allow for direct year to year comparisons, this was a good method for evaluating general levels and trends of distress formation. While rutting was measured, the level of rutting remained very low at less than 0.25 in all sections measured until pavement reconstruction. The longitudinal and transverse cracking distresses were also recorded with the automated survey for several years, but it was found that they differed too much from those recorded in the visual surveys (which are considered more precise). This was probably due to variations in calibration of the onboard instrumentation and/or the track the Pathways vehicle takes along the roadway thus resulting changes in the observations. Another possible source of variability could be the Pathways vehicle and instrumentation being replaced at various times throughout the project. A new photo-based visual distress method was introduced in the final performance monitoring phase to combine the more detailed nature of the visual distress survey with the quantitative record-based nature of the Pathways survey. More detailed information about the visual distress accuracy is presented in the visual distress section. The analysis was modified starting in 2013 to record only ride and rutting data for both the roadway areas of different base materials, and for the six individual pavement test sections. From that point forward, cracking data was acquired and analyzed from the manual distress survey, and then adding the more controlled digital distress survey introduced at the beginning of the phase 4 in 2015. Thus, IRI was the focus of the automated distress surveys.

Figure 3.3 shows the IRI results including the last phase of the study for all three sections. While the measurements after 2014 don't suggest an appreciable change in IRI over the final years, the results are generally in line with the previously reported results in the sense that a significant difference between roadway sections is still observed with Section 1 highest and Section 3 lowest. As will be observed in the cracking section, the 2018 increase in Section 2 IRI corresponded with more than doubled visually observed cracks. It was also noted in that section that the overall level of cracking was still low. In addition to showing the lowest overall roughness throughout the project, Section 3 also showed the lowest rate of increase in IRI at 0.058 IRI increase per year, versus 0.091, and 0.097 increases for Sections 2 and 3, respectively.

As will be described more in Chapter 4, test Section 1 has also typically shown the lowest base and subgrade modulus; probably impacting ride quality and contributing to cracking. Test Section 2 was typically mid-range in both ride quality and in base/subgrade modulus, again suggesting some relationship between the two. Test Section 3 showed the best ride characteristics, and that may have been influenced by the higher modulus of the CL-5M base and subgrade. The CPT testing results summarized in Chapter 4 also supports these conclusions. Based on the analysis of all the Pathways data, test Section 3 (Class 5 modified, PG58-34) appears to be the best overall performing test section on this project, despite regularly experiencing significantly higher traffic loading. Test Section 2 (PAB, PG58-34) has a slightly higher roughness increase than test Section 3 but also performed significantly better than test Section 1. The forensics in Chapter 4 also confirmed that the gradation differences persisted through the end of the pavement life, suggesting the larger rock size and less fine particles contributed to the better ride performance.

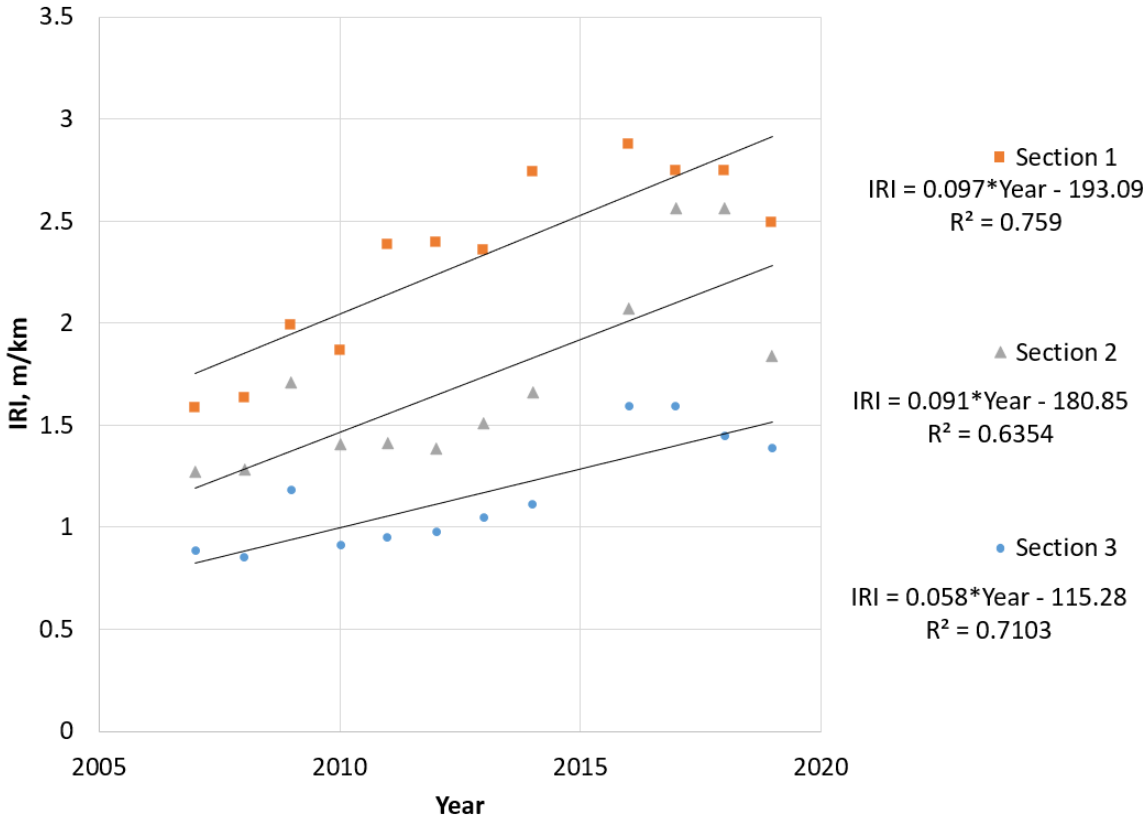

Figure 3.3 IRI Results for Each Section through Reconstruction

The data from 2010 through 2016 showed the most consistent pattern, so was further broken down for S&S vs non-S&S analysis, as shown in Figure 3.4. It can be observed that the non-S&S performed better than S&S in all sections. Section 1a (S&S) was rougher than 1b (non-S&S) and the two had the highest rate of roughness increase. Test Section 2b (S&S) showed higher roughness than 2a (non-S&S); and test Section 3b(S&S) showed higher roughness than 3a (non-S&S). Although not measured, it has been observed that on both Co Roads 117 and 104 the ride felt rough during winter periods due to expansion at the sawn joints, and then improved during the summer. Seasonal deformation of the sawn and sealed joints has also been observed elsewhere, leading to less use of S&S in Minnesota. The results of this study suggest non-S&S is better performing for ride than S&S.

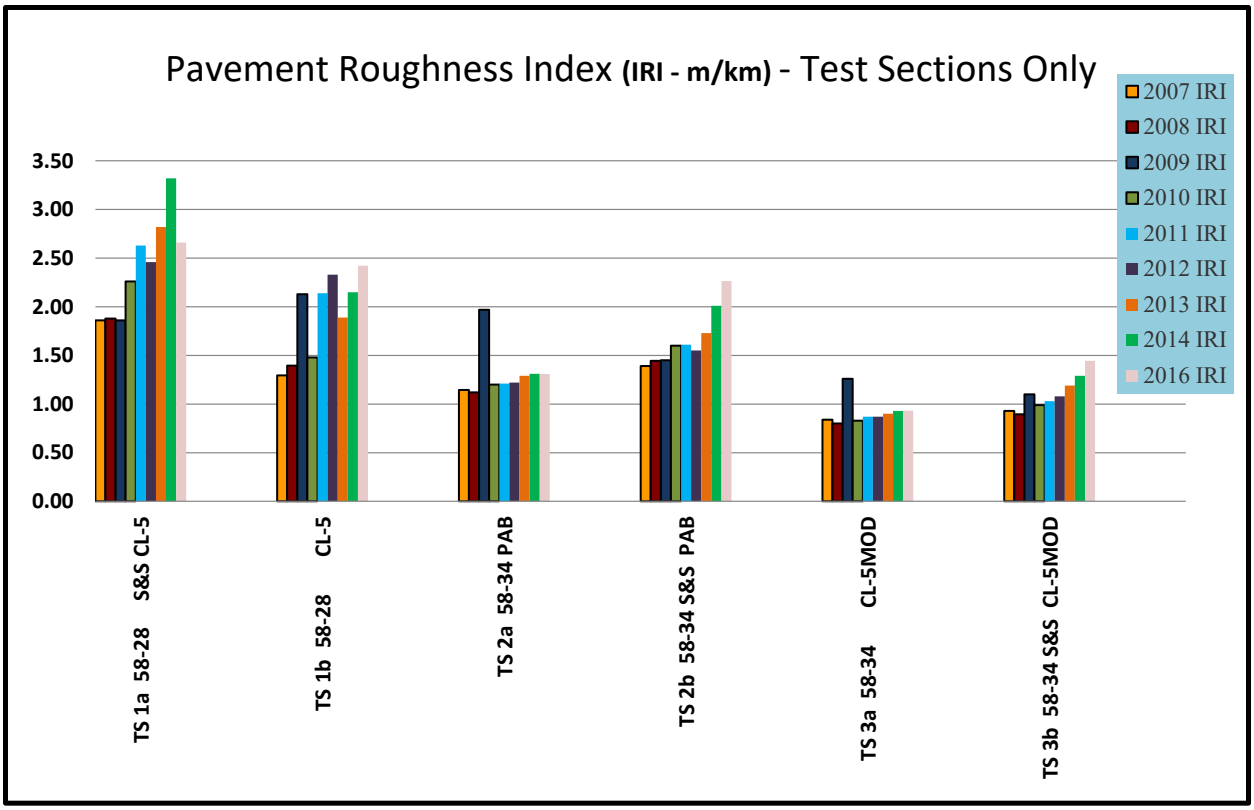

Figure 3.4 2007-2016 Pavement Roughness Index – Test Sections Only

3.3 Visual Distress Surveys

To carefully evaluate the relative differences of the test sections, visual (non-automated) pavement distress surveys were generally conducted annually on the project since 2008 through the initial 5-year period of the final phase. Although previous distress surveys have ranged in precision, an additional visual distress survey was conducted in 2015 then tied into the previous distress surveys as shown in Table 3.1 and Figure 3.5. However, it should be noted that the 2015 distress survey was conducted by new personnel which likely influenced the continuity of the distress map. Regardless, the visual distress surveys were able to track general trends, especially overall crack lengths.

Deterioration cracking (longitudinal and transverse) observed in all three road sections continued to grow in 2015. The survey showed that cracking in test Section 1a consisted in approximately 1028 feet of cracking. Section 1b had 997 feet of cracking, while Sections 2a, 2b, and 3b each had less than 200 feet of cracking. Section 1b had the largest increase in cracking by percentage and magnitude, moving from 535 ft in 2014 to 997 ft. of cracking in 2015. It should be noted that the visual distress survey method had a significant amount of uncertainty that was likely influenced by a change in personnel conducting the distress map in 2015. The more controlled photo-based method was not included for comparison with previous years since some of the increases from 2014 to 2015 could be an effect of moving to a more detailed photo-based system that counts some cracks missed occasionally by traditional visual surveys discussed earlier. The photo-based was used for comparison of the tail end of

the service life, while the visual is presented in Figure 3.5 to put it into context for historical comparisons and crack progression analysis.

Table 3.1 2015 Visual distress survey data summary for Test Sections

Date/ Section	2008	2009	2010	2011	2012	2013	2014	2015
Section 1a	0	0	0	100	150	228	948	1028
Section 1b	85	133	100.5	177	230	309	535	997
Section 2a	0	0	0	0	0	0	72	47
Section 2b	0	0	0	0	0	0	10	6
Section 3a	0	0	0	0	0	0	68	68
Section 3b	0	0	0	0	25	37	88	3

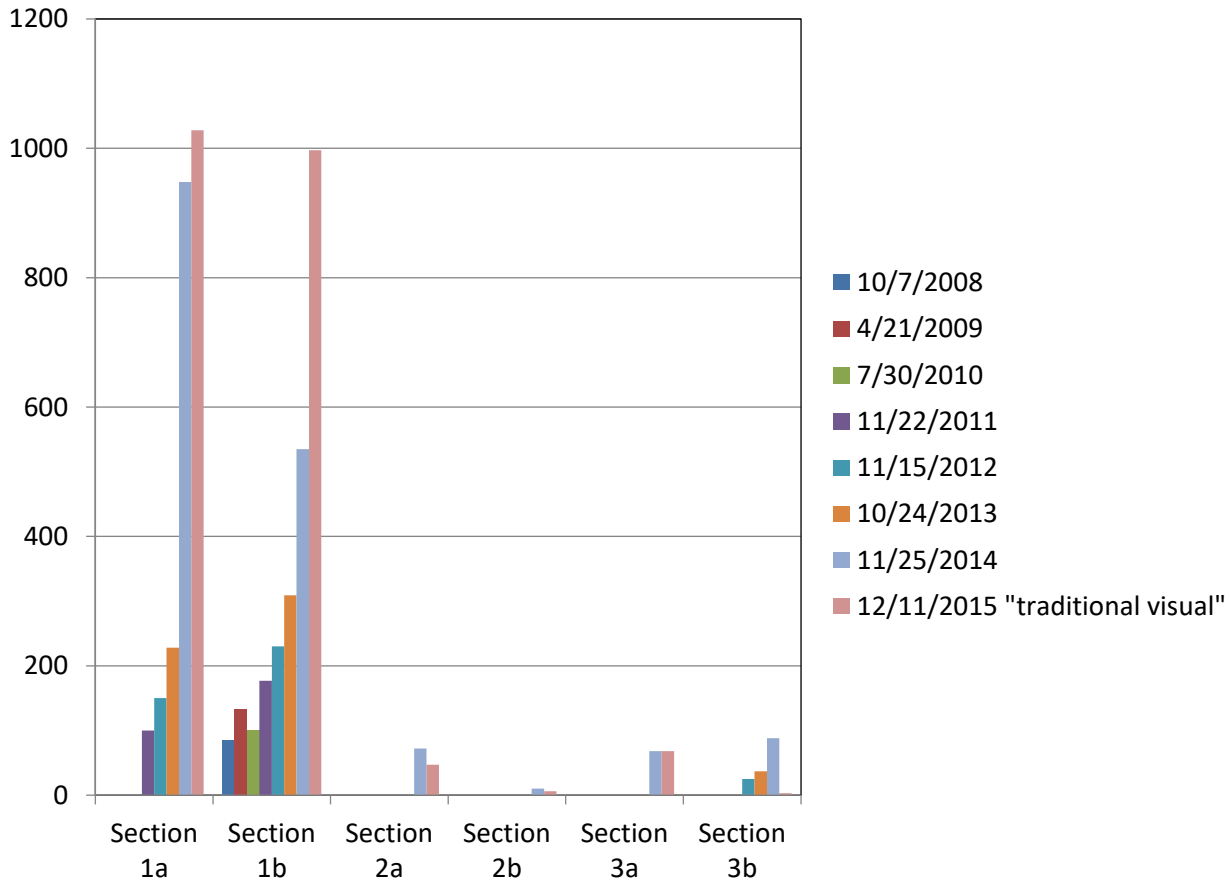

Figure 3.5 2008-2015 Approximate Cracking Length Observed by Visual Surveys

Since the progression of distress is more critical as the pavement fails, a more detailed approach was introduced in 2015 as part of the last phase of the study to verify the previous trends. This included use of photo-based visual distress identification in comparison with the traditional visual distress survey. Figure 3.5 shows a comparison of 2015 total cracking measurements of the same sections using the traditional visual and photo-based approaches in blue and red, respectively. It can be observed that, while the major trends are similar, the photo-based approach recorded a larger amount of cracking than the visual-based approach. To investigate the cause of the discrepancies, a comparison of both methods at specific 50 ft. locations, where the photo-based method identified significantly more cracking than the visual based approach, were evaluated. The photographs indicated that the larger cracking distance identified by the photo-based approach generally were caused by missed (false negative) locations using the visual-based approach. In a high percentage of the cases, distress that is visible in the photos was not represented in the corresponding visual distress survey. Figure 3.6 shows an example type of distress, superimposed on top of the chart that visual distress mapping occasionally did not mark.

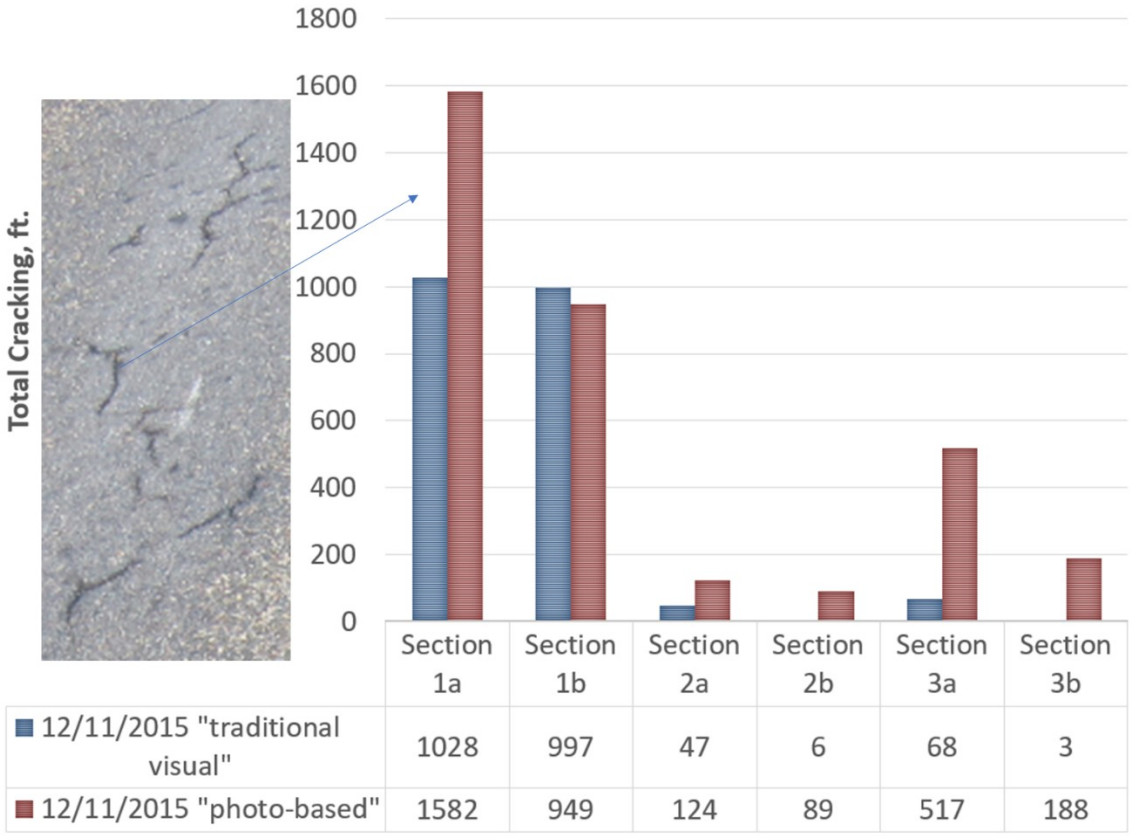

Figure 3.6 Photo-Based Versus Traditional Cracking Measurements for the Multiple Sections

Additionally, the photo-based method has the advantage of a recorded and catalogued analysis that can be re-evaluated for precision at later dates, unlike the traditional visual survey which cannot be re-evaluated since the pavement will be in a different condition by the time re-evaluation occurs. The photo-based approach is also less subjective to the user. Since, as will be shown below, the photo-based output is interactive in that the analysis used to create the current map can be evaluated by any user if they click on the photo corresponding to the area of interest. Based on the convenience, apparent higher accuracy, and more detailed records it provides, the photo-based method was used in phase 4 primarily to assess distress, while the visual map was used for historical comparison with previous data.

The output format of the photo-based distress map was similar to the past visual surveys where 50 ft. sections are broken into 12' X 10' subsections showing distress in both lanes. Figure 3.7 shows an example 50 ft.-section in Section 1A from 105+00 to 105+50. While the figure shown here is only a screenshot, the actual maps with corresponding linked photos were catalogued for access to all the 50 ft. subsections within Sections 1, 2, and 3. An example 10 ft. by 12 ft. photo-based distress mapping result from Section 1A 105+20 to 105+30 is shown in Figure 3.8. The black arrow shows the link used to pop up a photo corresponding to the mapped subsection. Transparent green boxes show the mapped area and corresponding photo.

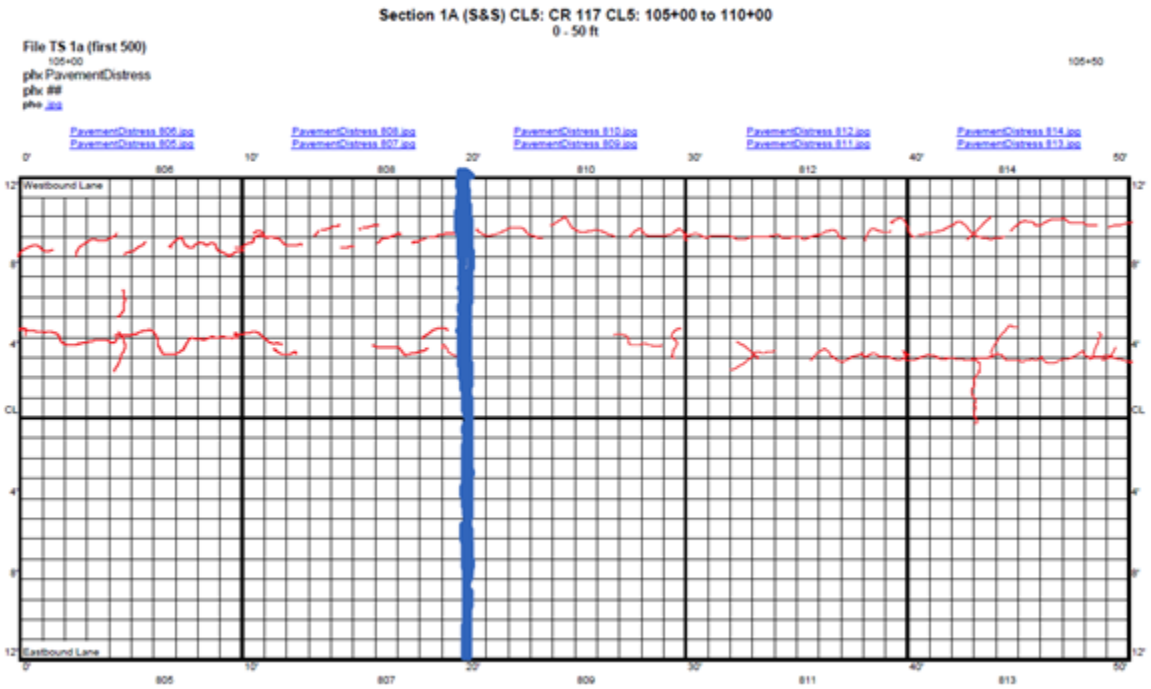

Figure 3.7 Example Photo-Based Distress Mapping Result from Section 1A 105+00 to 105+50

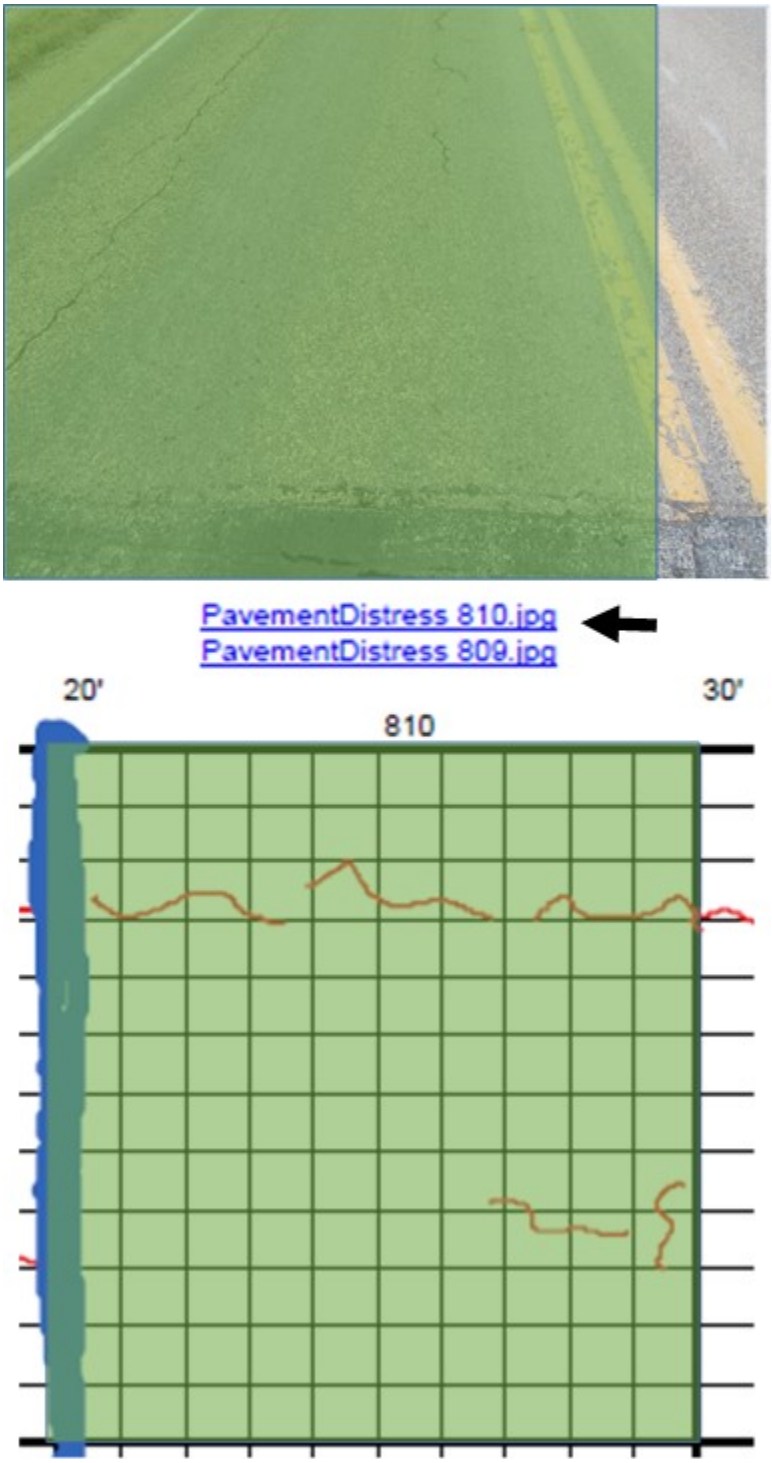

Figure 3.8 Example 10 Ft. by 12 Ft. Photo-Based Distress Mapping Result from Section 1A 105+00 to 105+30, Where the Transparent Green Box Shows the Mapped Area and Corresponding Photo

The cracking continued to show an increase leading up to failure and pavement reconstruction. Figures 3.9 and 3.10 summarize the general increase in each section as well as a more precise breakdown of the increase in Section 1A (which exhibited the most overall cracking) in the last 2 years of distress mapping.

Figure 3.9 compares crack length in each section as of the final data as compared to the previous distress collected 2018. Figure 3.10 further breaks down the section with the most cracking (Section 1A) into 50 ft-sections. It can be observed that while Section 1 still experienced increased cracking and exhibited the most cracking overall, Section 2b, and all of Section 3 showed the most significant increase in cracking toward the end of the pavement service life. The overall cracking was greatly increased as would be expected as the pavement was nearing reconstruction.

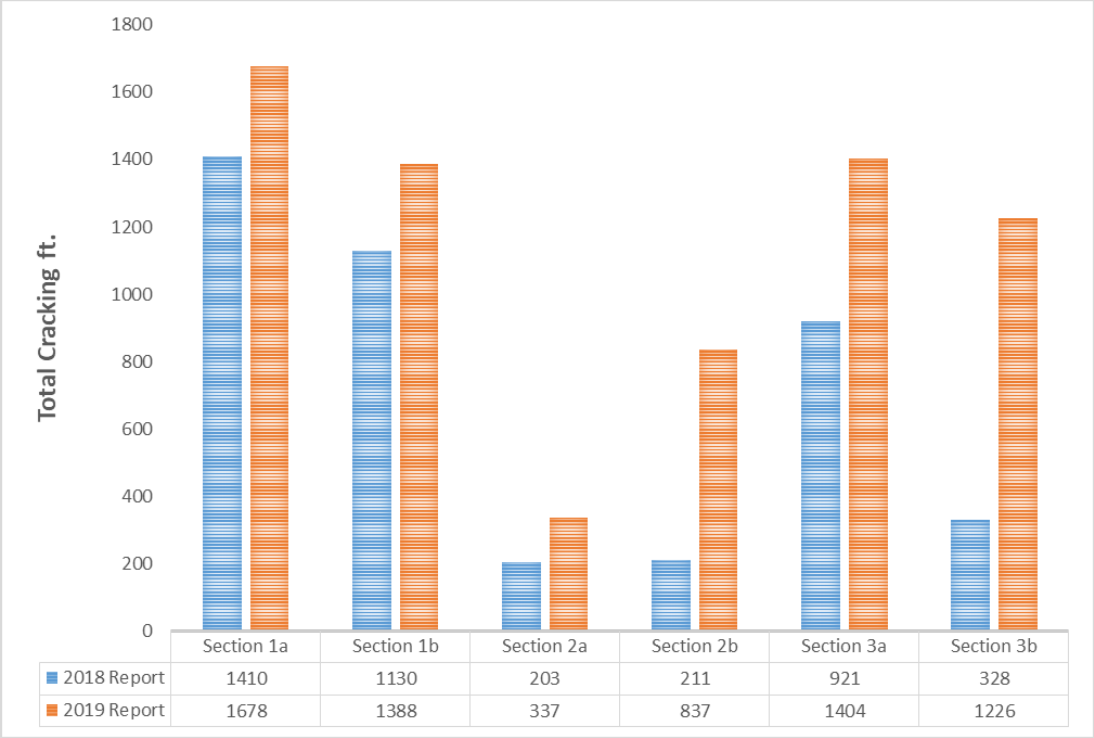

Figure 3.9 Comparison of Visual Crack Length in Each Section Showing Minimal Distress Increases in Sections 1A, and 1B, and Relatively Substantial Increases in Sections 2A, 2B, 3A, and 3B

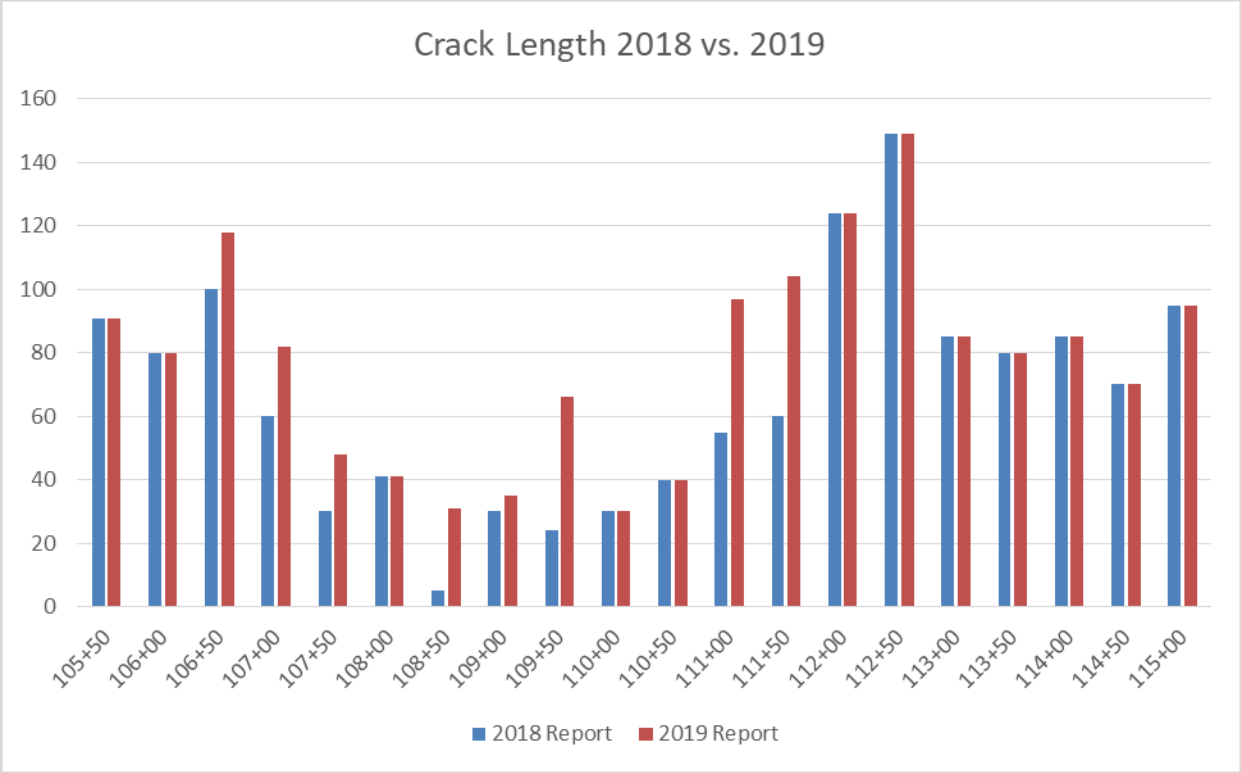

Figure 3.10 Breakdown of Section 1A by 50 Ft.-Sections Comparison of Visual Crack Length in Each Section.

Distresses reported previously and continuing in the last phase, included seasonal expansion of the sawn joints resulting in intensified scuffing directly adjacent to them between the wheel paths, minor surface wear, turning movement distress of the chip seal and minor influence cracking, missing chip seal in a couple locations, separation of the longitudinal construction joint, moderate sealant deterioration, edge cracking, and medium severity deterioration.

A representative assortment of photographs taken during the photo-based survey of significant distresses and cracking are described and shown in this section, updating the pictures taken during the second to last phase of the project. Test Sections 1a and 1b showed an abrupt increase in cracking in 2014, which continued in this phase of the project, including longitudinal cracking in the wheel paths (Figure 3.11), and along the centerline (Figure 3.12). The longitudinal cracking is in places interconnected with transverse cracks, indicating the mechanism of fatigue (alligator) cracking is continuing (Figure 3.13). Much of the cracking in Section 1 continued to progress in severity and appeared worse in the westbound lane of Sections 1a and 1b in the previous survey significantly worse in the last phase of the project.

Sealant material in the sawn joints was showing deterioration which continued until pavement reconstruction. Multiple thermal cracks in test Section 1b progressed to cross the entire roadway and appeared to have movement and width to accelerate the sealant deterioration. Although most cracking in Section1a was low-to-medium severity prior to the last phase, several cracks approached high severity (see figure 3.14) as the pavement approached the end of service life. In Section 1b, a significant number

of cracks widened and deteriorated to the point of high severity. Some secondary cracking occurred on the inside edges of the cracks and at the pavement edges (Figure 3.15). Very minor surface cracking was visible in the middle of the lane in Sections 2 and 3 in small areas. This appeared to be shrinkage cracking in the surface of the chip-sealant material and was not yet extending into the pavement (Figure 3.16).

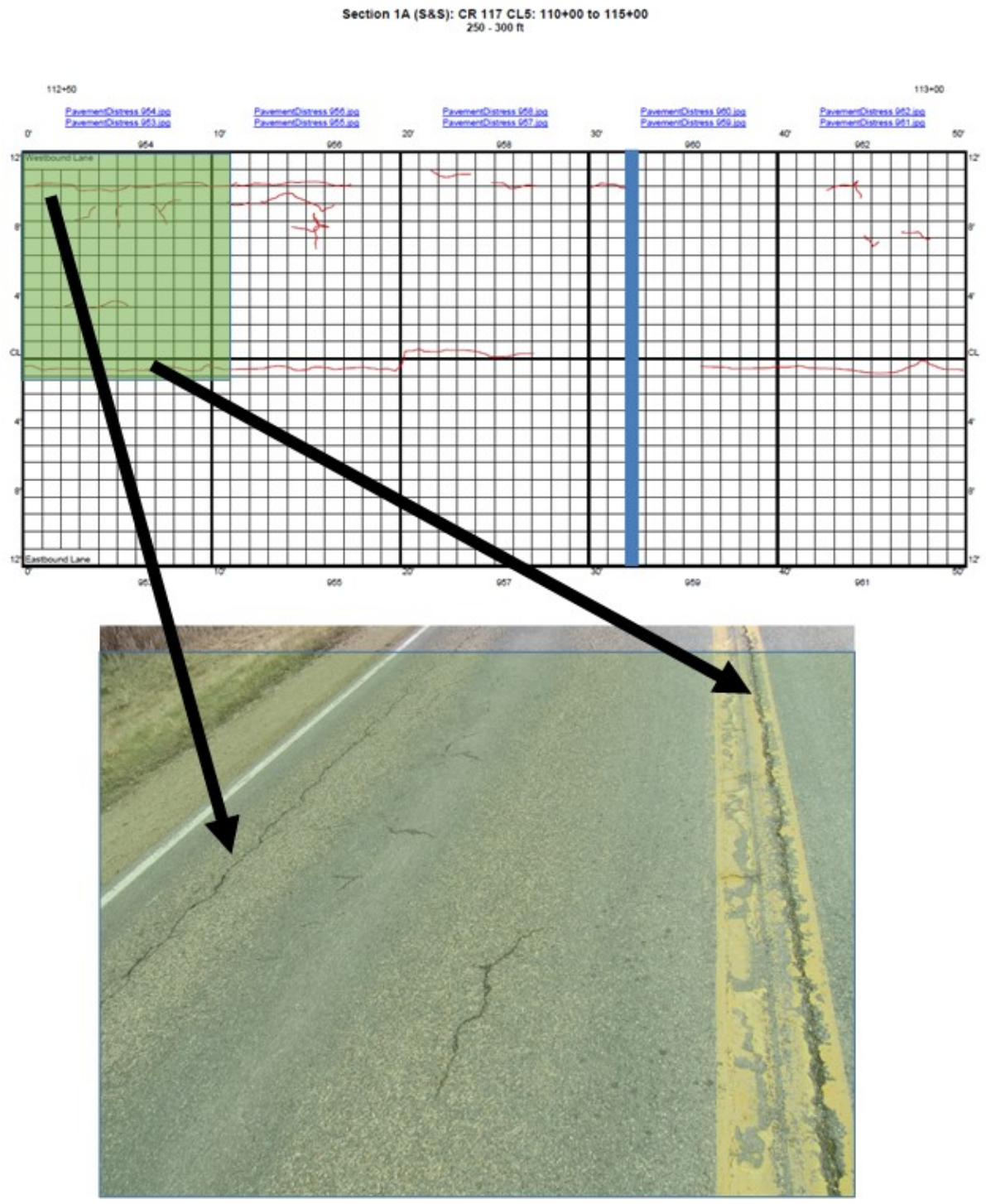

Figure 3.11 Wheel path Cracking Observed in Section 1A

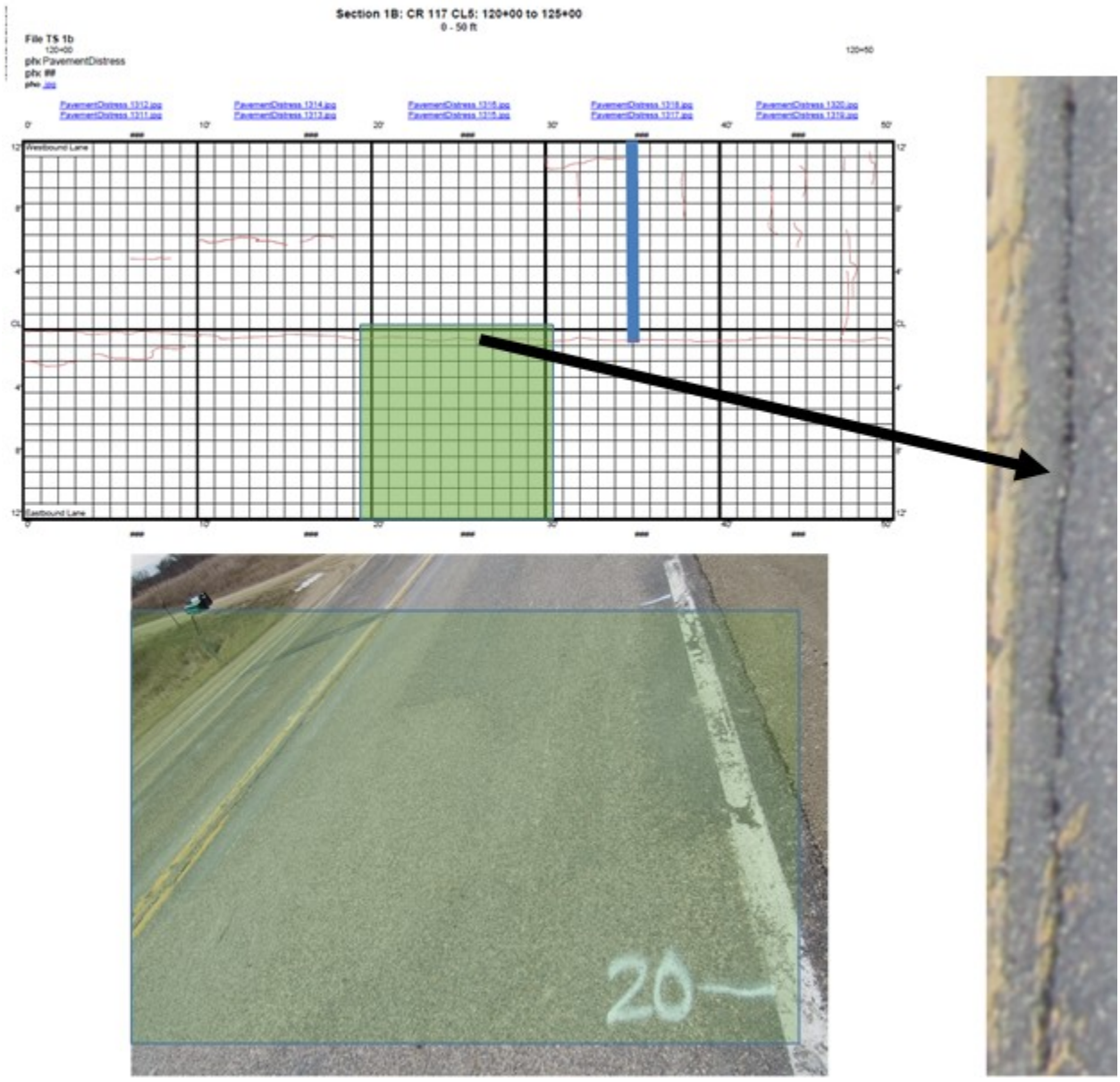

Figure 3.12 Centerline Construction Joint Deterioration and Cracking, Section 1B

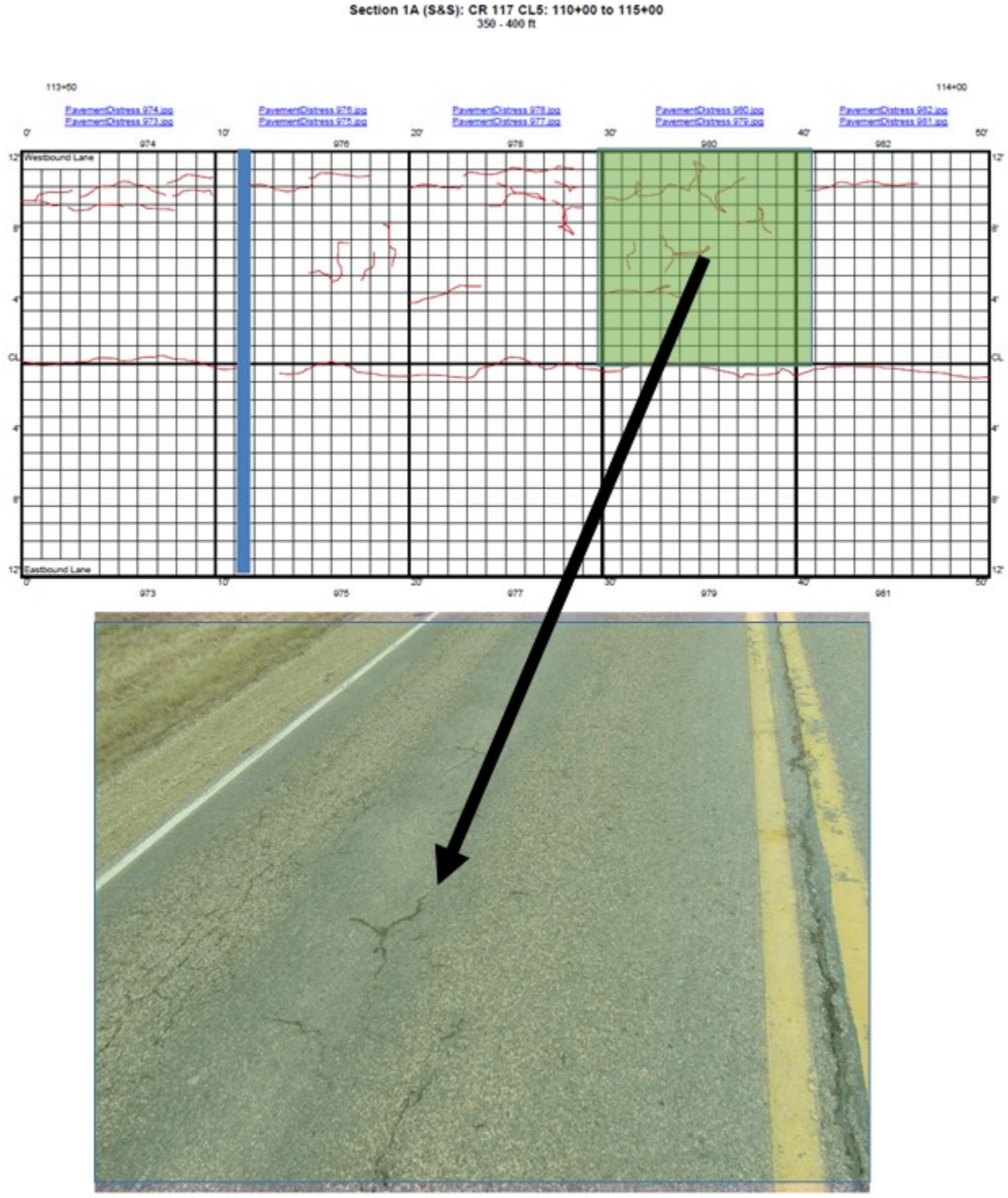

Figure 3.13 Fatigue Cracking in Section 1A

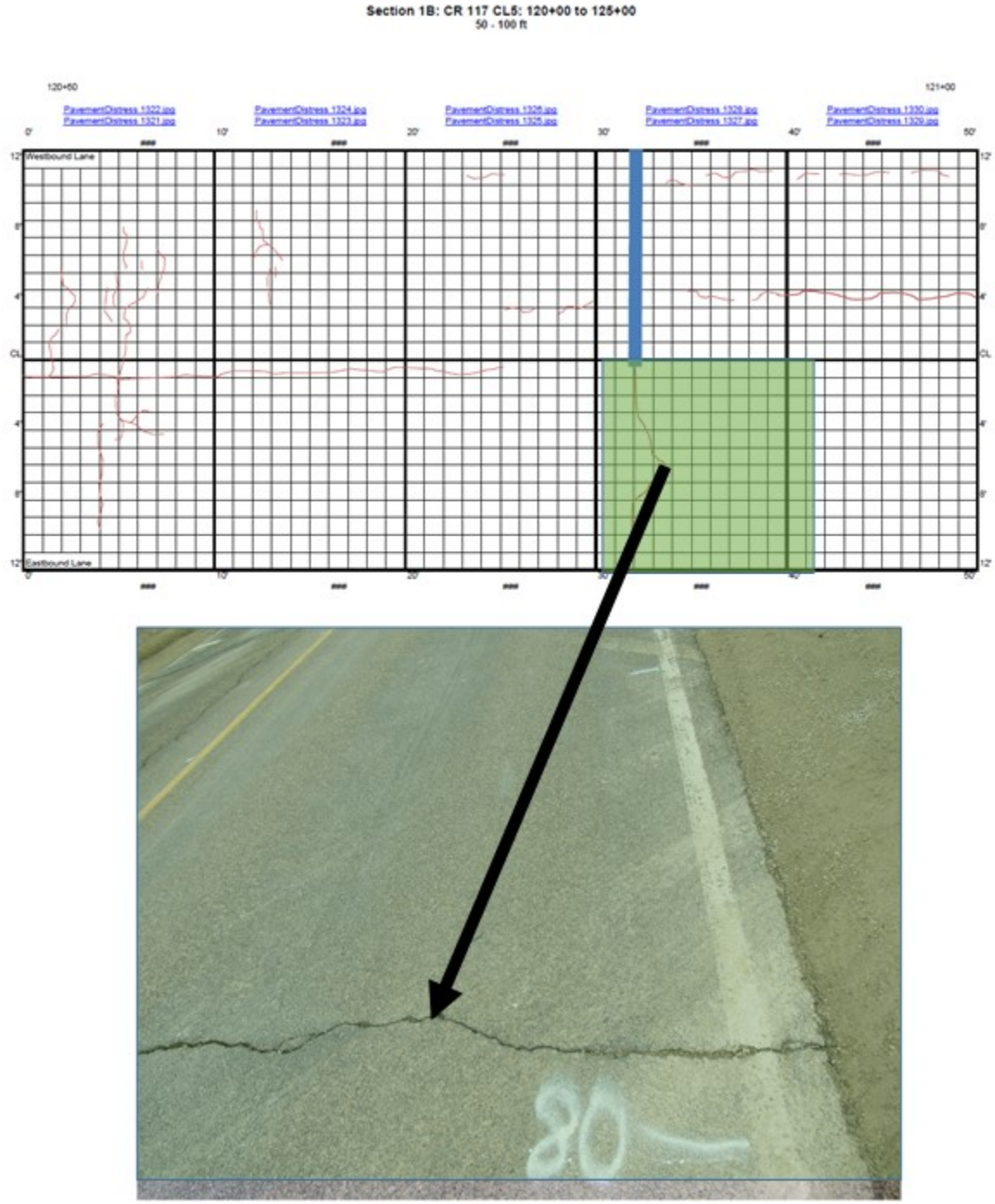

Figure 3.14 Transverse Crack in Section 1B

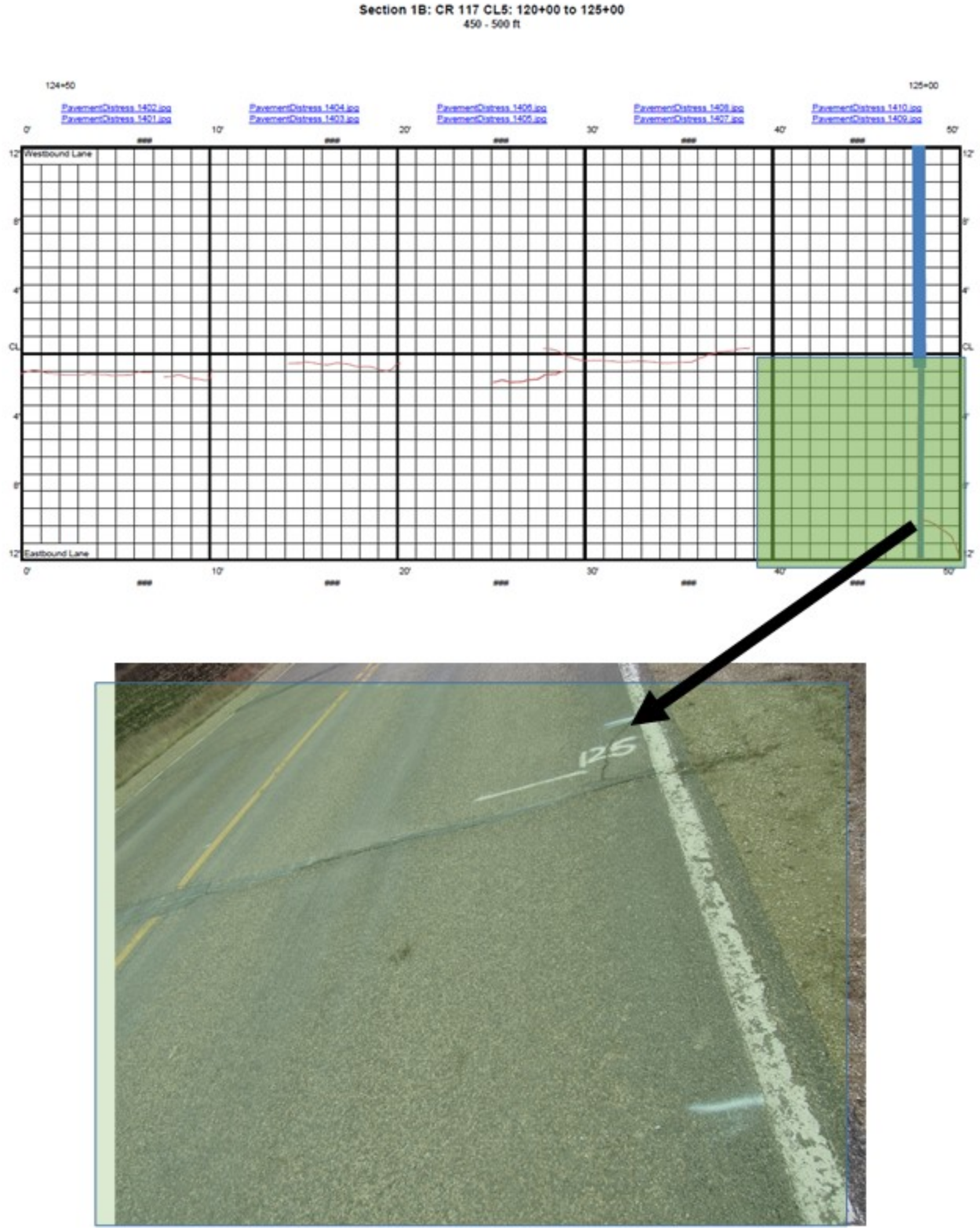

Figure 3.15 Secondary Cracking, Section 1B

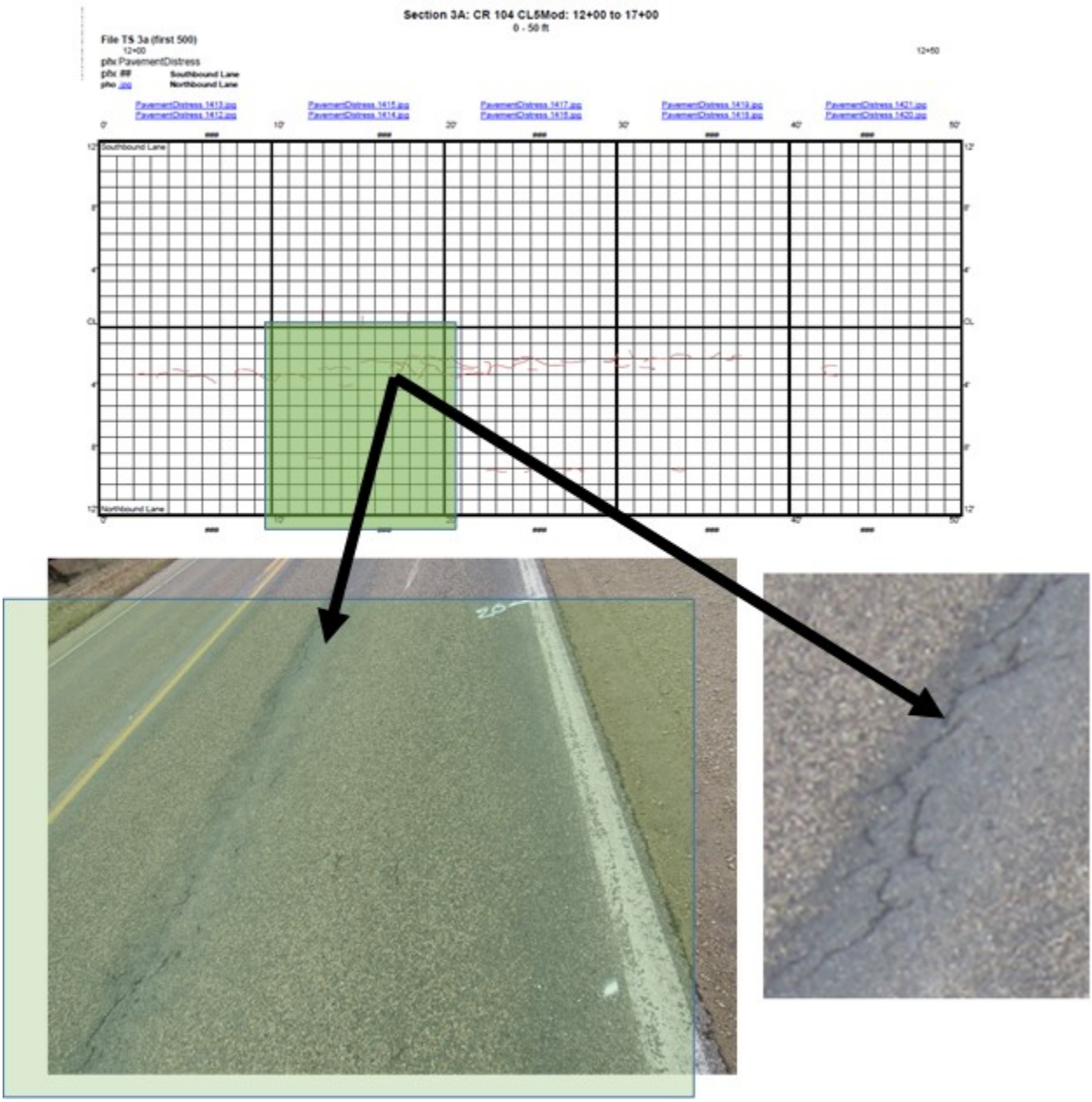

Figure 3.16 Minor Surface Cracking Beginning Section 3

Chapter 4: Project Data Analysis and Forensics

4.1 Falling Weight Deflectometer (FWD) Data Analysis

The final phase of this project adds to previous findings from Falling Weight Deflectometer (FWD) data by increasing the scope of analysis. The previous phase reported results from multiple dates within 2010, 2012, and 2014, so that now the analysis is focused on comparisons identifying year-by-year trends including multiple dates within 2008-2012, and 2014. Each year of data collection included data from just prior to the spring thaw, during spring thaw, summer, and fall.

4.1.1 FWD Major Trends

The additional analysis in the final phase of the project allowed for the calculation of layer moduli values when there were wide ranges in base and subgrade moisture, and pavement temperature. These two variables are most critical in impacting the strength of the unbound (base) and bound (asphalt) materials respectively. The summary of the three years of the back-calculated moduli values has previously been shown by comparing section vs section data analyzed using ELMOD software. The layer thicknesses from the construction plans were used. The materials stiffness through different seasons of the three years was well represented by the testing. The data from each of these years is shown in Tables 4.1 through 4.6.

Table 4.1 2008 Average Back-Calculated Resilient Moduli

Layer Resilient Moduli									
2008 Date (Mo/Day)	Test Section Number								
	1			2			3		
	Asphalt	Base	Subgrade	Asphalt	Base	Subgrade	Asphalt	Base	Subgrade
3/10	2030000	507500	134471	2030000	507500	141992	2030000	507500	144655
3/11	2030000	507500	124320	1840956	507500	121853	1861164	417337	144210
3/13	1369213	138623	93633	661884	103976	124335	1707726	374325	145000
3/14	1493832	43904	86462	694174	48093	105710	1463553	212165	145000
3/19	1644710	30774	60499	766330	26764	79656	1203851	25396	133275
3/20	1542670	25663	52899	689815	23222	66666	1102823	17130	121202
3/25	1389672	21698	46357	610685	21242	41755	795031	12358	107639
3/26	1492610	18958	35471	595040	20293	36854	920302	16135	67445
3/28	1354222	12883	28069	494803	19264	24372	806821	13406	58703
4/4	1646341	19899	14765	644651	19681	13361	881718	20204	30710
8/28	535362	23012	12704	221091	23200	25074	195103	36067	39104

Table 4.2 2009 Average Back-Calculated Resilient Moduli

Layer Resilient Moduli									
2009 Date (Mo/Day)	Test Section Number								
	1			2			3		
	Asphalt	Base	Subgrade	Asphalt	Base	Subgrade	Asphalt	Base	Subgrade
3/5	2011898	507268	141856	1615031	469739	144143	2022115	504869	144452
3/9	2021538	507042	134067	1565274	401715	131976	1998635	504017	144610
3/10	1544990	286404	125206	1354014	229626	141234	1933912	466033	144734
3/13	2024539	507500	141917	1906048	507080	141082	1968087	507500	143990
3/16	1293115	23432	122011	586768	56319	135336	1206668	165518	145000
3/18	1266829	12521	110846	506094	17538	76760	582418	14666	141833
3/19	1656125	8712	99238	833310	13456	72252	874656	15447	137380
3/20	1739081	22769	69986	1154010	13812	83056	1253584	12102	143327
3/23	1695322	16017	25576	806595	17198	24460	1423894	7185	97087
4/30	1504819	25302	15367	635482	23775	17767	1038152	22552	32544
7/9	799574	21606	13703	306825	23159	17492	374202	33730	33064
10/19	1518646	27864	17639	756843	20099	32883	1106160	31419	44477

Table 4.3 2010 Average Back-Calculated Resilient Moduli

Layer Resilient Moduli									
2010 Date (Mo/Day)	Test Section Number								
	1 (Stations 105-115 & 120-125)			2 (Stations 153-158 & 159-168)			3 (Stations 12-20 & 30-40)		
	Asphalt	Base	Subgrade	Asphalt	Base	Subgrade	Asphalt	Base	Subgrade
3/10	1620867	36254	40433	761762	33033	48340	1130868	50577	50853
3/12	1531915	19437	48341	706313	19762	51184	1032003	36335	37498
3/18	1053243	5185	42407	567665	7569	38587	791796	7398	49766
3/25	1635728	6958	28833	907220	8420	29718	1311534	9886	39124
4/7	1238109	6954	27070	665634	10582	28088	913319	12807	34581
5/24	451290	7317	28562	289321	13470	31728	257582	21549	31706
7/15	381595	5627	29555	269807	12372	33890	214115	23917	33866
8/10	399492	6542	30415	280947	15176	35471	225808	26455	36344
9/21	691801	9032	35120	393170	13933	37156	359544	27766	35821
10/13	1029897	9696	33389	559472	13334	37457	632510	27425	35858
11/19	1604533	14110	34386	848522	12501	38598	1132880	25207	35687

Table 4.4 2011 Average Back-Calculated Resilient Moduli

Layer Resilient Moduli									
2011 Date (Mo/Day)	Test Section Number								
	1 (Stations 105-115 & 120-125)			2 (Stations 153-158 & 159-168)			3 (Stations 12-20 & 30-40)		
	Asphalt	Base	Subgrade	Asphalt	Base	Subgrade	Asphalt	Base	Subgrade
3/8	1219093	193217	73472	877601	147253	77309	817579	111917	122197
3/14	2314001	118692	53320	1212130	59655	44621	1768015	131407	80795
3/16	1621207	34450	43186	584357	14766	46675	964840	35335	44197
3/30	1389494	3828	70003	780364	6684	33194	1187919	7359	44248
4/14	1280457	4354	50004	723970	8259	32534	952790	10079	36986
9/1							313266	25686	34129
9/28	554729	8402	37042	364319	13547	36389	600867	25273	35828
10/17	1397058	9819	47891	717480	12360	39247	918603	25815	36027
11/16	1896602	9888	49557	943326	13507	39331	1350195	31965	35418

Table 4.5 2012 Average Back-Calculated Resilient Moduli

Layer Resilient Moduli									
2012 Date (Mo/Day)	Test Section Number								
	1 (Stations 105-115 & 120-125)			2 (Stations 153-158 & 159-168)			3 (Stations 12-20 & 30-40)		
	Asphalt	Base	Subgrade	Asphalt	Base	Subgrade	Asphalt	Base	Subgrade
2/15	2228920	256812	54151	776970	210387	66080	1074349	492330	78724
4/5							377510	19768	33849
6/21	449041	6123	32991	261150	13700	33535	229290	19545	35688
8/31	275036	26203	9058	218665	27380	15482	187473	25893	35338
11/13	1803407	26483	10451	993064	11652	31313	1263057	23114	40193
11/20	1304152	15971	53686	844764	12707	40115	1043089	25474	35107
11/29	1743582	14706	45108	806357	11389	41758	1215119	36126	34686
12/17	1970446	13286	47180	1087914	13903	40496	1215119	36126	34686

Table 4.6 2014 Average Back-Calculated Resilient Moduli

Layer Resilient Moduli									
2014 Date (Mo/Day)	Test Section Number								
	1 (Stations 105-115 & 120-125)			2 (Stations 153-158 & 159-168)			3 (Stations 12-20 & 30-40)		
	Asphalt	Base	Subgrade	Asphalt	Base	Subgrade	Asphalt	Base	Subgrade
3/30	1393095	11321	65329	673243	12810	69469	1113749	33545	50484
4/22	984009	3751	42286	426147	10285	27330	562587	11491	35102
5/9	1125704	6263	26920	534889	11073	28782	677310	15557	33603
5/30	274914	5888	24642	171734	15780	28390	142084	20043	32079
6/26	252013	8718	27227	193848	14171	31662	171959	19879	32695
8/9	418350	7645	28592	235143	15996	33275	188189	29636	35860

In this final phase of the study, analysis was expanded to show that the average resilient modulus of the asphalt containing the PG 58-28 binder (Test Section 1) remains stiffer throughout the year than the asphalt containing the PG 58-34 binder (Test Sections 2 and 3). Figures 4.1 through 4.3 show the average resilient modulus of the asphalt year-by-year for Section 1, Section 2, and Section 3 respectively. It can be observed that the same general trend of stiffness for different pavement surface temperatures associated with different times of the year can be observed regardless of the year. Also, the higher pavement stiffness in Section 1 observed yearly with a concentration of data at and above 1500 ksi in the winter is likely contributing to the increased thermal cracking in the un-sawn test section. Sections 2 and 3 saw limited stiffness measurements approaching that level. Section 2 only saw this level in 2008/2009, while Section 3 only reached that average level in 2008/2009 and one date of testing in 2011. This confirms previous findings recommending polymer modified (lower temperature rated) asphalt binders in cold weather applications.

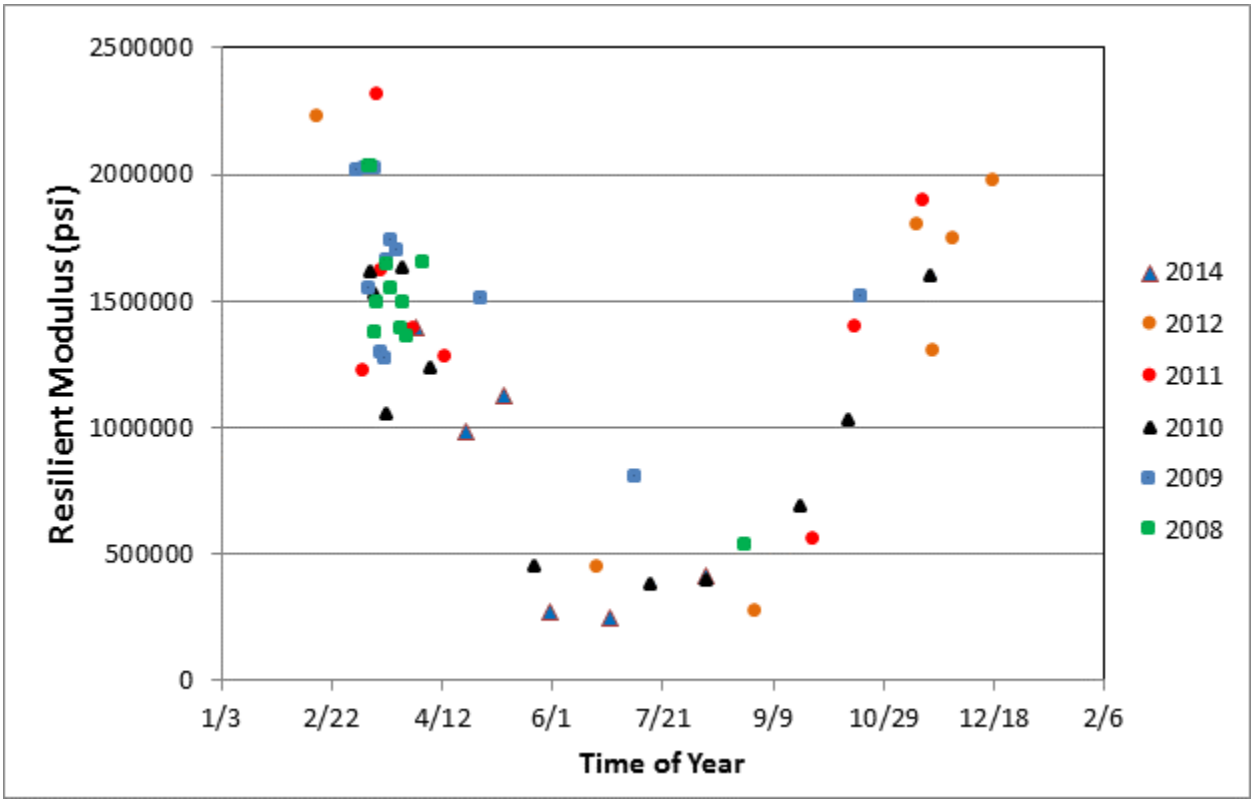

Figure 4.1 2008-2014 Average Back-Calculated Asphalt Pavement Resilient Moduli for Section 1

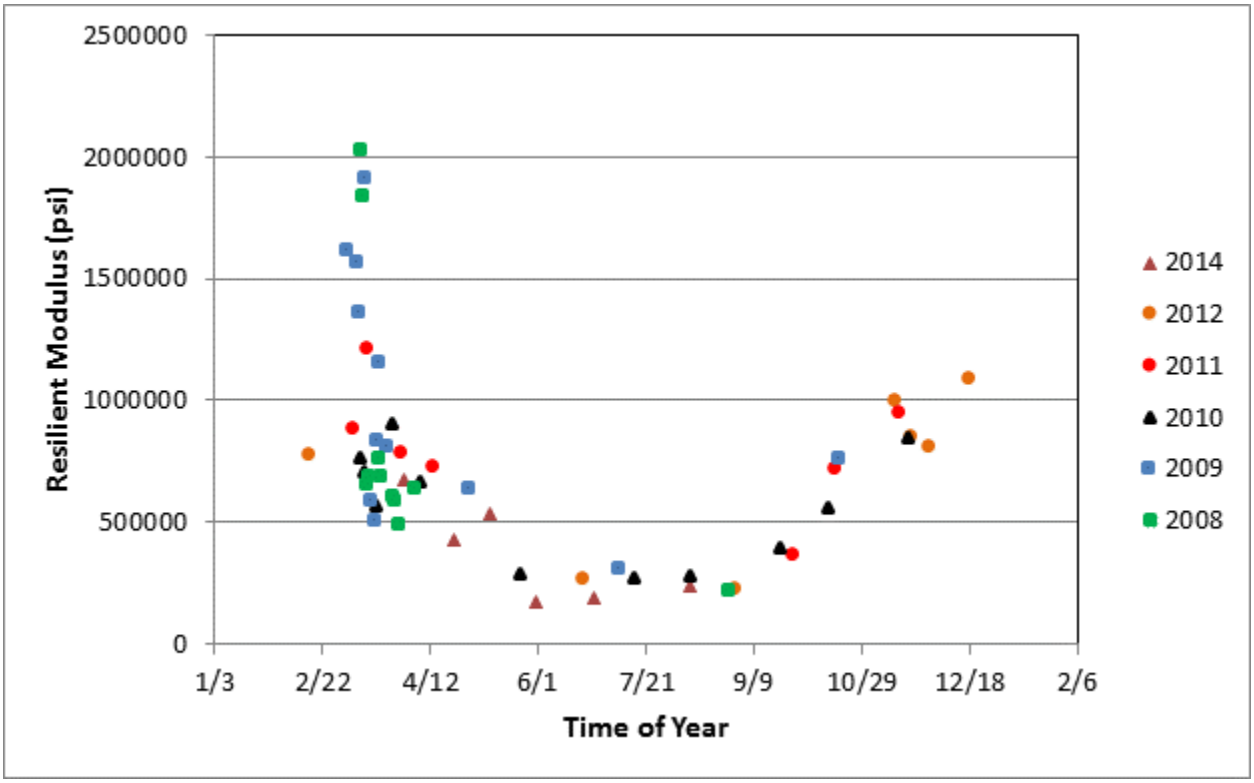

Figure 4.2 2008-2014 Average Back-Calculated Asphalt Pavement Resilient Moduli for Section 2

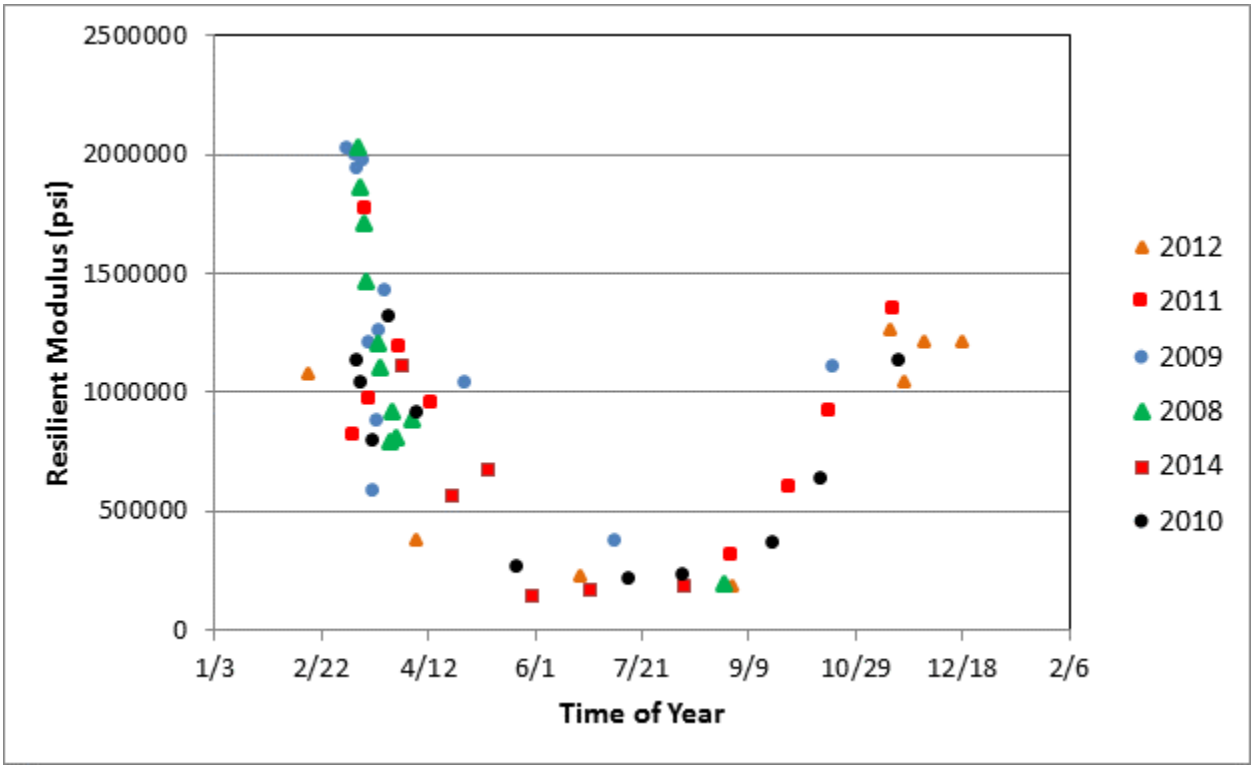

Figure 4.3 2008-2014 Average Back-Calculated Asphalt Pavement Resilient Moduli for Section 3

Annual FWD testing and analysis of the crushed limestone aggregate base resilient moduli on this project indicated that the base material in test Section 3 (the Class 5 modified section) is consistently stiffer than the PAB (Section 2) or conventional Class 5 (Section 1) test sections. The PAB section typically tested midrange between Sections 1 and 3. The difference between the three types became more apparent soon after the spring thaw.

Similar results are observed when looking at the year-by-year data for each section shown in Figures 4.4 through 4.6. The clear rebound of the resilient modulus is evident in every year when observing the Class 5 base in Figure 4.4. Section 2 showed a more modest rebound except for 2009 where there was over 23,000 psi on March 30th. Section 1 showed little to no rebound except for in 2009 in which over 23,000 psi was observed on March 30th. It can be observed that there is more spread from year to year in the base data as compared to the AC layer. This suggests more uncertainty in the measurement and analysis process and/or more year by year dependence of the stiffness on weather conditions. As discussed in the following subgrade section, these extreme cases may be an effect of aliasing between the base and subgrade layers since the modulus observed in the subgrade was comparatively unusually low in those years. Saturation level would be one factor that could contribute to the observed year to year variations in the base. Additional analysis using a back-calculation procedure designed to be more stable (Tonn2010) will be performed to further investigate this phenomenon.

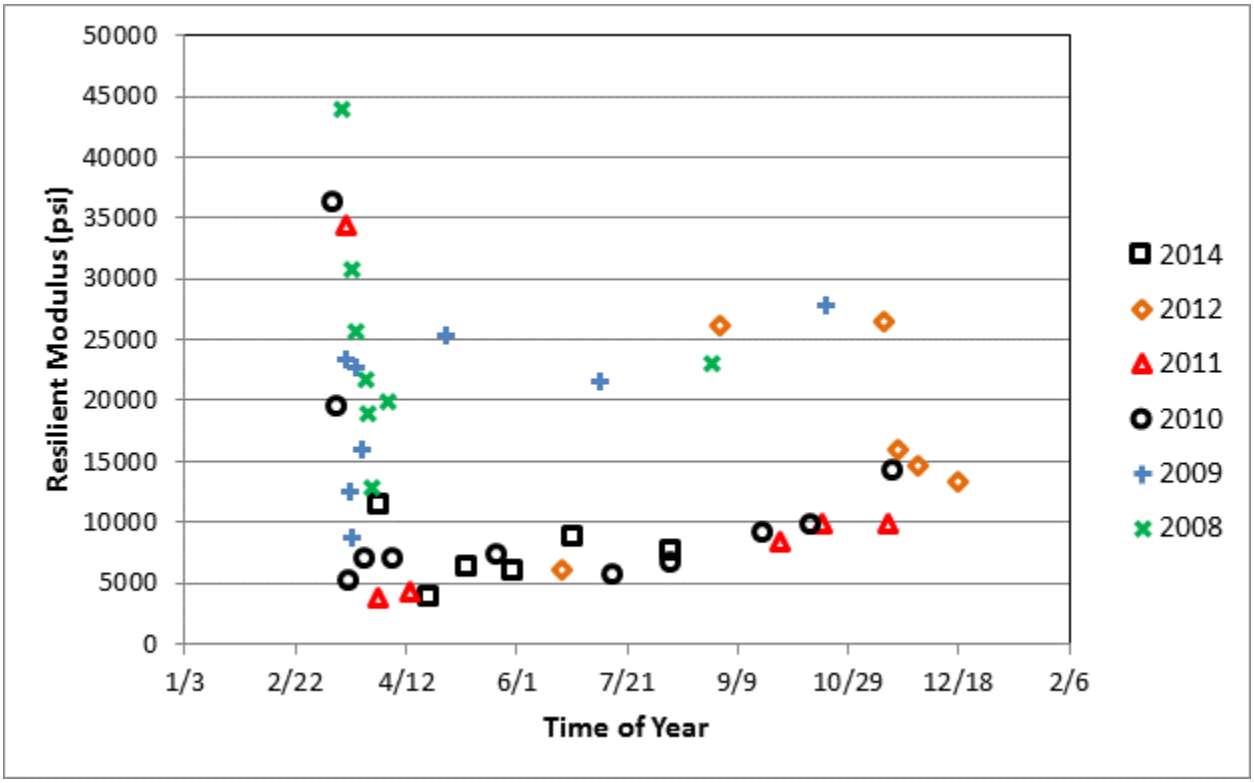

Figure 4.4 2008-2014 Average Back-Calculated Aggregate Base Resilient Moduli for Section 1

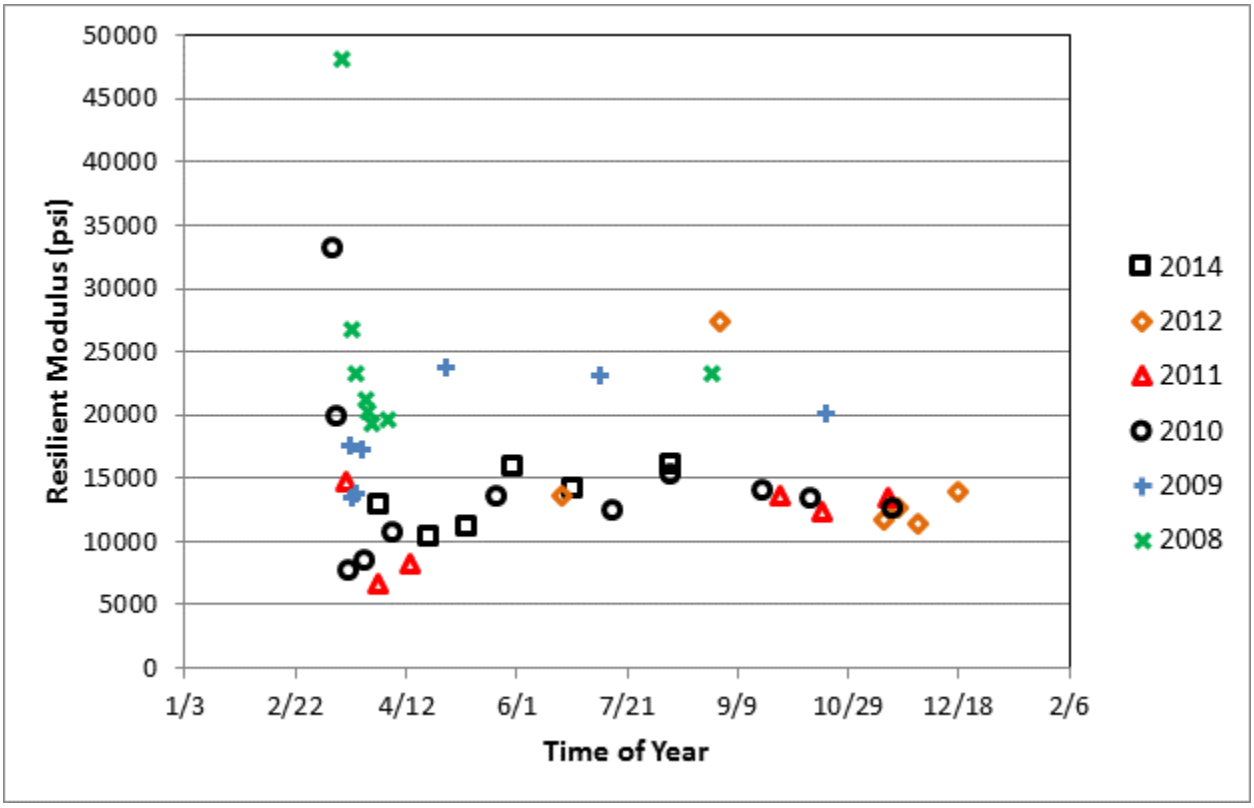

Figure 4.5 2008-2014 Average Back-Calculated Aggregate Base Resilient Moduli for Section 2

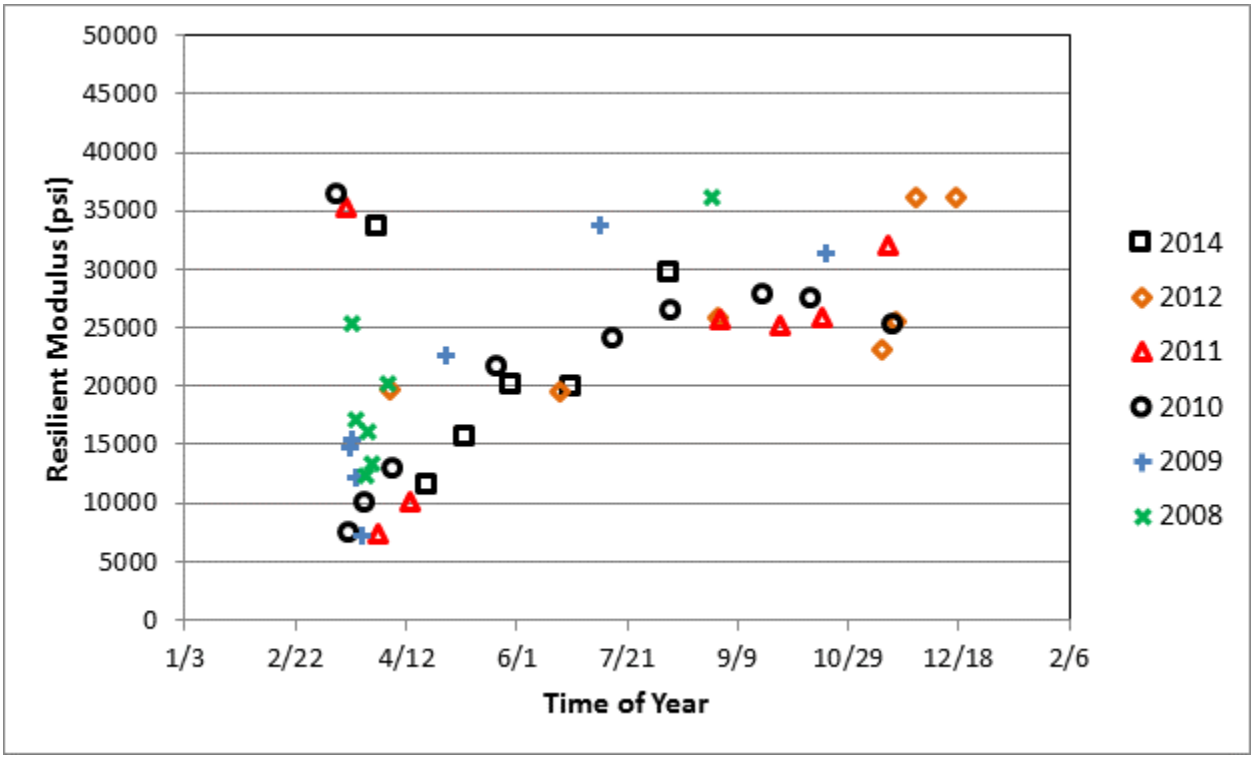

Figure 4.6 2008-2014 Average Back-Calculated Aggregate Base Resilient Moduli for Section 3

The differences in measured stiffness moduli of the three subgrades provided mostly inconclusive results throughout the study. Analysis of the subgrade FWD testing results for the three years of interest in the previous phase indicated that the subgrade in test Section 3 (PG58-34, Class 5 modified) typically had somewhat higher modulus values than test Sections 1 (PG58-28, Class 5) and test Section 2 (PG 58-34, PAB) which can also be observed year by year in Figures 4.7 through 4.9.

The research sections for this project were constructed by removing the existing pavement and then adding base material and new pavement on top of existing subgrades (that had some in-place base material) which were left undisturbed. Little was known about the relative support provided by the three subgrades at the time, but because they were in the same area and initially constructed near the same time, they were assumed to be very similar. It is assumed Sections 1 and 2 are more similar to each other as they are both on CR 117, while Section 3 is located on (the adjacent) CR 104. For this reason, CPT testing was performed during a previous research phase to help identify any differences. While previous reports can be referenced for results and more detailed conclusions, the major findings include:

- Section 1 appears to have the most cohesive materials, gets weaker most quickly with depth, and has some apparent organic material below 10 feet.
- Sections 2 and 3 showed very resistant materials with Section 3 having the most consistent (and granular) material down through the layers.

Some of the differences observed year-to-year are highlighted by breaking down the data by year for each Section with 2008/2009 showing lower than average values in Sections 1 and 2, and 2012 showing lower values than average in September and November. The repeatability of the data from year to year in Section 3 is the most stable as compared to Sections 1 and 2. These trends may be due to variable rainfall patterns or other physical phenomenon, but also may be due to aliasing between subgrade and base responses.

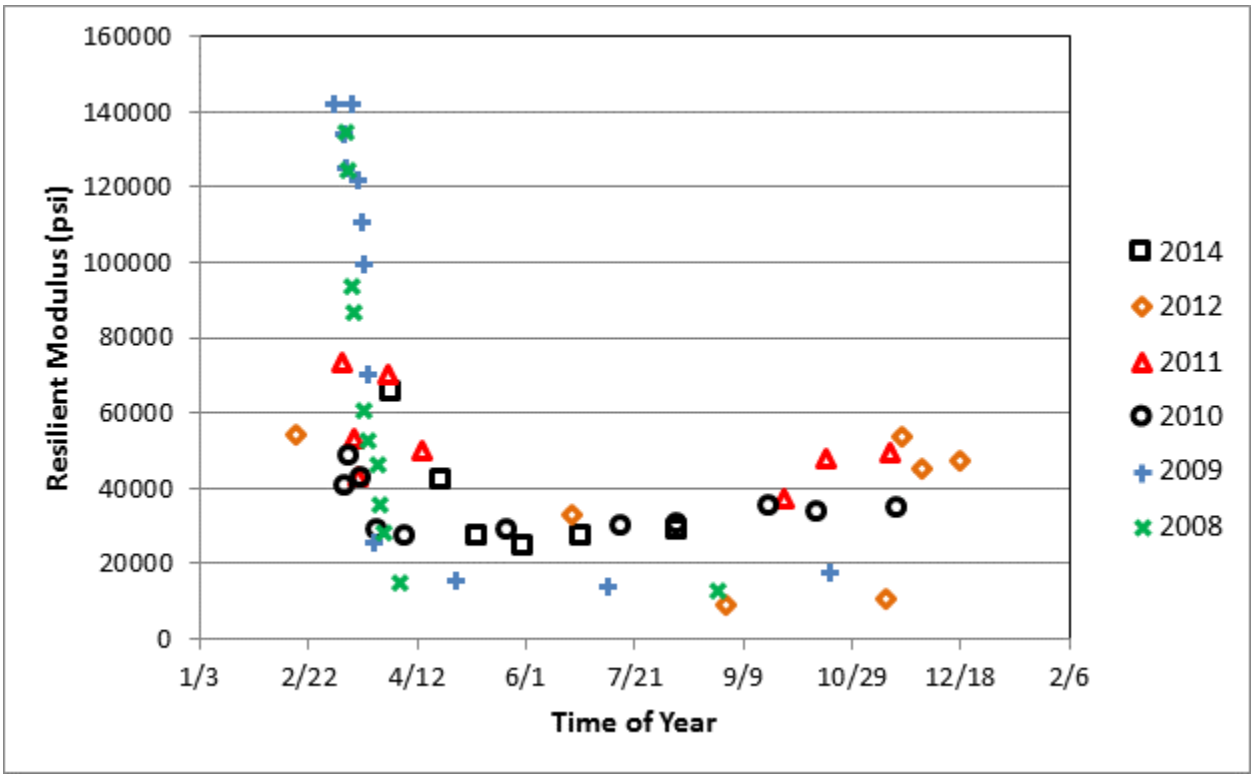

Figure 4.7 2008-2014 Average Back-Calculated Subgrade Resilient Moduli for Section 1

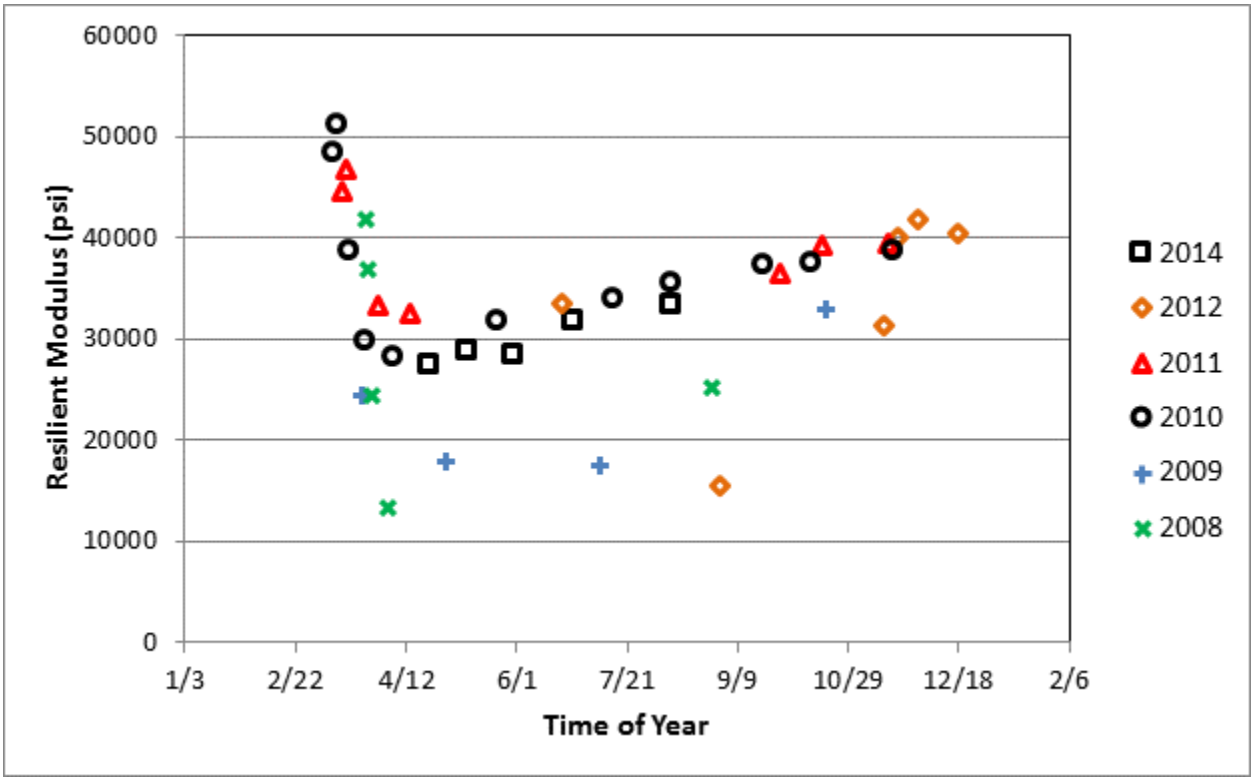

Figure 4.8 2008-2014 Average Back-Calculated Subgrade Resilient Moduli for Section 2

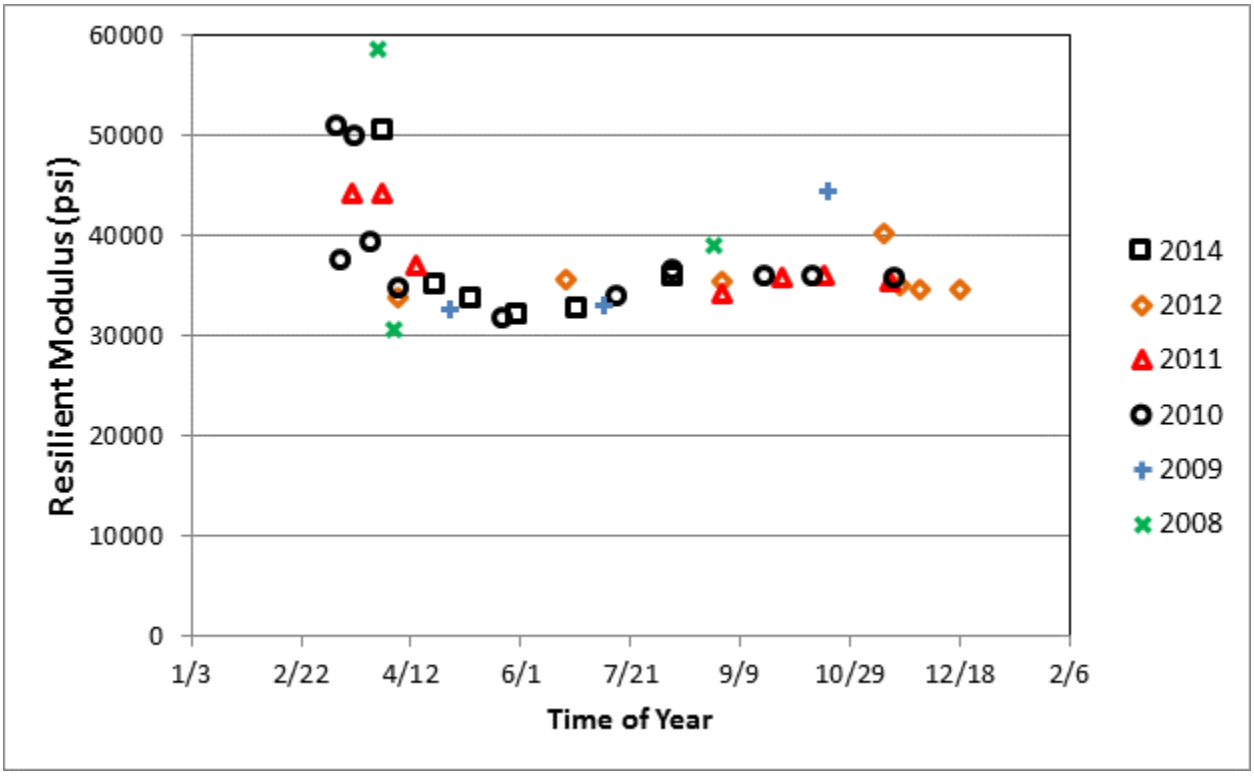

Figure 4.9 2008-2014 Average Back-Calculated Subgrade Resilient Moduli for Section 3

4.1.2 2010 Spring Thaw Period Intensive FWD Testing

During 2010, an intensive testing schedule was implemented to gain more information about the layer stiffnesses during the period when frost is leaving the subsurface layers; known as the "spring-thaw" period. This section contains the back-calculated and analyzed FWD data for the 2010 spring-thaw period. The thawing of the roadway layers at the project site progressed unevenly in 2010 due to variability in average daily temperatures (Figure 4.10). This resulted in some apparent thawing and refreezing and extended the total thaw period; however, the spring thawing period was fairly well represented by the testing that was performed. The variability in the average daily temperatures clearly affected the rate of thawing and resulting stiffness of the asphalt, the base, and subgrade materials.

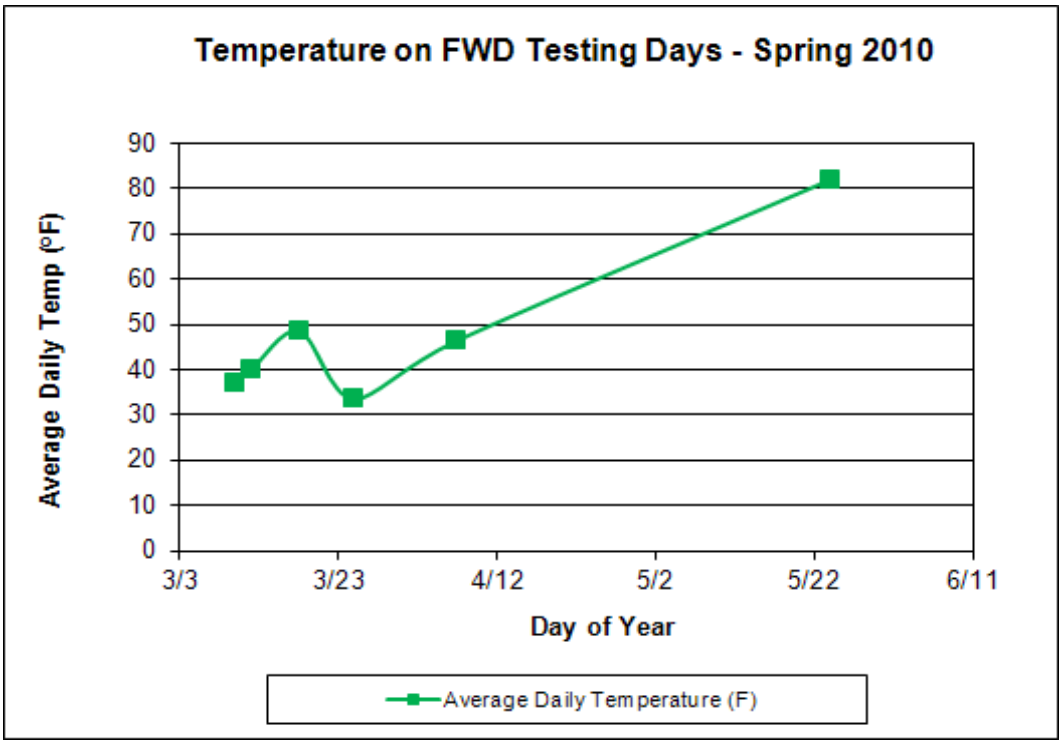

Figure 4.10 Average Daily Temperature (°F) During 2010 Thaw Period

A review of spring 2010 asphalt resilient modulus (Figure 4.11) shows a difference in the stiffness of the pavements of the three sections during the spring thaw. It is expected that Section 2 and 3 (both PG 58-34) would have very similar moduli, and Section 1 (PG 58-28) would be similar to them in the summer, but somewhat stiffer in the winter. There may have been some variability in the sections with 58-34 binder; in the cooler period, the Section 3 pavement appears stiffer than the Section 2 pavement with the same binder. However, later in the summer the two are nearly identical. The Section 1 pavement has approximately twice the stiffness of the Section 2 pavement in cooler periods; and this is expected. The high cold-weather stiffness in the Section 1 asphalt is likely the cause of the thermal cracking in the un-sawn test section (Section 1b).

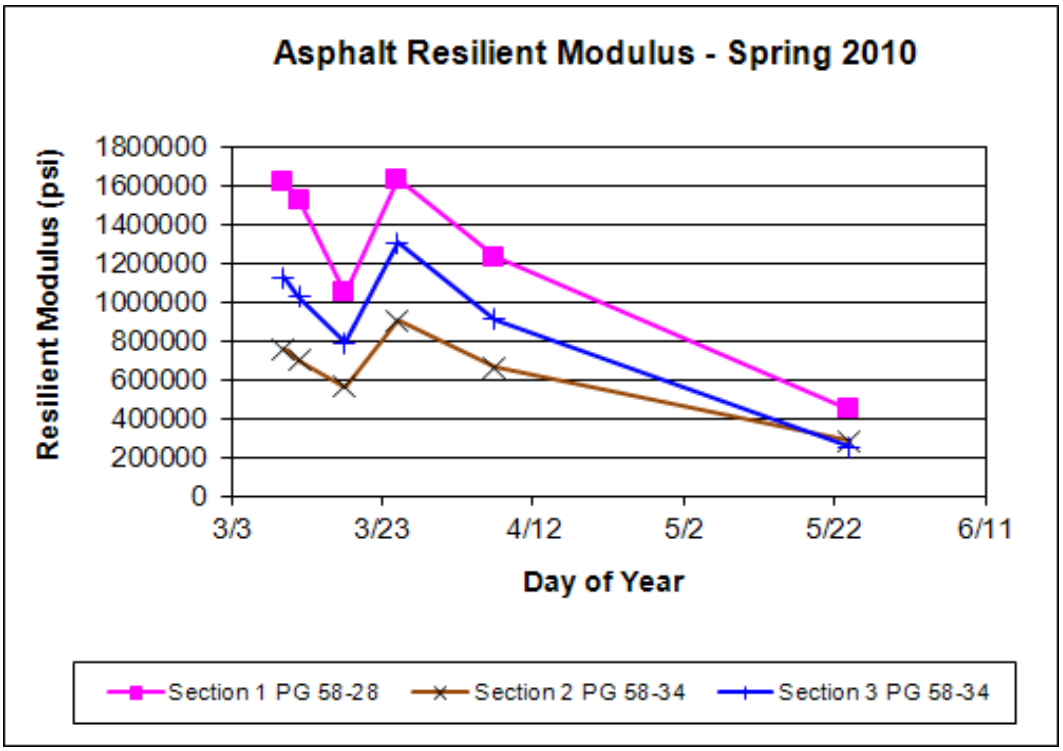

Figure 4.11 Asphalt Resilient Modulus, Spring 2010

A review of aggregate spring 2010 base resilient modulus (Figure 4.12) shows some difference in the stiffness of the three base materials during the spring thaw. Similar to data acquired in the previous research phases, the conventional Class 5 lost more stiffness and recovered slower than the Class 5 modified section. The Class 5 modified section also appeared to begin significant thawing later and had a slower drop-off in stiffness than either the Class 5 or PAB sections.

As previously stated, the conventional Class 5 does not meet the MnDOT gradation specification (exceeds 0.075 mm [#200] fraction specs), while the Class 5 Modified material would meet Standard Class 5 gradation passing #200 fraction specifications. Higher water retention due to excessive fine materials in the conventional Class 5 section would explain the higher frozen stiffness, rapid and extreme stiffness loss during the thawing period, and slower recovery observed in Section 1.

The PAB performed nearly identical to the Standard Class 5 in the frozen condition but was somewhat stiffer during the thaw and recovery. In previous years, the PAB has performed more similar to the Class 5 section through the recovery period. It is possible different rainfall patterns in previous years versus 2010 may have had different influences on base stiffness.

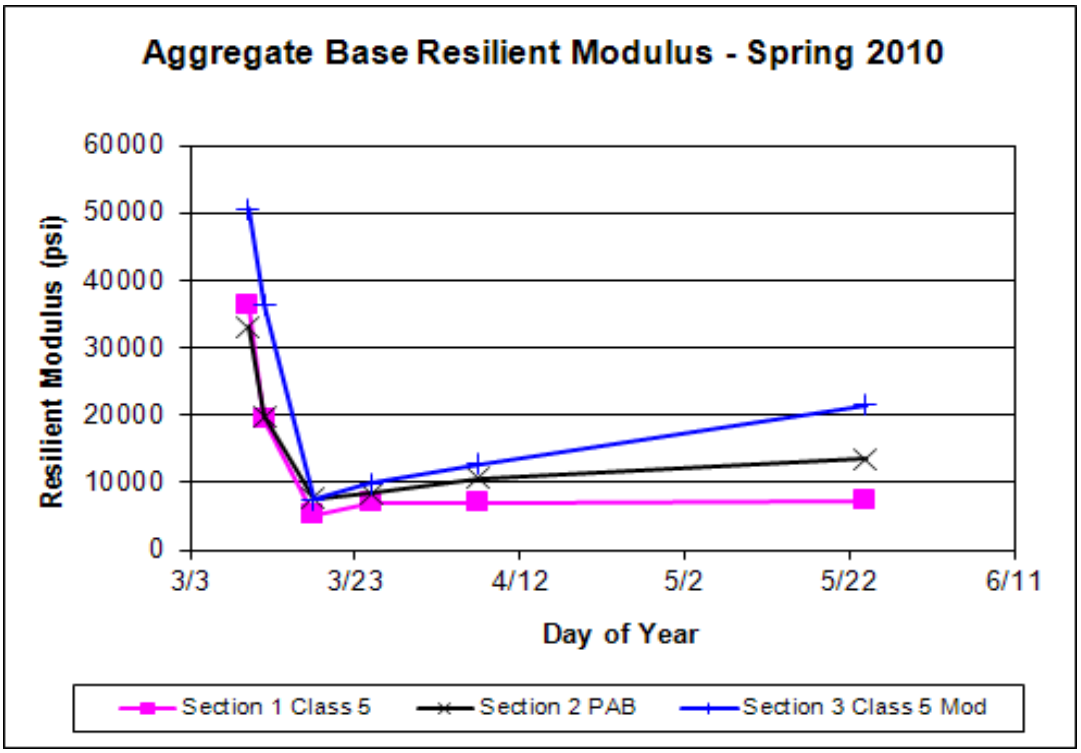

Figure 4.12 Aggregate Base Resilient Modulus, Spring 2010

A review of the spring 2010 subgrade resilient modulus (Figure 4.13) shows that the subgrade under test Section 3 (County Road 104) remained considerably stiffer than that under test Sections 1 and 2 (CR 117) during the thaw period. The subgrade resilient modulus values for test Section 3 also remained higher during the early recovery period, as was observed in past years. The subgrade modulus values for test Sections 1 and 2 were consistently approximately equivalent and may be due to the sections being constructed on the same roadway (CR 117) and most likely constructed with the same materials.

As also noted in in previous research, the somewhat lower modulus values recorded in April than the recorded on last test day in March most likely indicated that the roadway was not tested at the true low stiffness point (when all frost is out), which probably occurred near March 30. Previous years testing has shown the subsurface layers on this project reached a clearly defined low point at the end of the thaw period and typically were well into stiffness recovery in April.

The subgrade under test Section 3 was considerably stiffer in the spring (and throughout the year) than under test Sections 1 and 2. CPT testing (see Section 4.3) has also shown that it is probably more granular in nature and likely more drainable. This could also account for at least part of the large difference in strength of the base layers in the roadways since the PAB in test Section 2 was very low in material passing the 0.075 mm (#200) sieve (2.3 percent). It should be able to drain if a path is available. However, it is possible that a more impermeable subgrade leaves the Section 2 base layer saturated longer in spring, resulting in lower modulus values. It is also possible that the aggregate base that was

left in place during the reconstruction of test Section 2 is less permeable, rendering the improved permeability of the PAB of less consequence if moisture cannot escape it.

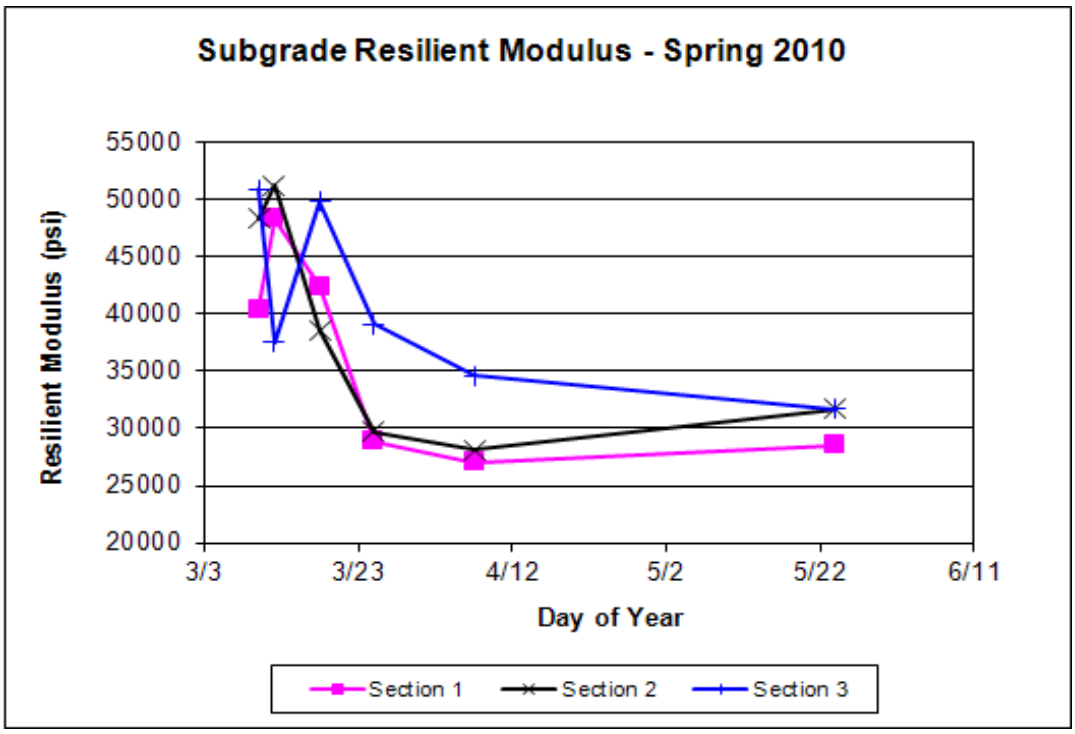

Figure 4.13 Subgrade Resilient Modulus, Spring 2010

4.1.3 2012 Fall Freezing Period Intensive FWD Testing

During late 2012, an intensive testing schedule was implemented in order to gain more information about the layer stiffnesses during the period when the subsurface layers begin to freeze; here referred to as the "fall freezing" period. This section contains the back-calculated and analyzed FWD data for the 2012 fall freezing period.

The freezing of the roadway layers at the project site progressed unevenly in fall 2012 due to variability in average daily temperatures (Figure 4.14). This resulted in some apparent thawing and refreezing and extended the total freeze period. The variability in the average daily temperatures also affected resulting measured stiffness of the asphalt, the base, and subgrade materials. The FWD equipment is not designed to operate in extreme cold weather environments, and testing had to stop after December 17, 2012 due to equipment problems before complete freezing of the subsurface layers occurred.

It is not known how deep the zone of freezing progressed during this testing period. However, based on measurements previously taken during frozen periods before the spring-thaw, it appeared the pavement was frozen at the time of the last test. The base and subgrade materials may have begun to freeze but were likely not yet completely frozen. This resulted in some unexpected data and rendered this test less effective than anticipated.

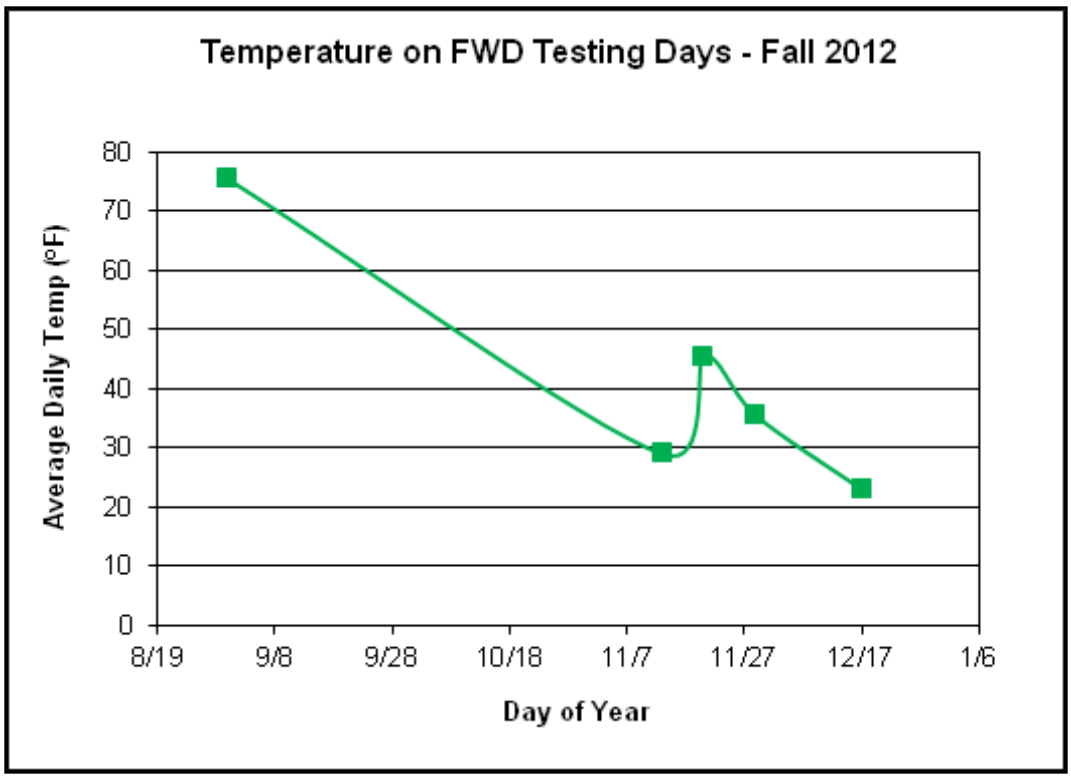

Figure 4.14 Average Daily Temperature (°F) During 2012 Freeze Period

A review of the fall 2012 asphalt resilient modulus (Figure 4.15) shows that the stiffness of the three pavements varied inversely to temperature during the fall. As expected, Sections 2 and 3 (PG 58-34) have very similar moduli, and Section 1 (PG 58-28) was more similar to them in the summer and then significantly stiffer than the others by the time of the last test in December. It is also noted that the Section 1 pavement (PG 58-28) already had significantly higher stiffness than Sections 2 and 3 (PG 58-34) at the beginning of the freezing period when temperatures were only near freezing, and not just during the coldest times of the year.

As also observed in previous spring-thaw data, it appears that there may have been some variability between Section 2 and 3 in the stiffness of the 58-34 binder at the time of construction. The pavement in Section 3 appears stiffer than the Section 2 pavement during freezing as it did during spring-thaw. As also observed previously, the Section 1 pavement has approximately twice the stiffness of the Section 2 pavement in cooler periods. The higher stiffness in Section 1 asphalt observed during spring-thaw, fall freezing, and winter is likely contributing to thermal cracking there, and supports the current practice of using polymer modified asphalt binders.

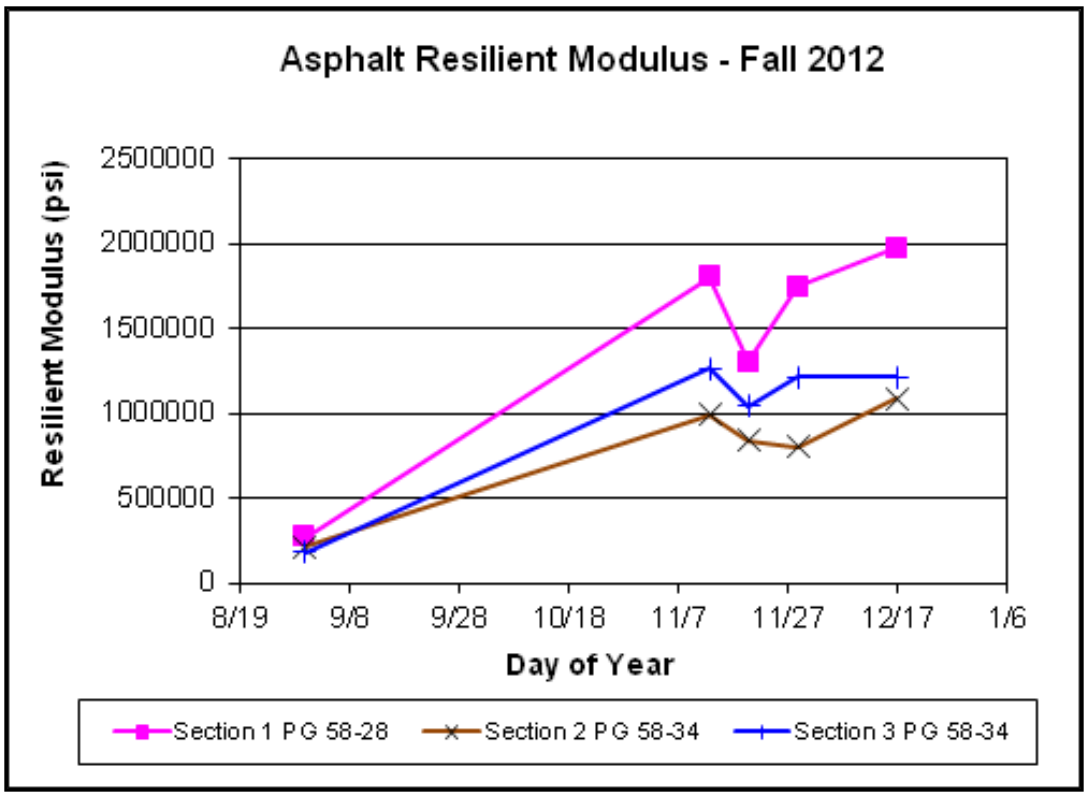

Figure 4.15 Asphalt resilient Modulus, Fall 2012

A review of the fall 2012 aggregate base resilient modulus (Figure 4.16) shows somewhat unexpected differences in the stiffness of the three base materials. The conventional Class 5 section responded in an apparent opposite way to the Class 5 modified section during the fall freezing period. The Class 5 modified section increased in stiffness during the freeze period and the standard Class 5 lost stiffness. The PAB section also appeared to lose stiffness earlier and had a more rapid bottom in stiffness than the conventional Class 5 section, but then began to recover better by the end of the freeze period. As previously stated, the Standard Class 5 does not meet the MnDOT specification for gradation (exceeds 0.075 mm [#200] fraction specs), while the Class 5 Modified material would meet Standard Class 5 gradation passing #200 fraction specifications. It is possible that higher water retention due to excessive fine materials in the Class 5 caused a lower stiffness during this period because actual freezing did not yet occur by the date of the last test, but more rain and snowfall increased in November. It is not known why the PAB would decrease in stiffness so dramatically during the fall. The equipment problems encountered during this testing period was also a possible factor in this unusual data, or as mentioned earlier, the different rainfall patterns in recent years appear to have had different influences on base stiffness.

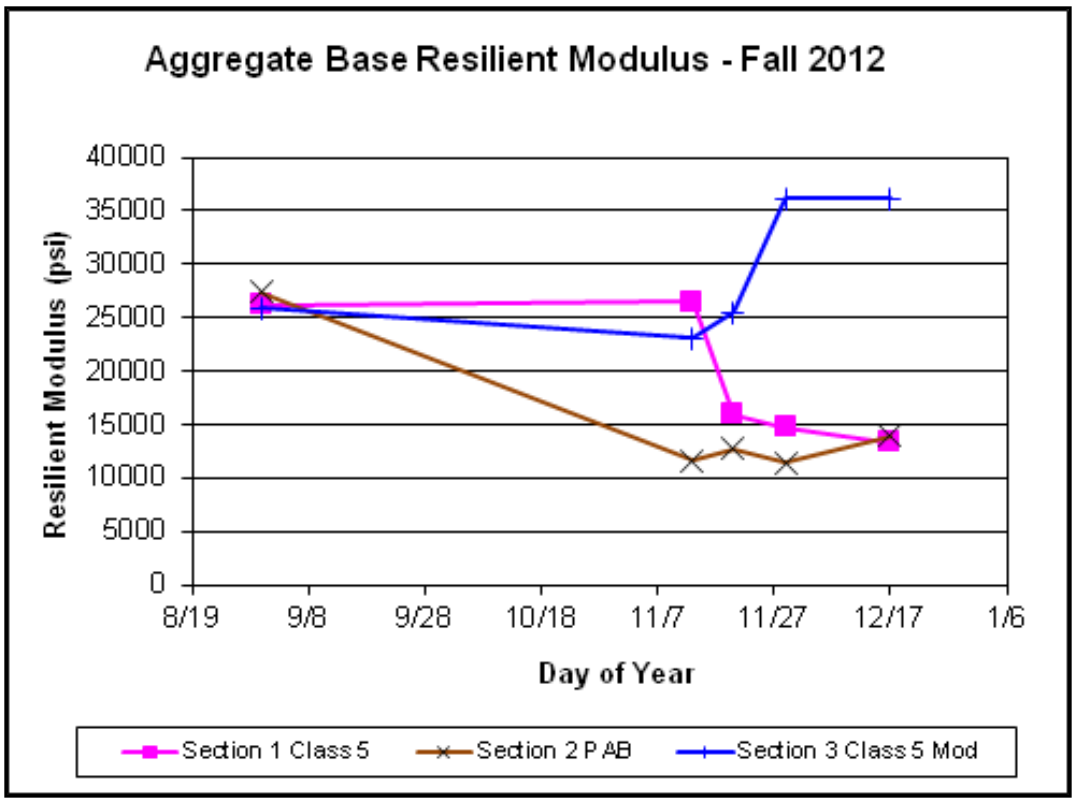

Figure 4.16 Aggregate Base Resilient Modulus, Fall 2012

A review of the fall 2012 subgrade resilient modulus (Figure 4.17) shows that the subgrade under test Section 3 (County Road 104) lost stiffness somewhat during the freeze period while that under test Sections 1 and 2 (CR 117), stiffness increased. During this period, the subgrade below the Class 5 acted more as expected and generally followed the temperature variations during the period.

Sections 2 and 3 subgrade stiffness values did not clearly follow the temperature data. The frost penetration may not have extended down to subgrade depth (in Section 2 and 3) by the time of the last testing, or the assumed better draining Sections 2 and 3 may have had less internal moisture to freeze. Because of the equipment problems encountered during this test, the results must be considered somewhat unreliable, and this type of testing probably will not be attempted again on this project with the FWD equipment currently available.

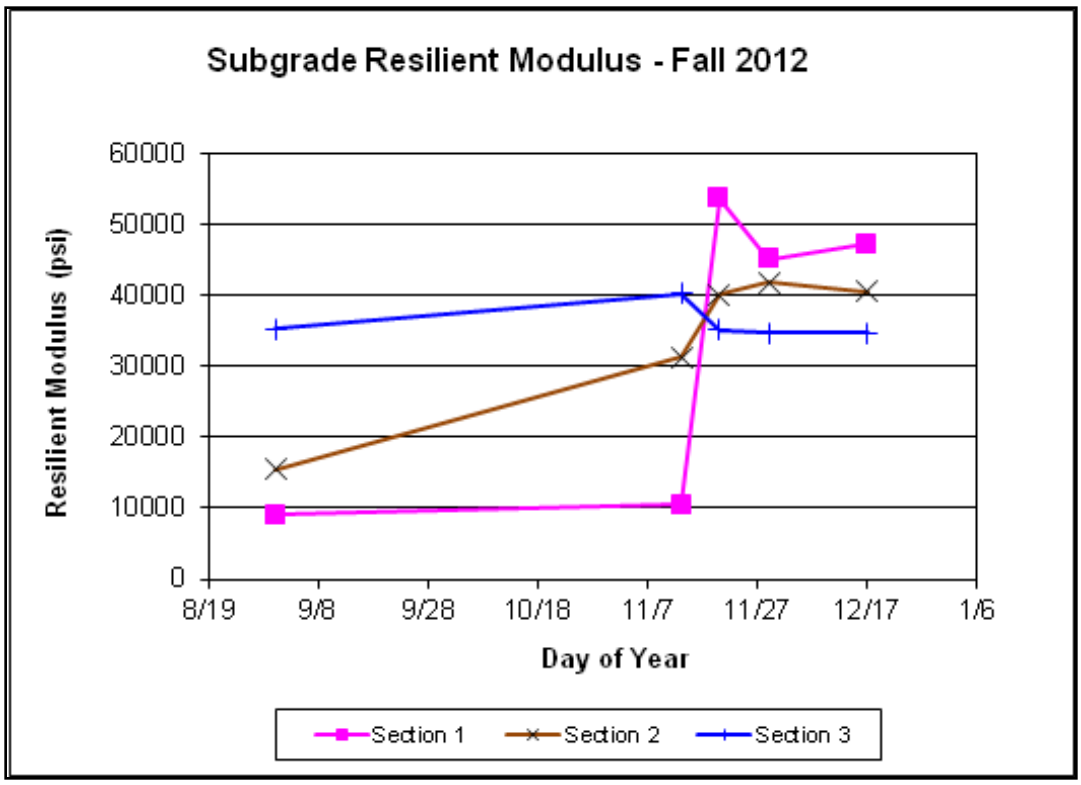

Figure 4.17 Subgrade Resilient Modulus, Fall 2012

4.2 Ground Penetrating Radar Forensic Analysis

Ground penetrating radar is included in the scope of this phase of the project to inform other analysis such as the distress maps and FWD analysis. Pavement thickness variation is one parameter that affects FWD analysis and potentially pavement distress if the thickness is deficient in some areas. Thus, pavement layer thickness evaluation was performed on this project. Figure 4.18 shows the GPR antenna (yellow object mounted to the front of the van) during data collection on new asphalt pavement construction.

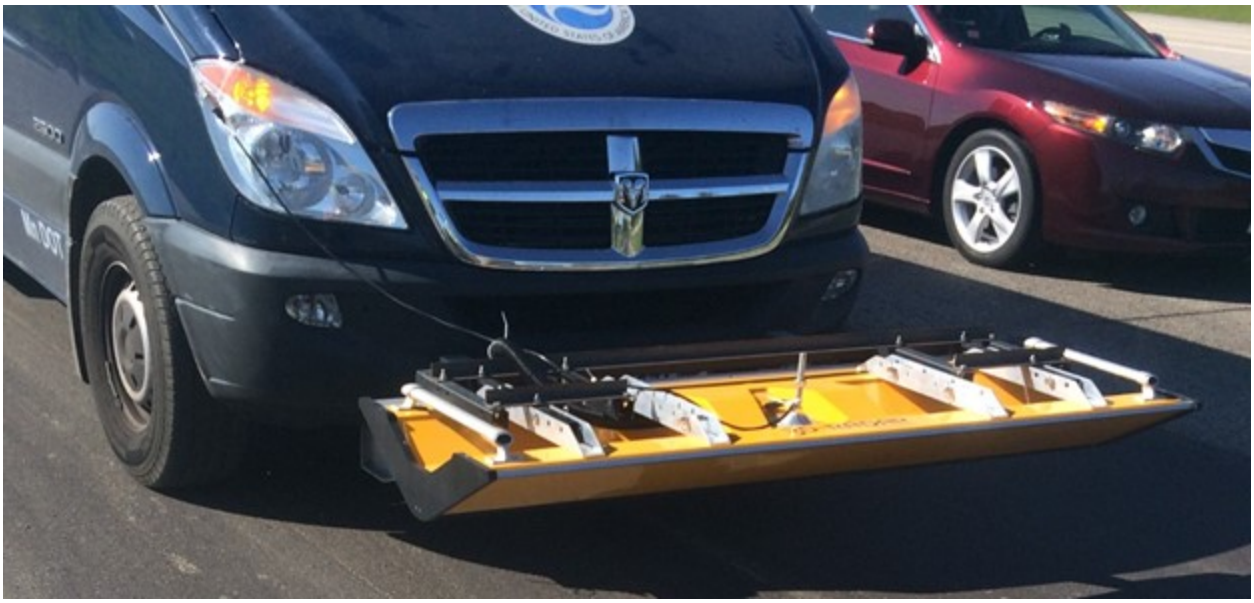

Figure 4.18 GPR Antenna (Yellow Object Mounted to the Front of the Van) During Data Collection on Asphalt Pavement Construction

3D radar data was collected in the center 5 ft. of both lanes for all 3 sections at a data grid spacing of 3 in. by 3 in. Figure 4.19 shows an example 3D Reconstruction at showing the 3D radar measured AC thickness in the center 5 ft of Eastbound Section 1a starting at stationing 105 to station 115. This information is all contained in the title. The title of each figure specifies the layer it is measuring the depth of, section being measured, and stationing of the start and end of the test data being presented using the convention "A_B_C_DtoE" where:

- A- specifies the layer being evaluated (all AC in this case since asphalt is the only layer presented in this report)
- B – specifies the current section being tested
- C – specifies the direction of travel (which lane is being tested)
- D – specifies the starting station (0 in the longitudinal axis of the plot corresponds to this location)
- E – specifies the ending station (the highest number in the longitudinal axis of the plot corresponds to this location)

The data is presented in the following 3 axes:

- Depth, in. – specifies the depth below the surface where the AC layer bottom caused a reflection (this information is also contained in the color of the presented layer where thicker layers are lighter/more yellow in color and thinner layers are darker/more red in color
- Transverse, ft. – specifies the location within the lane width (in this case 0 is at 6 ft away from the longitudinal joint, and negative values move toward the longitudinal joint)
- Longitudinal, ft. – specifies the distance traveled along the pavement from the beginning of the data set (specified in the title where 0 equals the first number from the title).

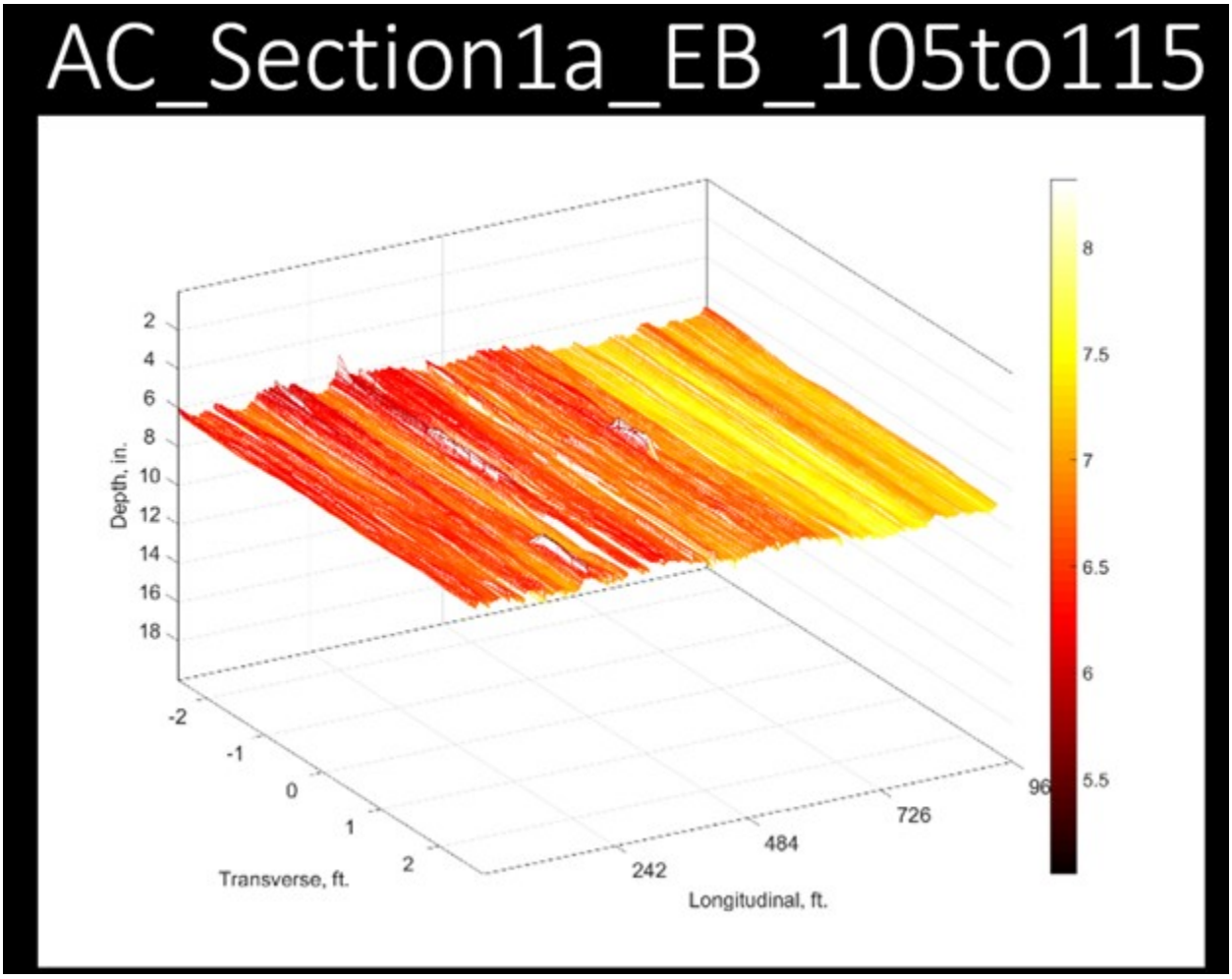

Figure 4.19 3D Reconstruction at Showing the AC Thickness in the Center 5 Ft. of Eastbound Section 1A Starting at Stationing 105 to Station 115

Figures 4.20 through 4.30 show the asphalt layer thickness in the middle of the lane in both directions for all the sections. It can be observed that there is some thickness variation from section to section and similarly within different sections and some variation between sections (more yellow dense spots in Section 1), but not enough to affect the comparisons reported. This was good confirmation that the differences in performance are likely not a function of asphalt thickness, as all 3 sections showed consistent thickness close to the nominal 6 in. depth, and the thickest section was the poorest performing section. This provides more confidence in the conclusions about the effectiveness of the different base materials and other findings are legitimate by ruling out a potentially significant confounding factor.

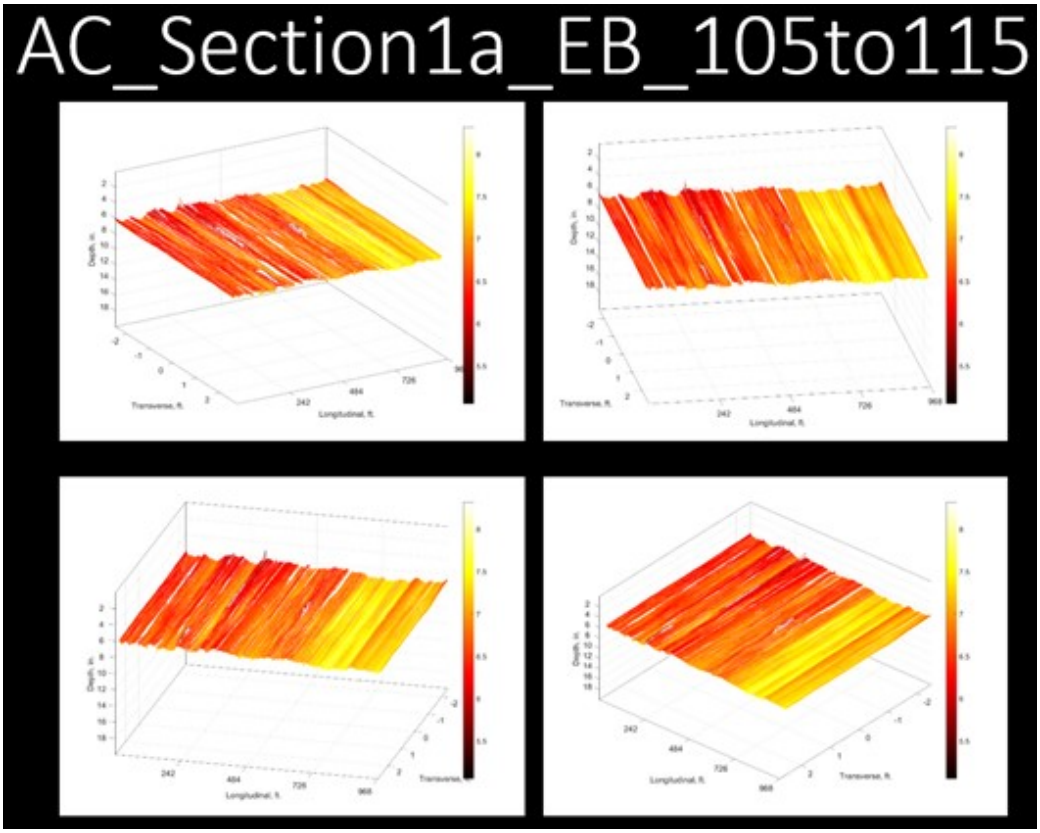

Figure 4.20 3D Reconstruction at 4 Different Angles Throughout the Title Specified Section

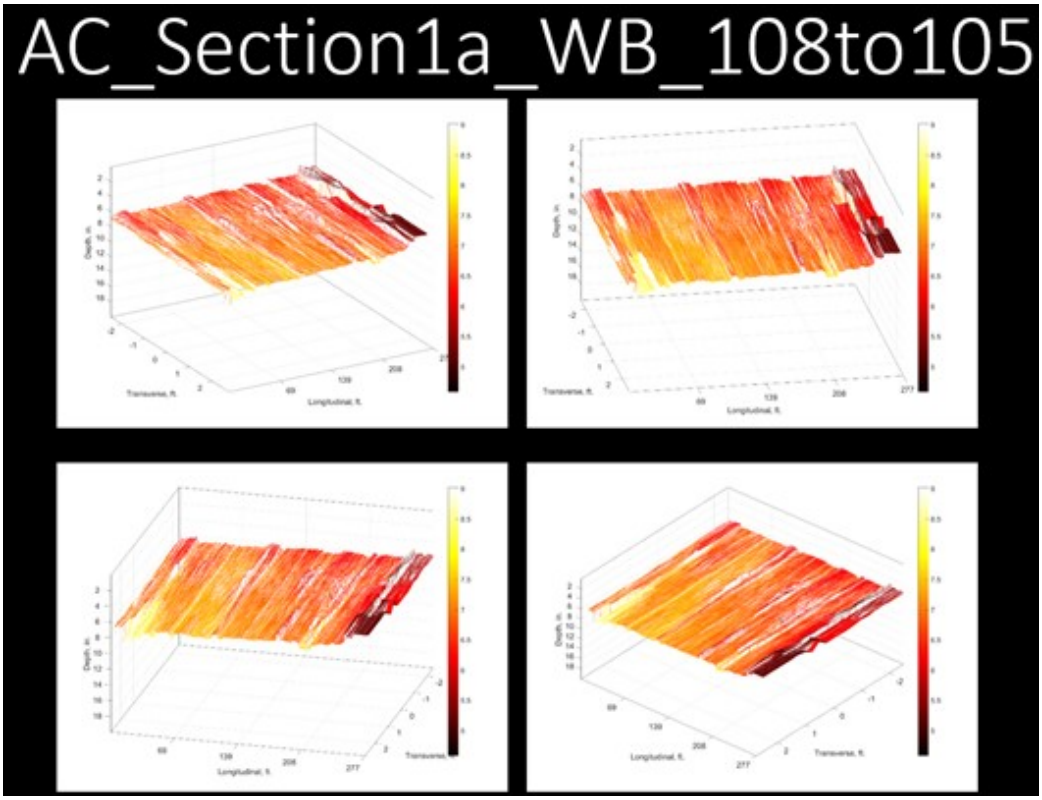

Figure 4.21 3D Reconstruction at 4 Different Angles Throughout the Title Specified Section

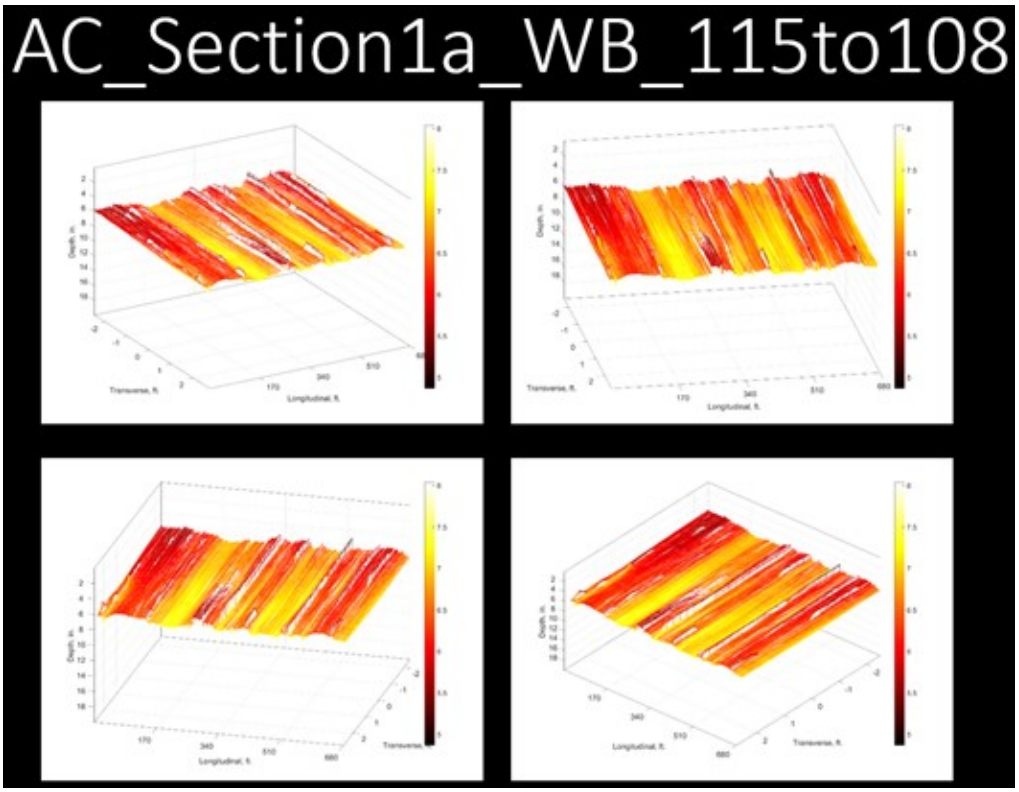

Figure 4.22 3D Reconstruction at 4 Different Angles Throughout the Title Specified Section

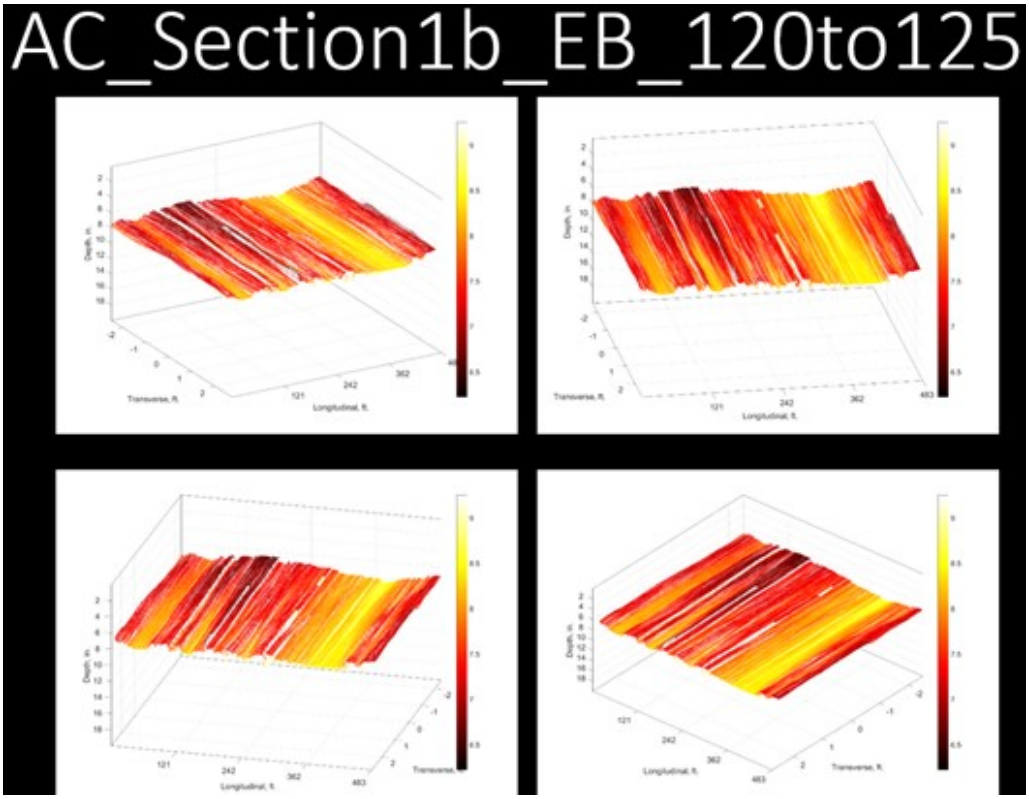

Figure 4.23 3D Reconstruction at 4 Different Angles Throughout the Title Specified Section

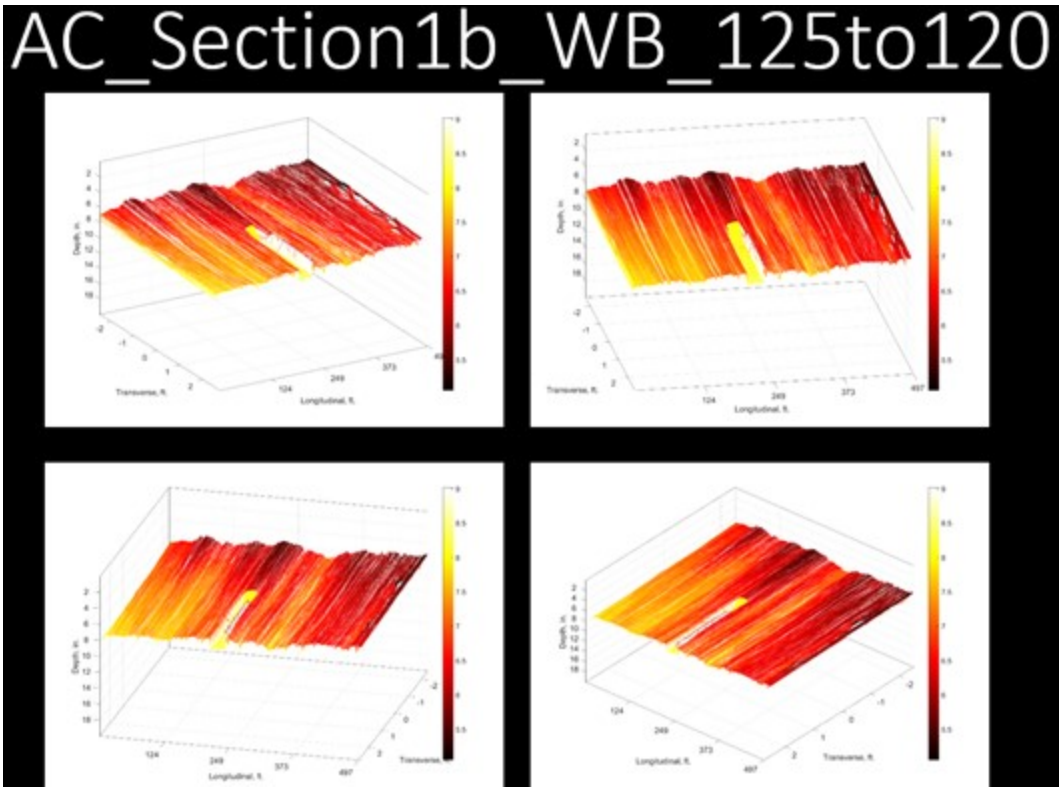

Figure 4.24 3D Reconstruction at 4 Different Angles Throughout the Title Specified Section

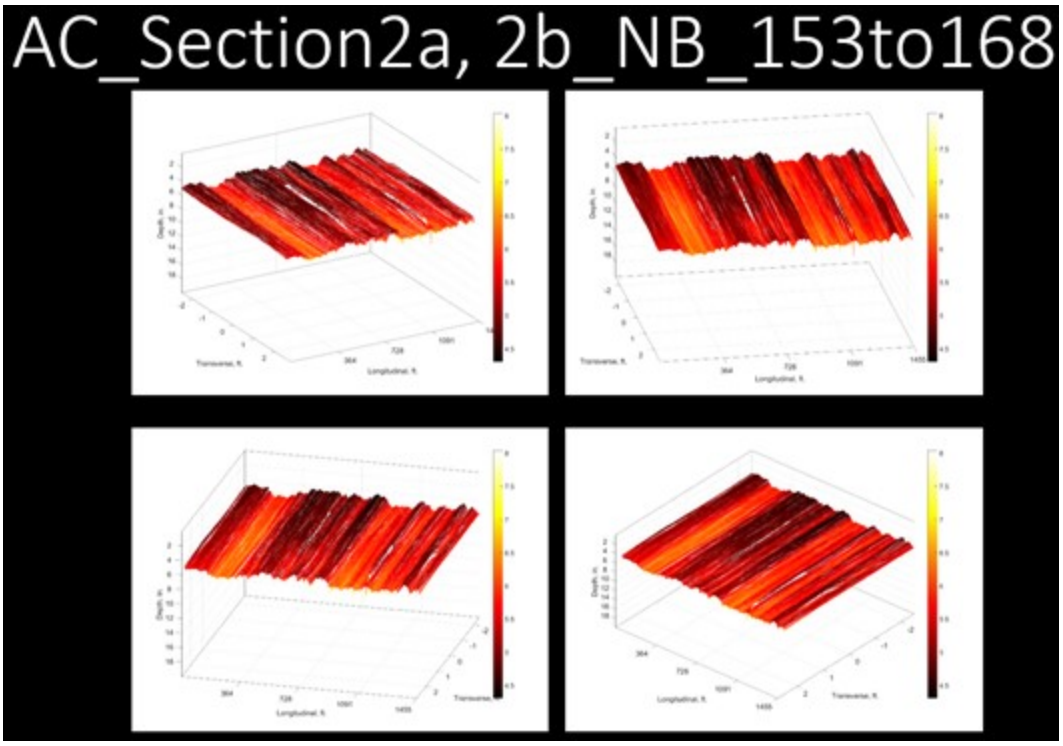

Figure 4.25 3D Reconstruction at 4 Different Angles Throughout the Title Specified Section

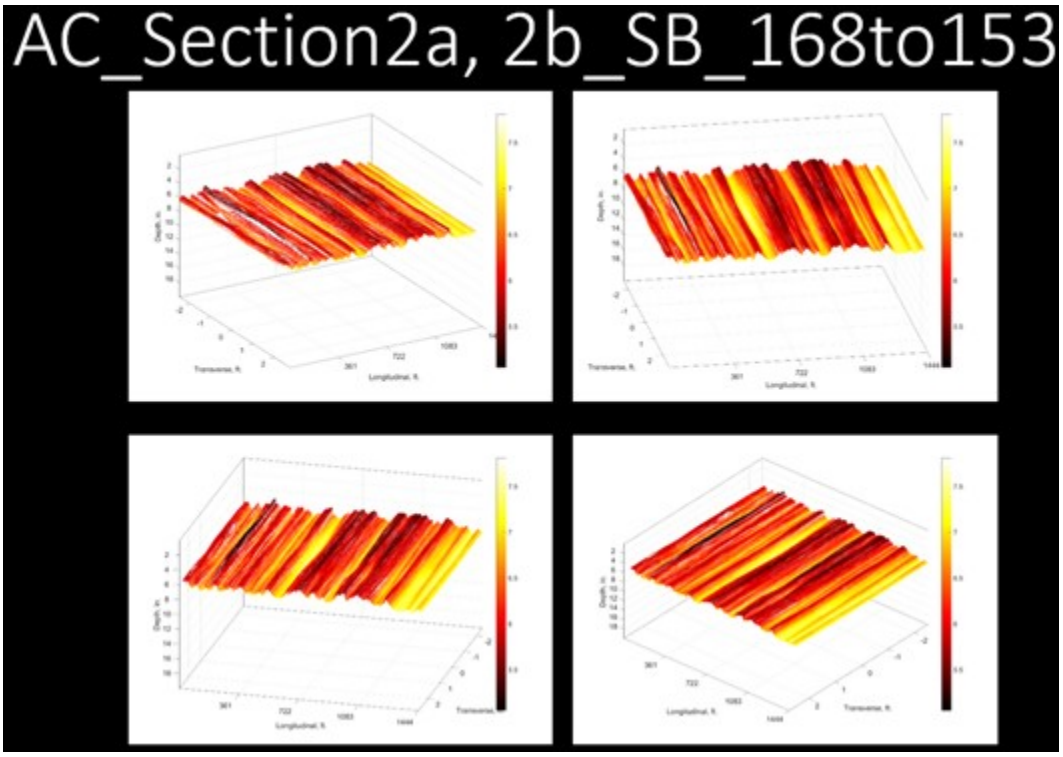

Figure 4.26 3D Reconstruction at 4 Different Angles Throughout the Title Specified Section

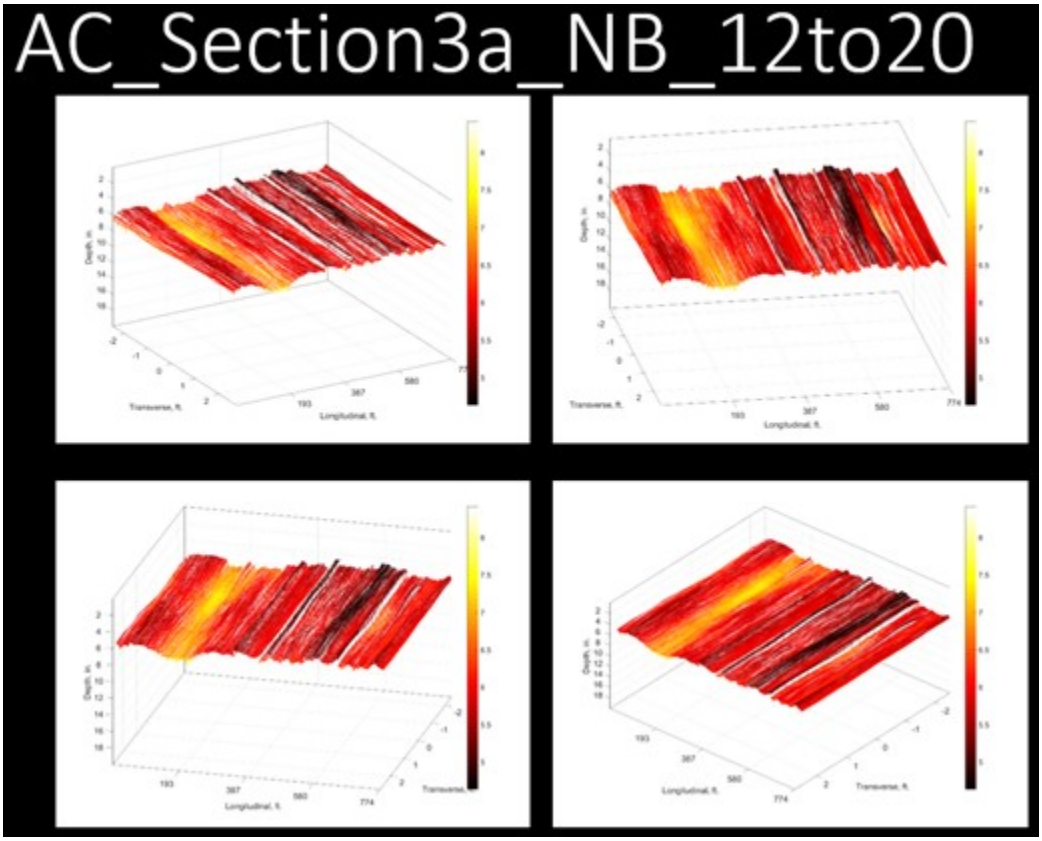

Figure 4.27 3D Reconstruction at 4 Different Angles Throughout the Title Specified Section

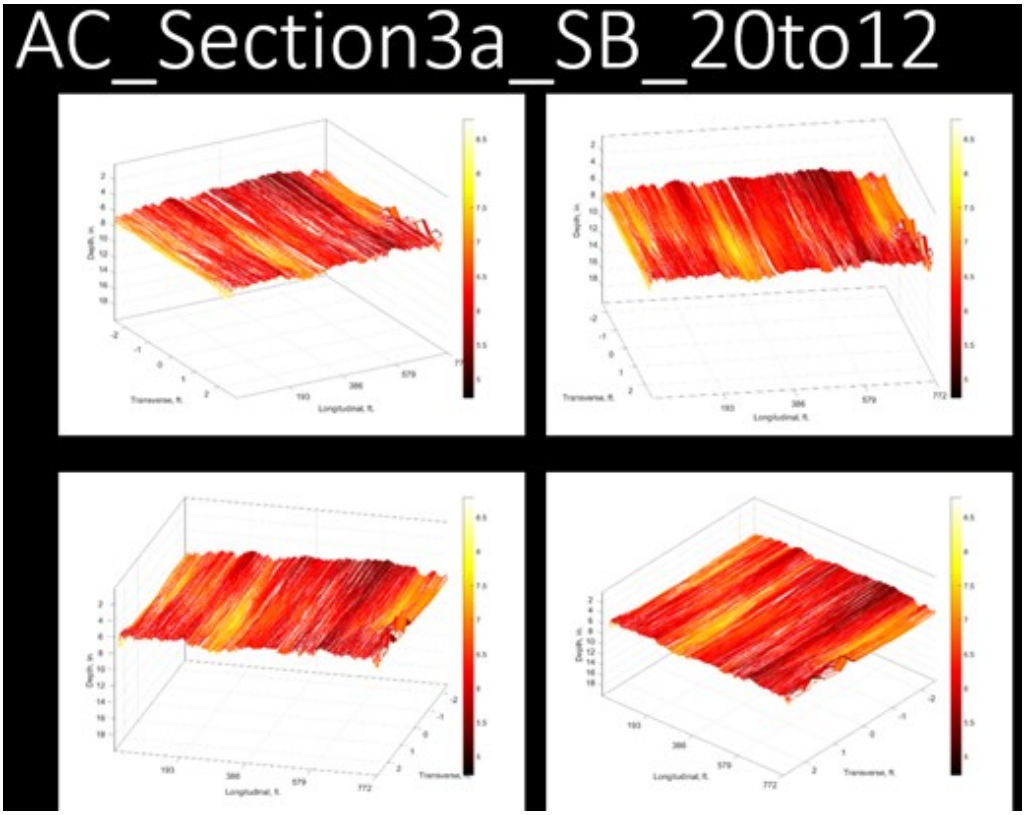

Figure 4.28 3D Reconstruction at 4 Different Angles Throughout the Title Specified Section

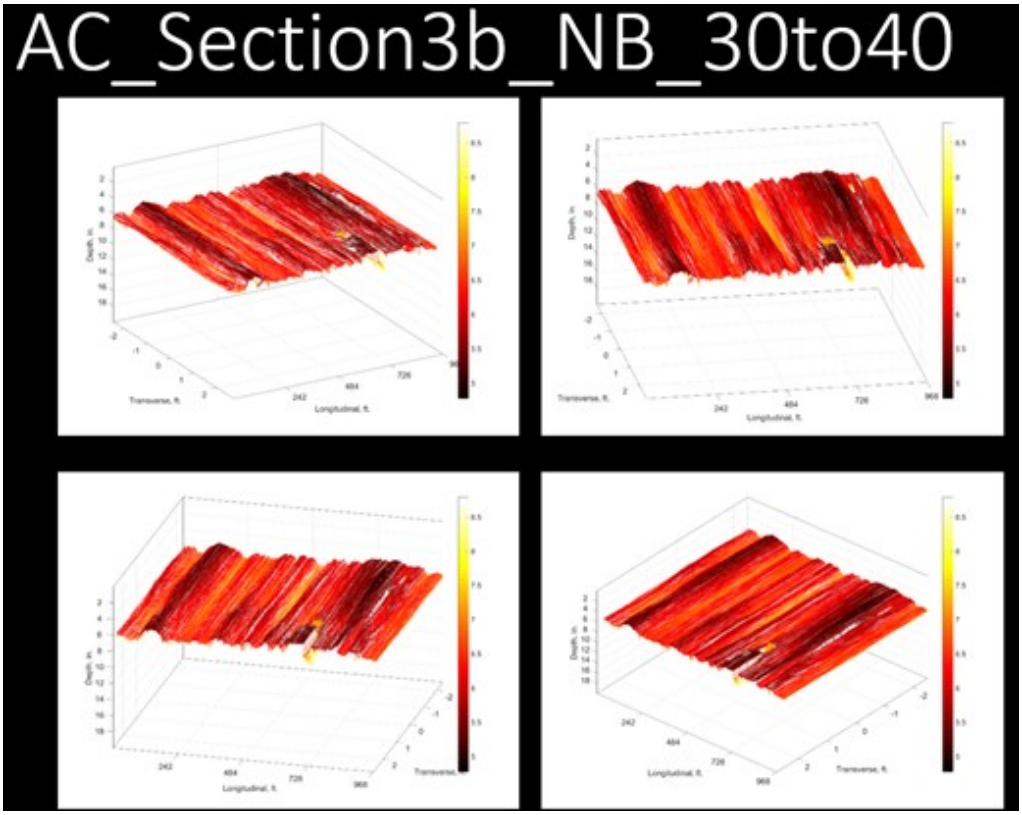

Figure 4.29 3D Reconstruction at 4 Different Angles Throughout the Title Specified Section

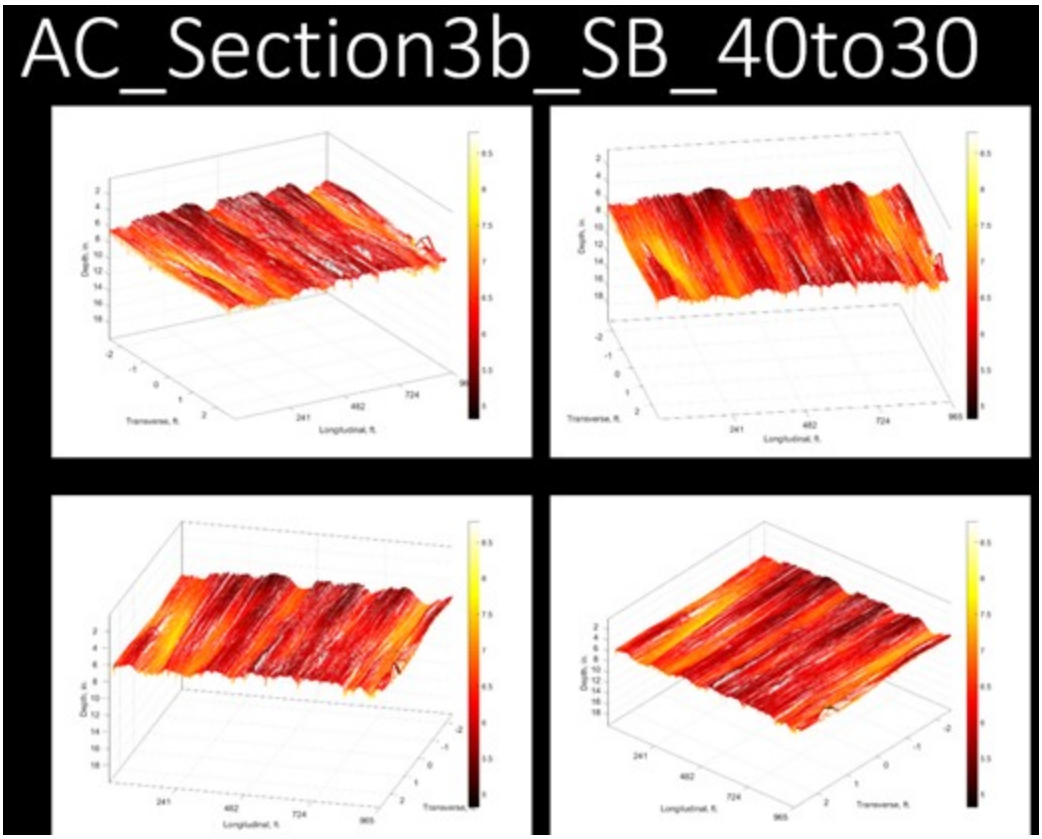

Figure 4.30 3D Reconstruction at 4 Different Angles Throughout the Title Specified Section

4.3 Cone Penetrometer (CPT) Methodology and Results

In order to better classify the strength (and not just stiffness) of the subsurface materials, cone penetrometer (CPT) testing was performed in October 2011 on both county roads 104 and 117 following the ASTM D5778 – 12 procedure. The device was inserted through the gravel shoulder directly alongside each of the six test sections. The map below (Figure 4.31) shows the CPT testing locations (as red dots) adjacent to the test sections, near the right pavement edge of the eastbound/northbound lane.

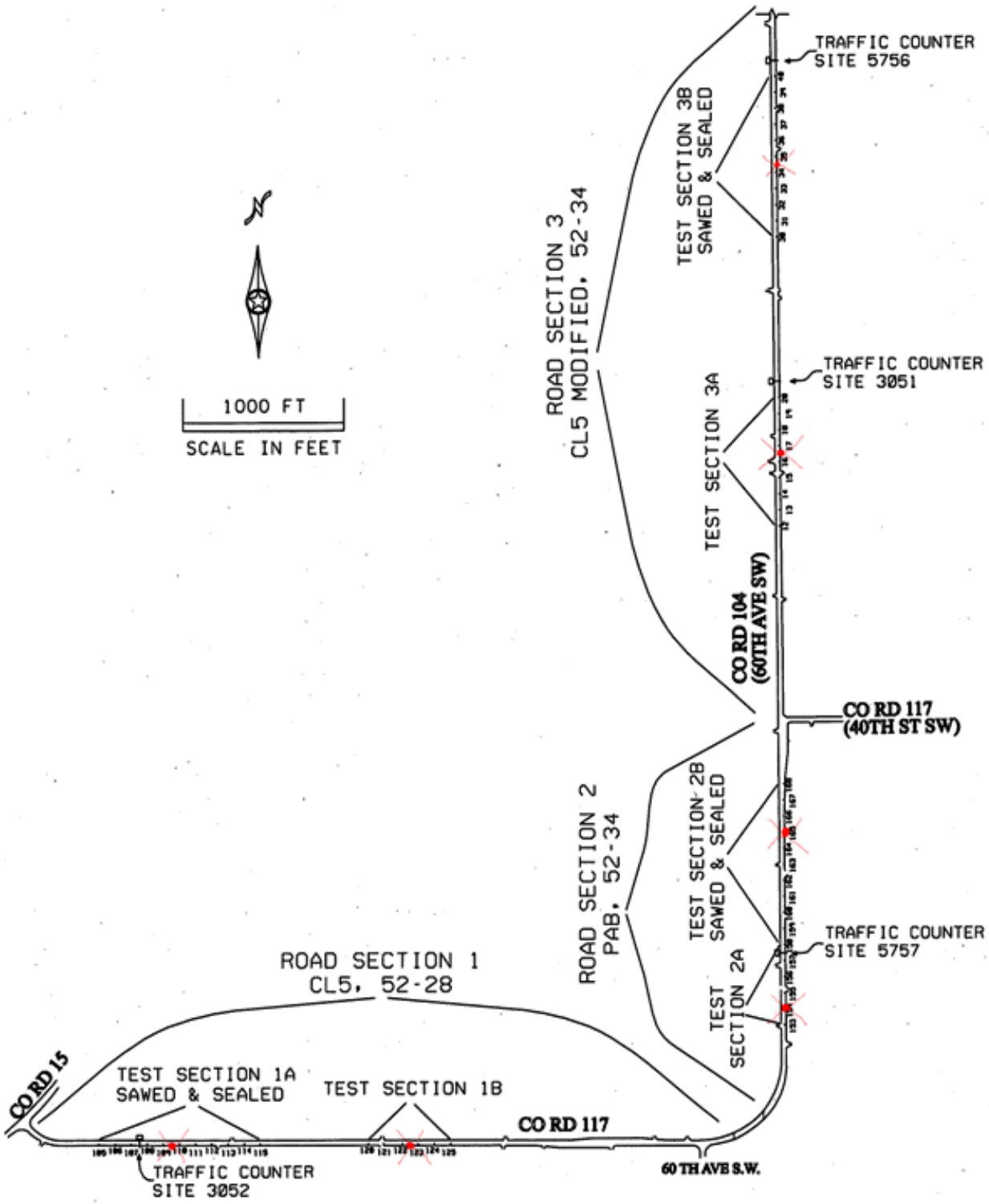

Figure 4.31 Cone Penetrometer (CPT) Testing Locations

The CPT testing procedure incorporates a vehicle-mounted device, which pushes a tube downward into the soil. A probe tip at the end of the tube has sensors which measure the tip resistance (psi) and the frictional resistance of the probe's sleeve travel through the soil material. The probe tip can also estimate the moisture content of the material. The depth of investigation can be varied; for these tests the target investigation (sounding) depth was 12 feet. The downward travel of the probe stops when materials encountered are very dense, such as hard-packed soil or bedrock. When probe travel ceased close to the surface on this project, additional attempts were made to reach 12 feet near the same location. An illustration of a CPT probe and vehicle is shown in Figure 4.32, below.

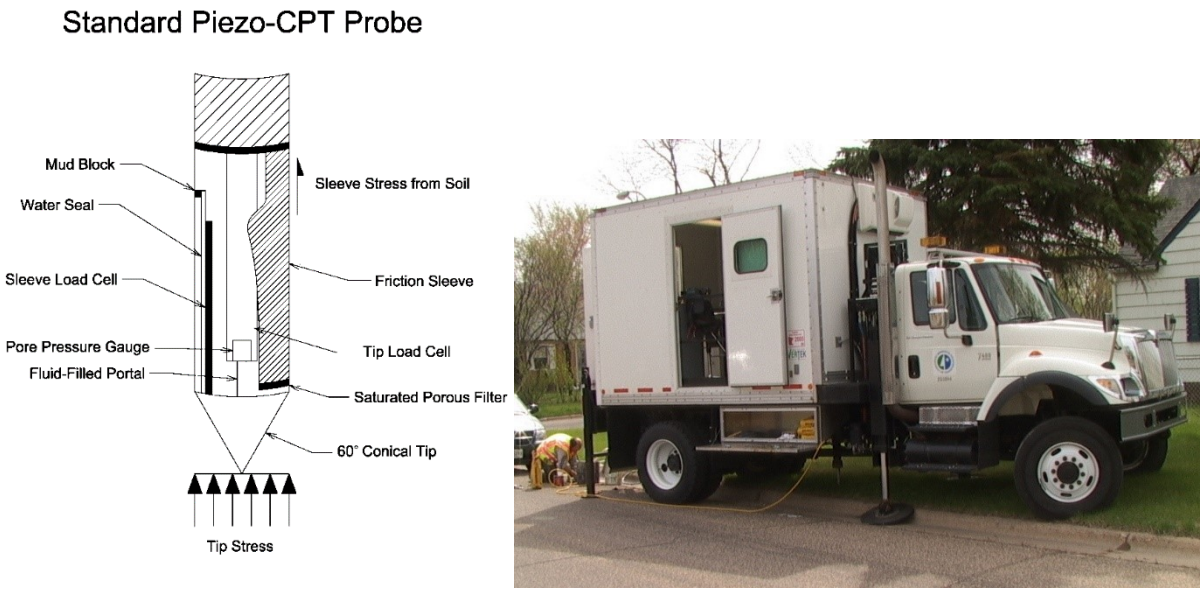

Figure 4.32 Cone Penetrometer (CPT) Probe and Vehicle

The strength of the materials encountered by the probe as it travels downward is estimated by evaluating the interaction (ratios) of the measured probes values. Different soil behavior types are then approximated by the ratios of probe resistance values, are expressed as tip stress (psi), and can be charted at increasing depths below the surface. The tip resistance values indicate strength of the layers. The following three soil types can be identified by the CPT relationships of tip resistance, sleeve friction, and moisture levels.

A. Granular Soils - High tip resistance, high sleeve friction, low friction ratio

B. Cohesive Soils - Low tip resistance, high sleeve friction, high friction ratio; high dPWP

C. Organic Soils - very low tip resistance, very low sleeve resistance, very high friction ratio >6%

The chart shown below (Figure 4.33) was used to classify the subsurface material types encountered by the CPT device on this project.

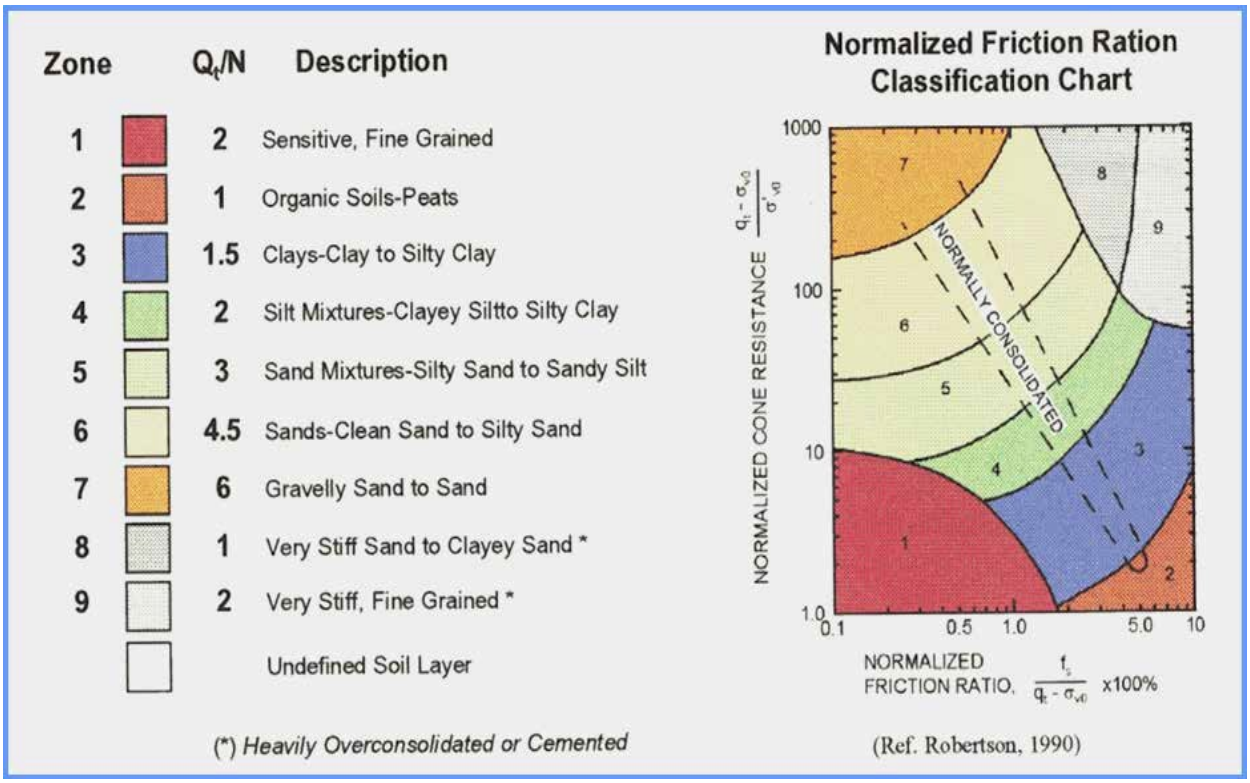

Figure 4.33 CPT Soil Type Classification Chart [5]

The chart in table 4.7 shows the tip stress (psi) results of the CPT testing. The scale on the left of the sheet shows the (1 foot) soil layers at increasing depths below the surface. The test sections and the sounding attempts are shown across the top. Additional soundings were performed close to the original location when the probe was stopped by very dense materials at less than 12 feet from the surface. The larger crushed limestone base material used on this project was penetrated by the probe without difficulty and reasonable data was obtained for the upper layers. The colors describe the type of material - based on apparent strength - as measured by the probe.

Of primary interest in this effort was to investigate the top two (one foot thick) layers – containing the base and upper subgrade materials. An analysis of the CPT data indicates that the top layers were clean, granular, and reasonably strong in all 3 sections, however the top 2 feet of Section 3 was clearly stronger than either Section 1 or 2. This indicates that the Class 5 modified base used on this project was performing better in strength terms than the other two base types. This result has also been indicated consistently with the FWD data analysis. Test Section 2 CPT testing also shows strength values between Section 1 and 3, which is expected as this has also been correlated in the FWD analysis. Section 1 has the lowest strength in the top two feet, indicating that the standard Class 5 base on this project is the weakest of the three types; even in the relatively dry conditions at the time of the CPT testing in October. At deeper levels, Section 1 also appeared to have the most cohesive materials, had the highest rate of decreasing strength with depth, and had some apparent organic material below 10 feet. The

weaker material at depth in Section 1 correlated with the previous observations of lower subgrade modulus and may have contributed to the high average roughness index found there.

Test Section 2 apparently had very resistant materials deeper, as only one probe attempt penetrated below 4 feet, and none below 8 feet. Section 3 appeared to have the best overall character throughout the depth of measurement; strongest at the top and most consistent (and granular) down through the layers. The probe was also not able to penetrate below 6 feet in test Section 3a, which also indicated very stiff materials in that location.

Unfortunately, CPT moisture readings for this testing produced negative values (and therefore unreliable) (except for Section 1), so they were not used in the analysis. It is not known why the moisture readings were unreliable. However, possibilities are; Sections 2 and 3 were unsaturated but moist, extraordinarily dry, in a zone of capillary rise, or the cone had poor calibration of the pore pressure sensor. As the testing was done in October, it was possible that the crushed limestone materials were very dry and absorptive, and produced the negative values. Better moisture data could be obtained by deploying the soil-moisture-resistivity (SMR) probe; however, it was not employed on the project as it was not needed to estimate the strength of the materials.

Table 4.7 CPT Measured Tip Stress (PSI) for Each Sounding

		Test Section 1 soundings			Test Section 2 soundings				Test Section 3 soundings		
		c01a	c01b	co1b/2	c02a	c02a/2	c02a/3	c02b/2	c03a	c03a/2	c03b
DEPTH	0-1	2500	2500	2000	4000	3000	2500	2000	5000	5000	5000
	1-2	500	600	700	2500	2250	1500	2000	1500	1500	1500
	2-3	100	125	250	1000	1250	750	400	1750	1000	750
	3-4	250	250	250		1000	3000	250	500	500	2000
	4-5	300	250	250		2500		200	2000	1500	2000
	5-6	500	100	2500				100		3500	1250
	6-7	250	1000	1000				250			2000
	7-8	200	2000	500				150			2500
	8-9	150						250			3000
	9-10	100									3000
	10-11	50									3000
	11-12	200									3000

some cohesion based on Friction Raito and Pore Water Pressure
generally cleaner granular behavior
peat, organics, liquefied sands, or highly compressible materials

VALUES: denotes tip stress (psi) in layers; higher stresses are generally more granular soils

4.4 Base Layer Forensic Analysis

With the new gradations from samples taken in 2022 prior to reconstruction, an analysis of further particle degradation could be assessed. It can be observed from Table 4.8 that the post-compaction gradation changed on all three base types by the time the pavement failed. Looking at the percent passing #200 sieve size, the increase was from 12 to 14.7, 8.9 to 12.3, and 2.3 to 6.6, for Class 5, Class 5 modified, and PAB, respectively. Thus, all 3 sections showed an increase in fine materials over the life of the pavement at a similar magnitude (2.7, 3.4, and 4.3 increase in percent passing #200 sieve size for sections 1 through 3, respectively).

Table 4.8 Gradation Pre-Compaction, Post-Compaction, and Post-Failure of All 3 Sections

	Percent Passing Class 5			Percent Passing Class 5 Modified			Passing Permeable Aggregate Base		
Sieve Size, in.	Pre-Compaction	Post-Compaction	Post-Failure	Pre-Compaction	Post-Compaction	Post-Failure	Pre-Compaction	Post-Compaction	Post-Failure
3	100	100	100	100	100	100	100	100	100
2.5	100	100	100	100	100	100	97.3	100	98
2	100	100	100	100	100	100	84.7	100	89
1.5	100	100	100		100	99		100	80
1.25	100	100	100		99.4	97		52	74
1	100	100	100	90.4	95.3	93	37	37.5	66
0.75	100	100	98	77	86.9	86	23.3	23	54
0.625		98.5	96		77.1	79.5		15	46.5
0.5		90.4	89		66.7	73		10.5	39
0.375	77.9	79.5	80	47.9	57.7	65	8.7	8	32
#4	51.3	56.2	58	31	41.5	46	4.8	5.5	22
#8		38.5	43		30.8	35		4.5	16
#10	31.8	36	41	21.5	28.8	33		4	15
#16		28.2	34		23.7	27		3.5	13

#30		22.6	28		19.4	23		3	10
#40	18	20.8	26	12.9	17.7	21		3	9
#50		19.5	24		16.6	20		3	9
#100		17.5	21		14.6	18		2.5	8
#200	12	14.7	17.9	8.9	12.3	15.6		2.3	6.6

Figure 4.34 shows the percent passing at sieve size #4 or smaller for Class 5 (shown in gray), Class 5 modified (shown in blue), and PAB (shown in orange), for post compaction (indicated by squares) and post failure (indicated by Xs). It can be observed that each base type experienced an increase in small particle sizes, with the largest increase occurring for the PAB material. Despite this increase the PAB was still comprised of significantly fewer fines than both Class 5 and Class 5 modified. Class 5 modified was still comprised of fine material below the post compaction levels of the Class 5 standard and was significantly lower than the post failure Class 5 standard fine materials. This supports the finding that the gradation (specifically lack of small particle sizes) contributed to the improved performance of Class 5 modified and PAB relative to the control Class 5 material and confirms the previous recommendation that Class 5 modified is an effective substitute for Class 5 standard base.

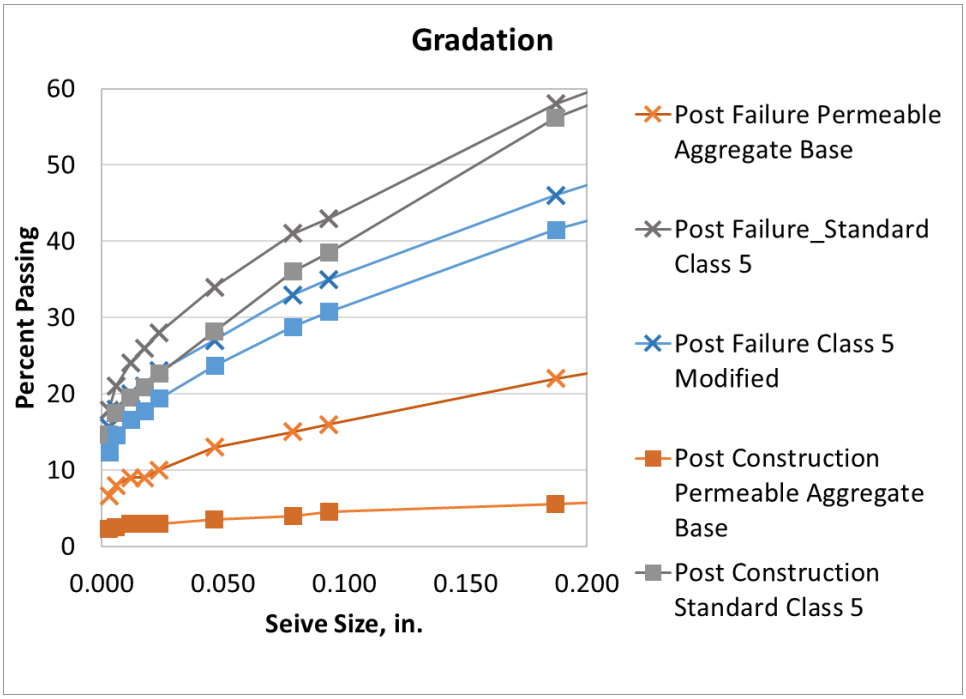

Figure 4.34 Percent Passing at Sieve Size #4 or Smaller for Class 5 (Shown in Gray), Class 5 Modified (Shown in Blue), and PAB (Shown in Orange), for Post Compaction (Indicated by Squares) and Post Failure (Indicated by Xs)

Chapter 5: Crushed Limestone Base Materials Survey

5.1 Agency Survey Description

During consultation with Olmsted County it was suggested that it may be useful to learn which other agencies in this region of southeastern Minnesota have used modified crushed limestone gradations, and the success of those changes. To assess the current practices for modifying the gradations of crushed limestone base materials, local government agencies were invited to participate in an online survey in 2013. The survey was developed by the MnDOT Office of Road Research, and an invitation was sent to local agencies near Olmsted County two times; first in March 2013 and then again in June 2013. Twelve southeastern Minnesota agencies responded, 4 cities and 8 counties. A few agencies responded twice; when they provided additional information the second time the two responses were combined. The respondents and the dates/times of participation are listed below:

City of Albert Lea	3/22/2013 2:17 PM
City of Albert Lea	6/30/2014 5:14 PM
City of Austin	6/30/2014 3:09 PM
City of Red Wing	3/25/2013 11:39 AM
City of Winona	6/30/2014 3:53 PM
Dodge County Hwy Dept.	3/25/2013 8:31 AM
Dodge County	7/7/2014 9:50 AM
Fillmore county	3/22/2013 11:19 AM
Fillmore County Hwy Dept.	3/22/2013 12:56 PM
Goodhue County Public Works	3/22/2013 11:13 AM
Goodhue County Public Works	6/20/2013 9:16 AM
Houston County DOT	3/25/2013 8:07 AM
Houston County	7/1/2014 7:16 AM
Mower County	3/22/2013 9:36 AM
Mower county	6/30/2014 8:12 PM
Olmsted County	4/5/2013 3:49 PM
Rice County Highway Dept.	3/22/2013 2:32 PM
Wabasha County	3/22/2013 1:44 PM
Wabasha County Highway Department	7/7/2014 2:58 PM

The survey was specifically intended to identify road sections where higher top-size crushed limestone base materials have been used, exactly how the gradations were modified, and the overall performance of those roadways. For each iteration of the online survey, the agencies were asked the following questions:

Q1: Respondent Information

Q2: Has your agency used a crushed limestone, with a modified Class 5 gradation specification for road base?
Q3: How have you modified the Class 5 gradation specification for crushed limestone materials?
Q4: (If yes to 3(A) above) Please describe known locations of the Class 5 top size modified materials?
Q5: Do you have performance data on any of the road sections with the Class 5 top size modified limestone base that you could share?
Q6: How would you describe the overall performance of the road sections with the top size modified limestone base?
Q7: Do you have any other comments about crushed limestone Class 5 (modified) base materials?

5.2 Agency Survey Results

The summation of the respondent's answers indicates that at least three different Minnesota counties have modified their crushed limestone base materials by increasing the top-size of the aggregate. The counties who responded positively are Olmsted County (the location of this project), Wabasha County, and Houston County.

All three agencies indicated that multiple projects were constructed with the materials and have varying traffic levels applied to them. Olmsted County has indicated in the past that it has used material similar to the Class 5 modified material at many locations, and that performance results have been good so far. The two counties other than Olmsted County reported that they have modified their gradations in a way similar to the PAB base used on this project in Section 2, The gradation they both identified specified the following limits: Sieve Size Percent Passing 3 inch 100; 2 inch 85-95; No. 4 10-50; No. 40 5-20; No. 200 2-10. One of those agencies reported generally good results so far; the second reported that roads with the modified base were too new for comment. Unfortunately, the only county to indicate that performance data was readily available for roads with crushed limestone bases was Olmsted County. The other two counties indicated that no detailed performance data was available.

Chapter 6 Conclusions and Recommendations

Performance-monitoring data showed that a combination of PG 58-34 binder with Class 5 modified base or PAB significantly outperformed the control section with PG 58-28 binder and Class 5 base. Additionally, the non-S&S sections outperformed the S&S sections. Finally, seasonal effects on stiffness where characterized showing significant asphalt layer and base stiffness loss during spring thaw, followed by the specific shape of recovery for the various layers. While confounding variables did not allow for breaking down the improvement due to the binder and base differences of the sections, respectively, the stiffness trends observed suggested both the 58-34 base, Class 5 modified base, and PAB base all contributed significantly to the better performance as compared to the control section.

The data from the automated and visual pavement distress surveys through the end of the pavement life indicated significant differences in the performance of the test sections. Both Sections 1a and 1b showed a rapid increase in cracking to a level that never became apparent in Sections 2 or 3. Test Sections 1a and 1b experienced more moderate-to-severe transverse cracking, while Sections 2 and 3 had mostly individual, low-severity transverse cracks. While part of this can be explained by thermal cracking and influenced by the higher asphalt binder stiffness in Section 1 as compared to Sections 2 and 3, the FWD, IRI, and CPT analysis suggested Section 1 suffered from reduced performance of the conventional Class 5 base. Forensics toward the end of pavement life (GPR and gradation) supported the hypothesized cause of reduced performance of Section 1 and reinforced the theory that increased fine material was a contributing cause of the reduced performance.

The average rutting in all sections never reached a significant level to the point of affecting pavement performance. FWD testing showed the asphalt containing the PG 58-28 binder remained stiffer than the PG58-34 and more so in cooler conditions as was expected. Test Section 1 demonstrated the worst roughness index of the three sections. It showed the most rapid decline in ride quality and ultimately led to the functional failure based on roughness criteria necessitating reconstruction. However, roughness increased somewhat in all sections. The non-sawed and sealed test sections demonstrated better ride quality than the rest of the sawed road, particularly during winter months. The sawn joints on this project appeared to suffer from the “tenting” phenomenon in winter periods (and then improve somewhat by the time of roughness testing in summer). This reinforces the previous decision to stop the sawing and sealing practice for asphalt roads in most of Minnesota.

There was likely a relationship between the aggregate base and subgrade stiffness of each of the test sections and the surface roughness. For example, Section 3 consistently demonstrated the best base and subgrade FWD measured resilient modulus and had good ride quality ratings while experiencing the highest traffic. Section 2 also continued to perform well despite lower FWD measured stiffness and slightly worse initial ride quality than Section 3. It is possible that the open-graded PAB material in Section 2 allowed more inter-particle movement (and somewhat less support) but facilitates drainage and provides flexibility and resilience.

Falling weight deflectometer (FWD) testing was performed annually to better understand the stiffness capability of the pavement and subsurface layers. FWD testing was performed at various times of the year, with an emphasis on spring testing in 2010, fall testing in 2012, and mid-summer testing in 2014, then additional analysis was focused on comparisons identifying year-by-year trends including multiple dates within 2008-2012 and 2014. The analysis of the 2010-14 FWD data demonstrated notable differences in stiffness between the different bituminous and aggregate base materials used in the project. During the spring-thaw and early summer, the conventional Class 5 base lost significant stiffness quickly and recovered more slowly than the other base types. Annual testing showed the Class 5 modified and PAB sections were consistently stiffer than the conventional Class 5. The subgrade soils remained somewhat stiffer on CR 104 (test Section 3) than on CR 117 (test Sections 1 and 2). The conventional Class 5 base lost stiffness during fall freezing; however, frost penetration may have progressed unevenly, moisture levels were unknown, and equipment problems rendered the results somewhat inconclusive. In this final phase of the study, analysis was expanded to show that the average resilient modulus of the asphalt containing the PG 58-28 binder (Test Section 1) remained stiffer throughout the year than the asphalt containing the PG 58-34 binder (Test Sections 2 and 3).

The research effort on this project has indicated that the Class 5 modified base material is the best performing of the three base types and may be considered an effective substitution for conventional Class 5 crushed limestone base materials of the type commonly available in Olmsted County, Minnesota. This conclusion was based on the following data: rutting, FWD, CPT, lab testing, and other Olmsted County project experience. The data led to an addition to the latest MnDOT standard Specification 3138 of a gradation category named CLASS 5Q. The Class 5 modified material used in this project in Section 3 would meet the new Class 5Q gradation specification.

More generally, the final phase of the project confirmed most of the same trends observed in the previous phases of the project. The major findings of the project included the following:

- The performance of larger top-size gradations of crushed limestone Class 5Q and PAB (Section 3 and Section 2) outperformed Class 5 standard (Section 1). Sections showed lower crack length and severity as well as IRI throughout the project, despite Section 1 showing the lowest levels of traffic.
- Non-S&S outperformed S&S, as less cracking and better IRI was observed throughout.
- FWD showed the different base material types of trends in relation to freeze-thaw cycles, and CPT analysis confirmed the better material properties of Class 5Q and PAB as compared to the Class 5Q.
- Forensics activities such as GPR thickness mapping and post pavement failure gradation conducted in the final phase confirmed the previously observed trends by eliminating possible confounding variables.
- Class 5 modified base material was demonstrated to be an effective substitution for conventional Class 5 crushed limestone base material.